

LUCAS MARTINIANO DE OLIVEIRA

**PATTERN RECOGNITION-BASED
IDENTIFICATION OF HAND MOVEMENTS
USING A NOVEL DATA CAPTURING DEVICE**

This dissertation is submitted to the Graduate Program in Computer Science at Pontifical Catholic University of Paraná in partial fulfillment of the requirements for the degree of Master of Science in Computer Science.

Curitiba

2018

LUCAS MARTINIANO DE OLIVEIRA

**PATTERN RECOGNITION-BASED
IDENTIFICATION OF HAND MOVEMENTS
USING A NOVEL DATA CAPTURING DEVICE**

This dissertation is submitted to the Graduate Program in Computer Science at Pontifical Catholic University of Paraná in partial fulfillment of the requirements for the degree of Master of Science in Computer Science.

Concentration track: Computer Science

Advisor: Dr. Carlos N. Silla Jr.

Co-advisor: Dr. Adam Arabian

Curitiba

2018

Dados da Catalogação na Publicação
Pontifícia Universidade Católica do Paraná
Sistema Integrado de Bibliotecas – SIBI/PUCPR
Biblioteca Central
Giovanna Carolina Massaneiro dos Santos – CRB 9/1911

O48p
2018

Oliveira, Lucas Martiniano de
Pattern Recognition -based identification of hand movements using a novel data capturing device / Lucas Martiniano de Oliveira ; orientador: Carlos Nascimento Silla Junior; coorientador: Adam Arabian. - 2018
109, [5] f. : il. ; 30 cm

Dissertação (mestrado) – Pontifícia Universidade Católica do Paraná, Curitiba, 2018
Bibliografia: f. 89-99

1. Processamento de dados. 2. Aprendizado do computador. 3. Mineração de dados (Computação). 4. Eletromiografia. 5. Mãos. 6. Reconhecimento de padrões. I. Silla Junior, Carlos Nascimento. I. Arabian, Adam. II. Pontifícia Universidade Católica do Paraná. Programa de Pós-Graduação em Informática. III. Título.

CDD 22. ed. – 004

ATA DE SESSÃO PÚBLICA

DEFESA DE DISSERTAÇÃO DE MESTRADO Nº 06/2018

PROGRAMA DE PÓS-GRADUAÇÃO EM INFORMÁTICA – PPGIa PONTIFÍCIA UNIVERSIDADE CATÓLICA DO PARANÁ - PUCPR

Em sessão pública realizada às 13h30 de **01 de Agosto de 2018**, no Auditório Guglielmo Marconi – Bloco 8, ocorreu a defesa da dissertação de mestrado intitulada “**Pattern Recognition-based Identification of Hand Movements Using a Novel Data Capturing Device**” apresentada pelo aluno **Lucas Martiniano de Oliveira**, como requisito parcial para a obtenção do título de **Mestre em Informática**, na área de concentração **Ciência da Computação**, perante a banca examinadora composta pelos seguintes membros:

Prof. Dr. Carlos Nascimento Silla Junior (Orientador)- PUCPR

Prof. Dr. Adam Arabian (co-orientador) – Seattle Pacific University

Prof. Dr. Julio Cesar Nievola – PUCPR/PPGIA

Prof. Dr. Alessandro Goedtel – UTFPR

Após a apresentação da dissertação pelo aluno e correspondente arguição, a banca examinadora emitiu o seguinte parecer sobre a tese:

| Membro | Parecer |
|---|---|
| Prof. Dr. Carlos Nascimento Silla Junior | <input checked="" type="checkbox"/> Aprovado () Reprovado |
| Prof. Dr. Adam Arabian | <input checked="" type="checkbox"/> Aprovado () Reprovado |
| Prof. Dr. Julio Cesar Nievola | <input checked="" type="checkbox"/> Aprovado () Reprovado |
| Prof. Dr. Alessandro Goedtel | <input checked="" type="checkbox"/> Aprovado () Reprovado |

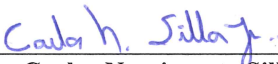
Portanto, conforme as normas regimentais do PPGIa e da PUCPR, a tese foi considerada:

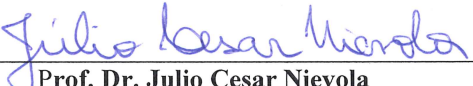
APROVADO

(aprovação condicionada ao atendimento integral das correções e melhorias recomendadas pela banca examinadora, conforme anexo, dentro do prazo regimental)


REPROVADO


E, para constar, lavrou-se a presente ata que vai assinada por todos os membros da banca examinadora. Curitiba, 01 de Agosto de 2018.



Prof. Dr. Carlos Nascimento Silla Junior


Prof. Dr. Julio Cesar Nievola



Prof. Dr. Adam Arabian


Prof. Dr. Alessandro Goedtel

Acknowledgements

First, I would like to thank both of my advisors, Dr. Adam Arabian and Dr. Carlos Silla Jr. for guiding and supporting me not only during this project but also over the years. You two have set an example of excellence as a researcher, mentor, instructor, and role model.

I would like to thank SPU for hosting me, all its staff and students for having me with open arms and help me with anything I needed. I will never forget it.

I'd like to thank my fellow graduate students at PUC who were part of my life during this research. I am very grateful to all of you in special Rodolfo and Zacarias, without you this job would be much more difficult and boring. I would also like to thank OSMARILIA.

I would especially like to thank my amazing wife Erin and my family for the love, support, and constant encouragement I have got over the years.

Thanks to CAPES for scholarship grant.

Abstract

In the world, there are nearly three million people living with upper limb loss. There is a need for novel approaches that go beyond the existing technologies to improve the life of amputees. This project applies new machine learning techniques in order to improve the current results for classification of hand movements for prosthetic devices presented in the literature. We performed experiments applying convolutional neural networks (CNN) and a hyper-parameter optimization technique, called Neural Architecture Search (NAS), as well as creating synthetic data using SMOTE in order to improve the CNN's classification performance on hand movement data from the NinaPro DB5, an open-sourced hand movement for prosthesis control dataset. The use of synthetic oversampling techniques, NAS and CNN considerably increased the classification performance of hand movements for prosthetic devices compared to the results presented in the literature. Additionally, we wanted to verify whether additional sensors to the EMG signals help to improve the classifier's performance. Due to the high cost of existing data capture devices, we built a new multi-sensor device for capturing hand movements. With this device we created the Sensor Glove data base (SGDB) with 21 hand movements performed by five different subjects. Subsequently, using the SGDB, we verified that the use of additional sensors along with the EMG signal significantly improve the classification performance.

Keywords: Data Glove, Prosthesis, Electromyography, Sensors, Hand, Pattern Recognition, Machine Learning, Data Mining, Deep Learning, Over-sampling.

List of Figures

| | |
|---|----|
| Figure 1 – Body Powered Prosthetic Arm | 19 |
| Figure 2 – Electric Powered Prosthetic Arm | 19 |
| Figure 3 – A schematic of the differential amplifier configuration. The electrodes are positioned in a bipolar configuration, in which there is one positive electrode, one negative electrode and a ground electrode. In this configuration, the EMG signal is the differential measure of the two electrodes. The use of this differential measure is favorable to eliminate interference from other biological activities of the patient or even the power grid. | 20 |
| Figure 4 – General Microcontroller Architecture. The Central Processing Unit (CPU) is responsible for the microcontroller data processing. It is this which interprets the commands, reads data and activates the input and output (I/O) ports or the peripherals if necessary; The Memory Unit is part of the microcontroller used for data storage; The I/O interfaces of a microcontroller are responsible for input and output information. | 21 |
| Figure 5 – Illustration of an IMU System | 22 |
| Figure 6 – FSR Construction | 22 |
| Figure 7 – How a flex sensor works. It is possible to determine the relative angle that the sensor is being bent by measuring its resistance. | 23 |
| Figure 8 – Basic principle of an IR proximity sensor | 23 |
| Figure 9 – Fictitious decision tree for Iris dataset | 31 |
| Figure 10 – Steps for Bagging | 33 |
| Figure 11 – Overview of a CNN applied in an image of 28×28 pixels | 35 |
| Figure 12 – NAS parent-child network architecture | 35 |
| Figure 13 – Example of SMOTE applied to the Iris dataset | 37 |
| Figure 14 – Examples of Vision Based Systems | 50 |
| Figure 15 – Examples of Data Gloves | 51 |
| Figure 16 – Sets of Movements from NinaPro Database | 57 |
| Figure 17 – Class distribution for the Ninapro database. The vertical axis shows the number of examples for all the subjects, the horizontal axis shows the class identification number. | 57 |
| Figure 18 – “Mock” data projected to \mathbb{R}^2 | 58 |
| Figure 19 – Confusion matrix shows the predictions from a classifier. | 59 |
| Figure 20 – Overview of the system | 75 |
| Figure 21 – Sensor Unit Overview | 76 |
| Figure 22 – Intel Edison kit for Arduino block diagram | 77 |

| | |
|---|-----|
| Figure 23 – Overview of the hardware connection | 78 |
| Figure 24 – Overview of base board and proximity sensor breakout board | 79 |
| Figure 25 – 3D Printed Box | 79 |
| Figure 26 – CPU + MCU Integration | 80 |
| Figure 27 – Activity diagram | 81 |
| Figure 28 – Final prototype. This picture shows the final configuration of the device. All principal electric components were placed in the 3d printed box to protect the equipment from sweat contact. | 81 |
| Figure 29 – Class distribution for the Sensor Glove database. The vertical axis shows the number of examples for all the subjects, the horizontal axis shows the class identification number. | 85 |
| Figure 30 – Neural Network Architecture for the <i>e</i> CNN trained with 500 epochs and dropout rate of 0.2 | 101 |

List of Tables

| | |
|--|-----|
| Table 1 – Upper Limb Amputation Types | 17 |
| Table 1 – Upper Limb Amputation Types | 18 |
| Table 2 – Example of a training set | 30 |
| Table 3 – Pattern Recognition-based Control of Upper Limb Prosthesis | 45 |
| Table 3 – Pattern Recognition-based Control of Upper Limb Prosthesis | 46 |
| Table 3 – Pattern Recognition-based Control of Upper Limb Prosthesis | 47 |
| Table 3 – Pattern Recognition-based Control of Upper Limb Prosthesis | 48 |
| Table 4 – Glove-Based Systems and Their Applications | 52 |
| Table 4 – Glove-Based Systems and Their Applications | 53 |
| Table 4 – Glove-Based Systems and Their Applications | 54 |
| Table 5 – Recall per class and overall accuracy and <i>MAvG</i> for a classifier. | 60 |
| Table 6 – Results for the subject dependent classifiers. | 62 |
| Table 7 – Results for the subject independent classifiers. | 64 |
| Table 8 – Results for subject dependent classifiers using SMOTE | 67 |
| Table 9 – Results for subject dependent classifiers using SMOTE-SVM | 68 |
| Table 10 – Results for subject independent classifiers using SMOTE | 71 |
| Table 11 – Results for subject independent classifiers using SMOTE-SVM | 72 |
| Table 12 – Results for subject independent classifier NAS-CNN using RMS as feature extraction. The first column presents the results using NAS-CNN with RMS from Table 11; The second column present the experiments using EMG and the CyberGlove II; The third column shows the experiments using EMG and CyberGlove II with syntethic examples from SMOTE-SVM. | 74 |
| Table 13 – Comparison of project’s requirements and prototype’s achievements | 82 |
| Table 14 – Price breakdown of our device | 83 |
| Table 15 – Results for the SGDB with EMG only and with all sensors. Using NAS-CNN classifier with RMS as feature extraction in a subject independent approach. | 86 |
| Table 16 – Neural Network Architectures generated by the NAS algorithm | 102 |

List of abbreviations and acronyms

| | |
|-----|------------------------------|
| Ab | Abduction Sensor |
| ADL | Activity of Daily Living |
| ALU | Arithmetic/Logic Unit |
| AS | Finger Joint Angle Sensor |
| BP | Body Powered |
| CC | Cepstral Coefficient |
| CeG | Centralized Grasp |
| ChG | Chuck Grip |
| CNN | Convolutional Neural Network |
| CPU | Central Processing Unit |
| CS | Contact Sensor |
| CSV | Comma Separated Value |
| CWT | Continuous Wavelet Transform |
| CyG | Cylindrical Grasp |
| DB | Database |
| DM | Data Mining |
| EE | Elbow Extension |
| EF | Elbow Flexion |
| EMG | Electromyography |
| FD | Frequency Domain |
| FFT | Fast-Fourier Transform |
| FMD | Median Frequency |
| FMN | Mean Frequency |

| | |
|-------------|------------------------------|
| FP | Fine Pinch |
| FR | Frequency Ratio |
| FS | Force Sensor |
| FSR | Force Sensitive Resistor |
| GA | Genetic Algorithm |
| GMM | Gaussian Mixture Model |
| HC | Hand Close |
| HE | Hall Effect Sensor |
| HG | Hook Grip |
| HIST | EMG Histogram |
| HLR | Humerus Lateral Rotation |
| HMM | Hidden Markov Model |
| HMR | Humerus Medial Rotation |
| HO | Hand Open |
| I/O | Input/Output |
| IFT | Inverse Fourier Transform |
| IMU | Inertial Measurement Unit |
| IR | Imbalance Ratio |
| K/M | Keyboard/Mouse |
| KG | Key Grip |
| LaP | Lateral Pinch |
| LDA | Linear Discriminant Analysis |
| M/A | Music and Arts |
| MAV | Mean Absolute Value |
| <i>MAvG</i> | Macro Average Geometric |
| MAVS | Mean Absolute Value Slope |

| | |
|-------|--|
| MCU | Microcontroller Unit |
| mDWT | marginal Discrete Wavelet Transform |
| ML | Machine Learning |
| MLP | Multi-Layer Perceptron |
| ms | Millisecond |
| MUAP | Motor Unit Action Potential |
| MYO | Myoelectric |
| NAS | Neural Architecture Search |
| OT | Optical Tracking |
| PA | Palm Arch |
| PCB | Printed Circuit Board |
| PG | Power Grip |
| PR | Pattern Recognition |
| PRE | Pressure Sensor |
| PS | Pressure |
| PSD | Power Spectrum Density |
| RF | Random Forests |
| RMS | Root Mean Square |
| SHAP | Southampton Hand Assessment Procedure |
| SL | Sign Language |
| SMOTE | Synthetic Minority Over-sampling Technique |
| SS | Strech |
| STFT | Short-time Fourier Transform |
| SVM | Support Vector Machine |
| TC | Thumb Crossover Sensor |
| TD | Time Domain |

| | |
|---------|------------------------------------|
| TG | Tool Grip |
| TS | Tilt Sensor |
| US | Ultrasonic Sensor |
| VAR | Variance |
| VR | Virtual Reality |
| WAMP | Willison Amplitude |
| WE | Wrist Extension |
| WF | Wrist Flexion |
| WL | Waveform Length |
| WNN | Wavelet Neural Network |
| WP | Wrist Prontation |
| WPT | Wavelet Packet Transform |
| WRD | Wrist Radial Deviation |
| WS | Wrist Supination |
| WUD | Wrist Ulnar Deviation |
| xyz-Fab | xth yth zth-Digit Finger Abduction |
| xyz-Fad | xth yth zth-Digit Finger Adduction |
| xyz-FE | xth yth zth-Digit Finger Extension |
| xyz-FF | xth yth zth-Digit Finger Flexion |
| ZC | Zero Crossing |

Contents

| | | |
|------------|---|-----------|
| 1 | INTRODUCTION | 14 |
| 1.1 | Objectives | 15 |
| 1.2 | Hypothesis | 16 |
| 1.3 | Structure of the document | 16 |
| 2 | CONCEPTUAL AND EMPIRICAL FOUNDATIONS | 17 |
| 2.1 | Amputation | 17 |
| 2.2 | Prosthesis | 18 |
| 2.2.1 | Body-powered | 18 |
| 2.2.2 | Electric-powered | 19 |
| 2.3 | Electromyography | 20 |
| 2.4 | Microcontrollers | 21 |
| 2.5 | Inertial Navigation | 21 |
| 2.6 | Force Sensitivity Resistor (FSR) | 22 |
| 2.7 | Flex Sensors | 23 |
| 2.8 | Proximity Sensor | 23 |
| 2.9 | EMG Feature Extraction | 24 |
| 2.9.1 | Time Domain | 24 |
| 2.9.1.1 | Mean Absolute Value (MAV) | 24 |
| 2.9.1.2 | Variance (VAR) | 24 |
| 2.9.1.3 | Mean Absolute Value Slope (MAVS) | 24 |
| 2.9.1.4 | Root Mean Square (RMS) | 25 |
| 2.9.1.5 | Willison amplitude (WAMP) | 25 |
| 2.9.1.6 | Zero Crossing (ZC) | 25 |
| 2.9.1.7 | Slope Sign Changes (SSC) | 25 |
| 2.9.1.8 | Waveform Length (WL) | 26 |
| 2.9.1.9 | EMG histogram (HIST) | 26 |
| 2.9.1.10 | Auto-regressive Coefficients | 26 |
| 2.9.2 | Frequency Domain | 26 |
| 2.9.2.1 | Power Spectrum (PS) | 26 |
| 2.9.2.2 | Mean Frequency (FMN) | 26 |
| 2.9.2.3 | Median Frequency (FMD) | 27 |
| 2.9.2.4 | Frequency Ratio (FR) | 27 |
| 2.9.2.5 | Short-time Fourier Transform (STFT) | 27 |
| 2.9.2.6 | Continuous Wavelet Transform (CWT) | 27 |

| | | |
|------------|---|-----------|
| 2.9.2.7 | Discrete Wavelet Transform (DWT) | 28 |
| 2.9.2.8 | Wavelet Packet Transform (WPT) | 28 |
| 2.9.2.9 | Marginal Discrete Wavelet Transform (mDWT) | 28 |
| 3 | MACHINE LEARNING | 29 |
| 3.1 | Supervised Learning | 29 |
| 3.1.1 | Support Vector Machines | 30 |
| 3.1.2 | Decision Trees | 31 |
| 3.1.2.1 | Bagging | 33 |
| 3.1.2.2 | Random Forests | 33 |
| 3.1.3 | Convolutional Neural Networks | 34 |
| 3.1.4 | Neural Architecture Search | 35 |
| 3.2 | Imbalance Classification | 36 |
| 3.2.1 | Synthetic Minority Oversampling Technique | 36 |
| 4 | PATTERN RECOGNITION-BASED MYOELECTRIC CONTROL | 38 |
| 5 | HUMAN MOTION SENSING TECHNIQUES | 50 |
| 5.1 | Vision Based Sensing | 50 |
| 5.2 | Wearable Sensing | 51 |
| 6 | EXPERIMENTS | 56 |
| 6.1 | Experimental Settings | 56 |
| 6.1.1 | The Ninapro DB5 database | 56 |
| 6.1.2 | Evaluation Metrics | 58 |
| 6.2 | Experiment #1: Exploring different algorithms | 60 |
| 6.3 | Experiment #2: Towards a subject independent model | 63 |
| 6.4 | Experiment #3: Improving the results with Synthetic Samples | 65 |
| 6.4.1 | SMOTE and SMOTE-SVM in a Subject Dependent Approach | 65 |
| 6.4.2 | SMOTE and SMOTE-SVM in a Subject Independent Approach | 66 |
| 6.5 | Experiment #4: Improving the results with additional sensors | 73 |
| 7 | PROTOTYPE DEVELOPMENT | 75 |
| 7.1 | System Overview | 75 |
| 7.1.1 | Project Specifications | 76 |
| 7.2 | Hardware Implementation | 76 |
| 7.2.1 | Electronic Design | 76 |
| 7.2.1.1 | Computing Platform | 76 |
| 7.2.1.2 | Electromyography Sensor | 77 |
| 7.2.1.3 | FSR, Flex and Proximity Sensors | 77 |
| 7.2.2 | Printed Circuit Board Design | 78 |

| | | |
|------------|---|------------|
| 7.2.3 | Mechanical Design | 78 |
| 7.3 | Software Implementation | 79 |
| 7.3.1 | Operating System | 79 |
| 7.3.2 | Application | 80 |
| 7.4 | Results | 80 |
| 7.4.1 | Costs | 83 |
| 7.5 | Data Collection | 84 |
| 7.6 | Low-cost sensor glove validation | 85 |
| 8 | CONCLUDING REMARKS | 87 |
| | BIBLIOGRAPHY | 89 |
| | APPENDIX | 100 |
| | APPENDIX A – NEURAL NETWORKS ARCHITECTURES | 101 |
| | APPENDIX B – SCHEMATICS | 103 |
| | APPENDIX C – MOVEMENTS SGDB | 109 |

1 Introduction

In the world, there are nearly three million people living with upper limb loss (LEBLANC, 2011). War and ground mines are the main reasons for amputation, but other injuries, such as a motor vehicle crash, a disease (e.g. diabetes, peripheral vascular disease, or cancer of a bone or joint), can contribute to the number of people who had their limbs amputated (WHO, 2004). In the United States, it was estimated in 2005 that about 1.6 million people were living with the loss of a limb. Among those living with limb loss, the main causes are traumatic incident (47.7 percent), non-diabetes-related infection (12.8 percent) and cancer (12.5 percent) (ZIEGLER-GRAHAM et al., 2008; AMPUTEE COALITION; O&P EDGE, 2011). According to the IBGE (2010) in Brazil, around 470,000 people were victims of amputations. In a study conducted in the city of Rio de Janeiro between 1992 and 1994, the estimated number of amputations were 3,954 cases, making an average annual rate of 13.9 per 100,000 inhabitants (SPICHLER et al., 2001). In Brazil, the main causes of amputation are diabetes-related vascular diseases (52 percent), traumatic incident (19 percent) and non-diabetes-related vascular diseases (19 percent), claimed ABBR (2016).

Prostheses were created to help amputees to live a normal life. It is believed the Indians were the pioneers of this idea. A poem from India, the Rigveda, dated between 3500 and 1500 BC, tells the story of a warrior queen who had her leg amputated during a battle and after recovering, an iron leg was placed, and she could return to the battlefield (VANDERWERKER, 1976). For a long time, the main concern in the prosthesis development was the aesthetic resemblance of the missing limb. Because of the shame felt by the amputee, the prosthesis functionality was usually set aside. However, after the development of mechanical prosthesis, the prosthesis control has become more functional and allowed the patient to perform some complex activities.

There are two different types of prosthesis: passive prosthesis and active prosthesis. Passive prostheses are devices for cosmetic purposes only, i.e. they do not have any functionality. The active prostheses, however, are devices that allow an amputee to perform some tasks and that can also be used with cosmetic purposes when needed (AMPUTEE COALITION, 2014).

Active prosthesis are either body-powered or electric-powered. Body-powered devices are usually operated by cables that requires the patient to use the movements of their body to control the open and close movements of the prosthesis. On the other hand, electric-powered prosthesis, commonly refereed as myoelectric prosthesis, uses electric signals from the body's muscles to actuate motors and perform opening and closing

movements.

Electrical signals, sent from the brain to the arm muscles, are used to control how the prosthesis should move. These are called Electromyography (EMG) signals. Those signals are captured using electrodes sit on the skin over specific muscles. The EMG signal is acquired from the muscle's contractions and sent to a microcontroller which processes the signals actuating the motors that controls the prosthesis (LICHTER et al., 2010).

The idea of using EMG for prostheses control is not new. In the 60s and 70s Finley and Wirta (1967), Lawrence, Herberts and Kadefors (1973) and Lyman, Freedy and Prior (1976) developed prostheses control schemes using EMG. However, the computing capacity and the EMG of the day were not enough powerful.

Currently, myoelectric hand prosthesis leading industrial developers are Ottobock, RSL-Steepier, LTI, Motion Control, and Touch Bionics. Despite all the technology embedded in them, they do not have a very good precision and prevent the user to make complex maneuvers, also limiting the number of movements the user can perform, resulting in unnatural movements (FARLEY, 2014). In academia, although recent researches like Atzori, Cognolato and Müller (2016) and Phinyomark, Khushaba and Scheme (2018) have made significant advances in the area, there is still a need for new approaches that go beyond the existing technologies to improve the life of amputees.

Experiments made by Kyranou et al. (2016) shows that the use of inertial information along with the EMG improves the classification accuracy. We believe that adding more information other than the EMG can improve even more the classification performance.

In this work, we apply new machine learning techniques in order to improve the current results for classification of hand movements for prosthetic devices presented in the literature. In addition, due to the high cost of data capture devices and low variety of sensors, we build a new multi-sensor device for capturing hand movements. With this device we created the Sensor Glove data base (SGDB) with 21 hand movements performed by 5 different subjects. Subsequently, using the SGDB, we verify the functionalities of the device we proposed and whether the use of additional sensors along with the EMG signal improves the classification performance.

1.1 Objectives

The main objective of this dissertation is to improve classification performance of algorithms used for prosthetic devices.

Specific Objectives:

- Create and/or adapt a device that captures movements of a person's hand;
- Create an annotated database of hand movements using the data capture device;
- Perform experiments to verify if the sensors of the proposed device are complementary to the EMG signal, thus improving the classification performance of machine learning algorithms;

1.2 Hypothesis

The hypothesis of this research is:

The incorporation of multiple sensors along with electromyography has the potential of improving the performance and robustness of a prosthetic device by increasing the classification performance of the machine learning algorithm.

1.3 Structure of the document

The remainder of this document presents the following organization:

- In this chapter we present the opening remarks, the motivation for the development of this project, as well as the objectives for the development and this section about the organization of the document;
- Chapter 2 presents the theoretical foundations for the understanding of this project;
- Chapter 3 presents an introduction to concepts and applications of machine learning;
- Chapter 4 presents an analysis of the related work in hand movement classification for prosthetic control;
- Chapter 5 presents a review of existing human motion sensing techniques;
- Chapter 6 focuses on the experiments applying new machine learning techniques to improve the performance of classifiers for hand movements;
- Chapter 7 discusses important aspects of the proposed device such as our implementation from hardware to software, as well as data collection and product validation;
- Finally, in Chapter 8, we summarize the entire dissertation;

2 Conceptual and Empirical Foundations

This chapter is organized in three parts: [Part 1](#) presents concepts related to the foundations of amputation and prosthesis; [Part 2](#) addresses the concepts of microcontrollers, electromyography, inertial measurement unit and a description about how the sensors work; part [Part 3](#) presents a review of the most common EMG feature extraction algorithms. All these topics are important to understand this project.

2.1 Amputation

According to NHS Choices (2014) amputation is the removal of a limb or part of one caused by trauma, medical illness, or surgery. In medicine, it is used to control pain or disease in the affected limb, such as the cancer and gangrene (COSTA, 2006).

Amputation may be classified as lower limb amputation and upper limbs amputation. As part of this project involves hand movements data collection, the lower limb amputations types will not be covered. Table 1 presents the different types of upper limb amputation.

Table 1 – Upper Limb Amputation Types

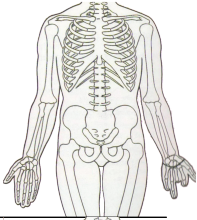
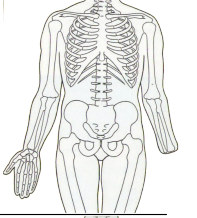
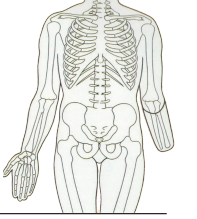
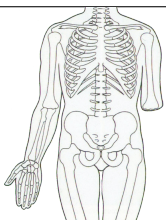
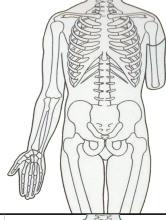
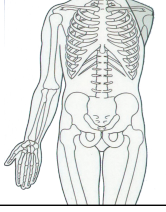
| Typical Forms | Description | Figure |
|--------------------------------------|--|---|
| Partial hand amputation | Complete or partial removal of the metacarpal or partial removal of the carpal bones, may or may not keep phalanges. |  |
| Wrist disarticulation | Complete removal of the hand, preserving the integrity of the distal forearm bones |  |
| Below elbow amputation (Transradial) | It is the bone section between the elbow joint and wrist |  |

Table 1 – Upper Limb Amputation Types

| Typical Forms | Description | Figure |
|---|--|--|
| Elbow disarticulation | Complete removal of the forearm bones (radius and ulna), preserving the distal humerus integrity (upper arm bone) |  |
| Above elbow amputation (Transhumeral) | It is the bone section between the shoulder joint and the elbow |  |
| Shoulder disarticulation and forequarter amputation | Complete removal of the humerus (upper arm bone), preserving the integrity of the clavicle and scapula. It is complete withdrawal of the member |  |

Source – Adapted from Limbless Association (2012)

2.2 Prosthesis

The dictionary definition of Prosthesis is an artificial replacement of part of the body, accidentally lost or intentionally removed (DICTIONARY.COM, 2015). In the article “Prosthetics in developing countries”, Strait (2006) explains that an upper-limb prosthesis incorporates five main components: a socket, that allows the prosthesis to connect to the patient’s residual limb, an extension section or forearm section, a suspension system, to secure the prosthesis, a wrist unit, that allows the user the ability to rotate terminal device, and a terminal device such as a hook or hand.

Functional Prosthesis can be separate in two different groups: Body-powered and Electric-powered prosthesis.

2.2.1 Body-powered

The body-powered prosthesis are fed by the energy of the body. They can be either voluntary closing or voluntary opening, for example on Figure 1, a voluntary closing prosthesis remain open (1) until the user pulls a cable, with the residual limb and/or the shoulder girdle (2), causing it to close with a grip force proportional to the amount of force the person puts on the cable (3) (MARKS, 1905).

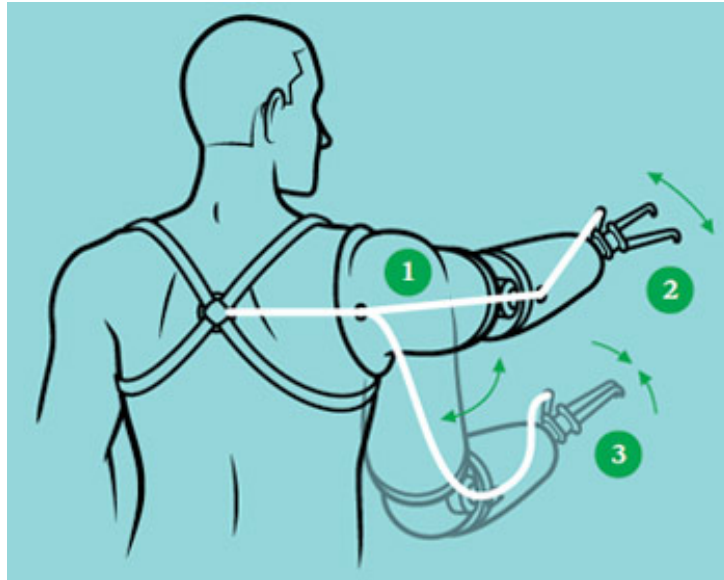


Figure 1 – Body Powered Prosthetic Arm

Source – Chorost (2012)

2.2.2 Electric-powered

The electric-powered prosthesis is supplied by an external power source, having components that are controlled by motors and powered by batteries. The system is usually controlled by a microcontroller using body signals to control the prosthesis. These body signals come from muscle contractions which generate electrical signals on the skin and are captured and used to control the electric prosthesis (STRAIT, 2006).

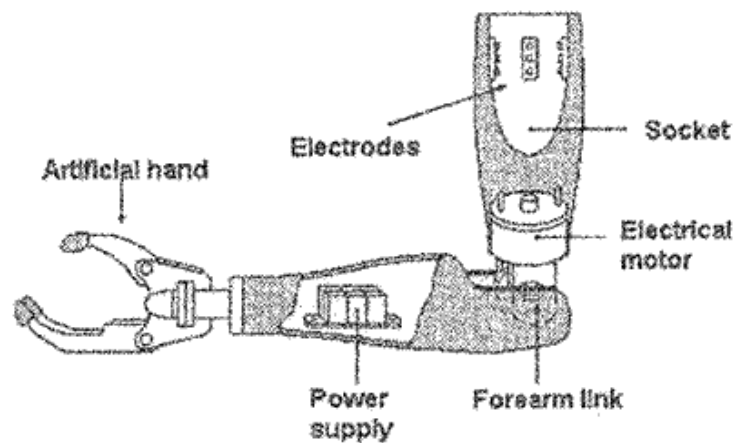


Figure 2 – Electric Powered Prosthetic Arm

Source – Bonivento et al. (1998)

2.3 Electromyography

“Electromyography is an experimental technique concerned with the development, recording and analysis of myoelectric signals. Myoelectric signals are formed by physiological variations in the state of muscle fiber membranes.” (BASMAJIAN; LUCA, 1985).

The EMG signal has physiological origin in motor neurons that innervate skeletal muscle fibers. Such neurons transmit nerve impulses, to arrive at the neuromuscular junction, release the neurotransmitter acetylcholine, which will cause the initiation of an action potential of the muscle on individual muscle fibers. This action potential propagates throughout the muscle membrane, causing muscle contraction (HALL, 2010).

The principle used to study the function of the muscles was established by an electrical engineer named Luigi Galvani. According to Galvani, a muscle contracts when it is electrically stimulated, and consequently, when contracted voluntarily, it generates electric current (KAMEN; GABRIEL, 2010). The sum of the electrical activity of the muscle fibers of the motor unit form the Motor Unit Action Potential (MUAP). Figure 3 illustrates how the MUAP can be captured by surface electrodes placed on muscles.

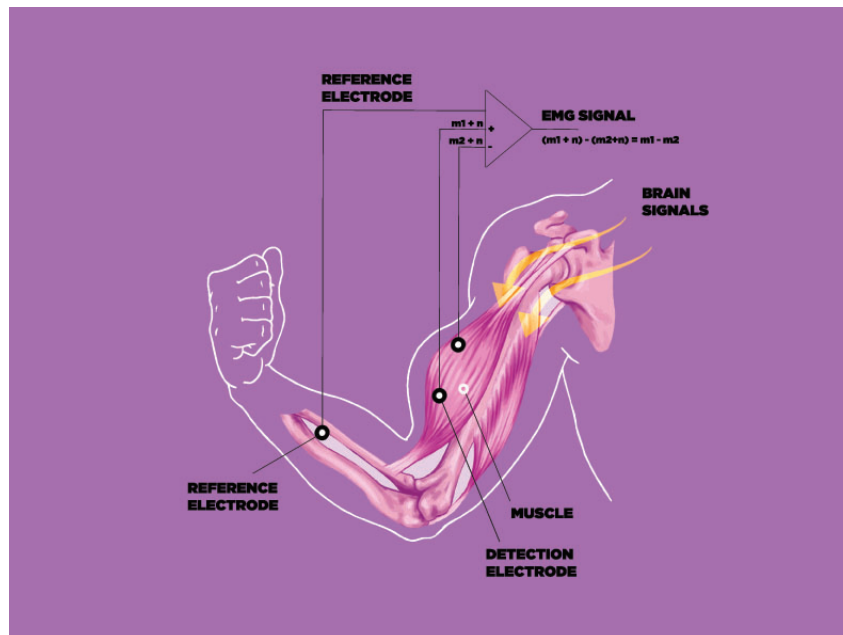


Figure 3 – A schematic of the differential amplifier configuration. The electrodes are positioned in a bipolar configuration, in which there is one positive electrode, one negative electrode and a ground electrode. In this configuration, the EMG signal is the differential measure of the two electrodes. The use of this differential measure is favorable to eliminate interference from other biological activities of the patient or even the power grid.

2.4 Microcontrollers

Microcontrollers are microprocessors that can be programmed for specific functions. In general, they are used to control circuits and are commonly found within other devices, being known as “embedded controllers”. The internal structure of a microcontroller has a processor and memory units and input and output peripherals. Figure 4 presents the basic functions of the microcontroller’s components according to Gerrish and Roberts (2004).

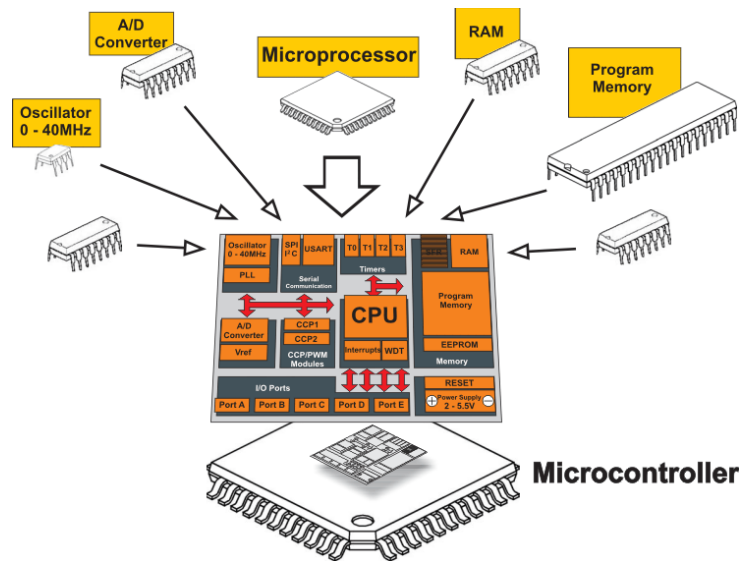


Figure 4 – General Microcontroller Architecture. The Central Processing Unit (CPU) is responsible for the microcontroller data processing. It is this which interprets the commands, reads data and activates the input and output (I/O) ports or the peripherals if necessary; The Memory Unit is part of the microcontroller used for data storage; The I/O interfaces of a microcontroller are responsible for input and output information.

Source – Verle (2016)

2.5 Inertial Navigation

The inertial sensors are grouped and controlled by an on-board electronic, thus creating an Inertial Measurement Unit (IMU). Figure 5 presents a typical IMU, which contains orthogonal triads of gyroscopes and accelerometers which provide measurements of angular velocities and linear accelerations, respectively. By processing these signals, it is possible to track the position and orientation of an object (STEWART; FERSHT, 1991; PANAHANDAH; SKOG; JANSSON, 2010; WOODMAN, 2007). IMUs are widely used in the control of hand-held devices, air-crafts, robots, autonomous vehicles, among others (ANG; Khosla ; RIVIERE, 2003; GRIGORIE; BOTEZ, 2014).

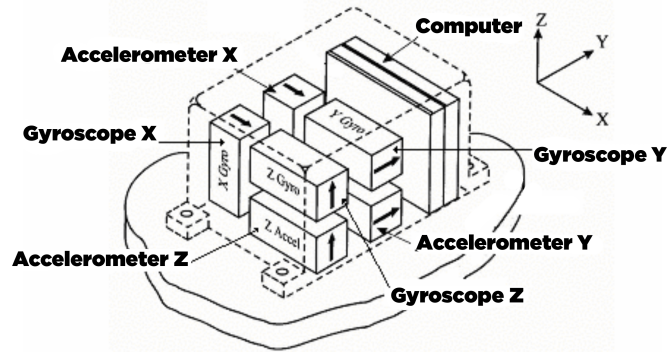


Figure 5 – Illustration of an IMU System

Source – Adapted from Verplaetse (1995)

2.6 Force Sensitivity Resistor (FSR)

In a force sensitivity resistor, its resistance will vary depending on the force applied to its sensitive area. The force is inversely proportional to the resistance. When no force is applied to it, its resistance increases causing an open circuit (ADAFRUIT LEARN, 2012). The FSR basically consists of two layers: a semiconductor element and an active element separated by a spacer. Stronger the FSR is pressed, more parts of the active area touch the semiconductor causing the resistance to drop (Figure 6).

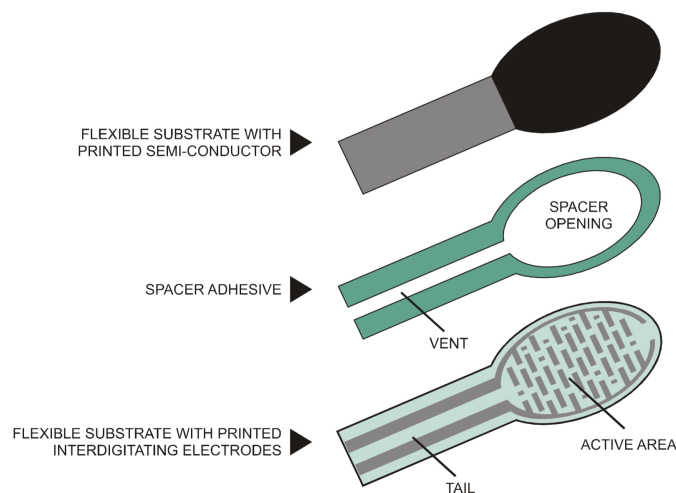


Figure 6 – FSR Construction

Source – Electronics (2015)

2.7 Flex Sensors

Flex sensors work similarly as FSRs. Its resistance will vary depending on the bending angle. The sensor has a conductive polymer ink with a certain resistance when the sensor is straight. Figure 7 shows that when the sensor is bent away from the ink, its resistance increases. When the sensor straightens out again, the resistance returns to its original value.

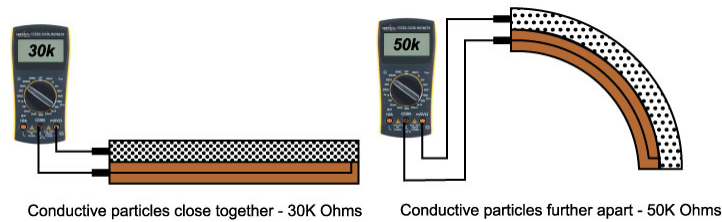


Figure 7 – How a flex sensor works. It is possible to determine the relative angle that the sensor is being bent by measuring its resistance.

Source – Grusin (2011)

2.8 Proximity Sensor

The proximity sensor is a sensor that can detect the distance from an object without physical contact. They are usually found in smartphones, soap dispensers and even robots (BENET et al., 2002; WININGS; SAMSON, 1997; HSIAO et al., 2009). The sensor consists of a transmitter and a receiver. Figure 8 illustrates the proximity sensor works. The transmitter emits infrared (IR) light at a given pulse. When an object enters the sensor's range, it will reflect the light back to the receiver, which measures the particles of light which were deflected by the object. From this measure it is possible to calculate the distance between the sensor and the object (ENGINEERSHANDBOOK.COM, 2006; CAMPBELL, 1984).

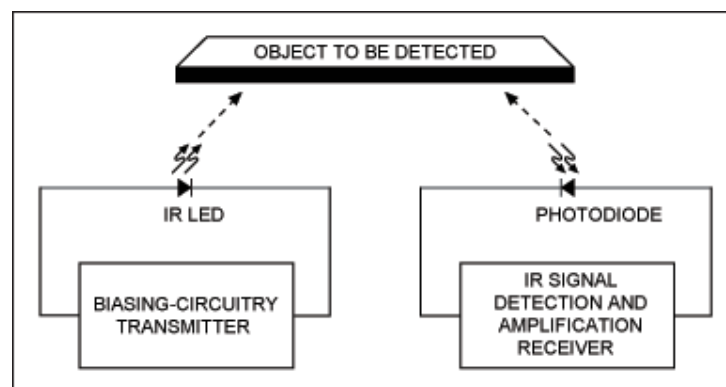


Figure 8 – Basic principle of an IR proximity sensor

Source – Mehta (2009)

2.9 EMG Feature Extraction

A wide variety of features are shown in Nazmi et al. (2016). The features can represent the amplitude of an EMG signal and its spectral content. Such features can be grouped into two categories:

1. time domain (TD);
2. frequency or spectral domain (FD);

2.9.1 Time Domain

Time domain features are often easily and quickly implemented because these features do not require any transformation. They are calculated by dividing the signal x into windows of length N . The k^{th} element of the i^{th} window corresponds to $x_i(k)$. Ten time domain features are shown in this study through an extensive and careful review of the literature.

2.9.1.1 Mean Absolute Value (MAV)

MAV is one of the most popular used in EMG signal analysis (HUDGINS; PARKER; SCOTT, 1993; PARK; LEE, 1998). The MAV feature is an average of absolute value of the EMG signal amplitude in a segment, which is defined in Equation 2.1.

$$MAV_i = \frac{1}{N} \sum_{k=1}^N |x_i(k)| \quad (2.1)$$

2.9.1.2 Variance (VAR)

VAR used by Park and Lee (1998), Tenore et al. (2009). It is defined as an average of square values of the deviation of that variable, which is defined in Equation 2.2.

$$VAR_i = \frac{1}{N} \sum_{k=1}^N (x_i(k) - \bar{x}_i)^2 \quad (2.2)$$

2.9.1.3 Mean Absolute Value Slope (MAVS)

MAVS is a modified version of the MAV feature (HUDGINS; PARKER; SCOTT, 1993; CHAN et al., 2000). It estimates the difference between mean absolute values of the adjacent segments $i + 1$ and i , which is defined in Equation 2.3.

$$MAVS_i = MAV_{i+1} - MAV_i \quad (2.3)$$

2.9.1.4 Root Mean Square (RMS)

RMS is a popular feature in EMG signal analysis (HUANG et al., 2005; SHENOY et al., 2008; PRAHM et al., 2017). It is modeled as amplitude modulated Gaussian random process which relates to constant force and non-fatiguing contraction.

$$RMS = \sqrt{\frac{1}{N} \sum_{i=1}^N x_i^2} \quad (2.4)$$

2.9.1.5 Willison amplitude (WAMP)

Willison or Wilson amplitude counts the number of times that the absolute value of the difference between the EMG signal amplitudes of two consecutive samples ($x_i(k)$ and $x_i(k+1)$) exceeds a predetermined threshold x_{th} (TENORE et al., 2009).

$$WAMP_i = \frac{1}{N} \sum_{k=1}^N f(|x_i(k) - x_i(k+1)|), \quad \text{with } f(x) = \begin{cases} 1, & \text{if } x > x_{th} \\ 0, & \text{otherwise} \end{cases} \quad (2.5)$$

2.9.1.6 Zero Crossing (ZC)

ZC is the number of times that the signal passes the zero amplitude axis (HUDGINS; PARKER; SCOTT, 1993). A threshold x_{th} must be included in the zero crossing calculation to reduce the noise.

$$ZC_i = \sum_{k=1}^N f(k), \quad \text{with } f(k) = \begin{cases} 1, & \text{if } x_i(k) \times x_i(k+1) < 0 \text{ and} \\ & |x_i(k) - x_i(k+1)| > x_{th} \\ 0, & \text{otherwise} \end{cases} \quad (2.6)$$

2.9.1.7 Slope Sign Changes (SSC)

Slope sign change (SSC) is another method to represent frequency information of the EMG signal. It is a number of times that slope of the EMG signal changes sign. The number of changes between the positive and negative slopes among three sequential segments is performed with the threshold function for avoiding background noise in the EMG signal.

$$SSC_i = \sum_{k=2}^{N-1} f((x_i(k) - x_i(k-1)) \times (x_i(k) - x_i(k+1))), \quad \text{with } f(x) = \begin{cases} 1, & \text{if } x > x_{th} \\ 0, & \text{otherwise} \end{cases} \quad (2.7)$$

2.9.1.8 Waveform Length (WL)

WL is the cumulative length of the waveform over time segment. It is related to the waveform amplitude, frequency and time (HUDGINS; PARKER; SCOTT, 1993; FARRY; WALKER; BARANIUK, 1996).

$$WL_i = \sum_{k=1}^{N-1} f(|x_i(k) - x_i(k+1)|) \quad (2.8)$$

2.9.1.9 EMG histogram (HIST)

According to Zardoshti-Kermani et al. (1995), HIST is a combination of the ZC and WAMP features. It divides the elements of the EMG signal into b equally spaced voltage bins and returns the number of elements in each bin.

2.9.1.10 Auto-regressive Coefficients

AR describes each sample of EMG signal as a linear combination of previous samples plus a white noise error term (ZARDOSHTI-KERMANI et al., 1995; PARK; LEE, 1998; HUANG et al., 2005; LIU; HUANG; WENG, 2007).

$$x_i(k) = \sum_{j=1}^N a_j x_i(k-j), \quad n^{th} \text{ order AR model} \quad (2.9)$$

2.9.2 Frequency Domain

The frequency domain features are based on the signal's estimated power spectral density (PSD) and are computed by parametric methods (OSKOEI; HU, 2006). However, these features compared to the TD features require more computational power to be calculated. Nine FD features are shown in this study through extensively and carefully review of the literature.

2.9.2.1 Power Spectrum (PS)

Power spectrum (PS) can be seen as an extension version of PKF and FR features (Qingju & Zhizeng, 2006). The PSR is defined as ratio between the energy P0 which is nearby the maximum value of the EMG power spectrum and the energy P which is the whole energy of the EMG power spectrum. Its calculation can be written by

2.9.2.2 Mean Frequency (FMN)

FMN is the average frequency (OSKOEI; HU, 2008). It is calculated as the sum of the product of the power spectrum and the frequency, divided by the total sum of

spectrogram intensity.

$$FMN_i = \frac{\sum_{j=1}^M (f_j P_j)}{\sum_{j=1}^M (P_j)} \quad (2.10)$$

2.9.2.3 Median Frequency (FMD)

FMD is the frequency at which the spectrum is divided into two regions with equal parts (OSKOEI; HU, 2006).

$$FMD_i = \frac{1}{2} \sum_{j=1}^M (P_j) \quad (2.11)$$

2.9.2.4 Frequency Ratio (FR)

FR was proposed by (HAN et al., 2000) in order to distinguish between contraction and relaxation of a muscle.

$$FR_i = \frac{\min(FFT(x_i))}{\max(FFT(x_i))} \quad (2.12)$$

2.9.2.5 Short-time Fourier Transform (STFT)

STFT is used to determine the sinusoidal frequency and phase content of local sections of a signal as it changes over time. It is done by dividing the input signal into segments. By doing this the signal in each window can be assumed to be stationary (ZECCA et al., 2002).

$$STFT[k, m] = \sum_{r=1}^{N-1} x[r]g[r - k]e^{-\frac{j2\pi mi}{N}} \quad (2.13)$$

where g , k , and m are the window function, the time sample, and the frequency bins, respectively.

2.9.2.6 Continuous Wavelet Transform (CWT)

CWT is a transform where a signal is integrated with a shifted and scaled mother wavelet function (ENGLEHART et al., 1999; ENGLEHART; HUDGIN; PARKER, 2001).

$$CWT_x(\tau, a) = \frac{1}{\sqrt{|a|}} \int x(t)\psi\left(\frac{t - \tau}{a}\right) dt \quad (2.14)$$

where $x(t)$ is the function representing the input signal, ψ is the complex conjugate of the mother wavelet function, and $\psi(\frac{t-\tau}{a})$ is the shifted and scaled version of the wavelet at time τ and scale a .

2.9.2.7 Discrete Wavelet Transform (DWT)

In a DWT is transform a signal is passed through a series of low-pass and high-pass filters, which are defined by the type of wavelet used, obtaining the approximation coefficients (cA), from the low-pass filter and the detail coefficients (cD), from the high-pass filter. This process can be repeated in further levels of decomposition, increasing the frequency resolution and the approximation coefficients (CHOWDHURY et al., 2013).

2.9.2.8 Wavelet Packet Transform (WPT)

WPT is a generalized version of the continuous wavelet transform and the discrete wavelet transform. The basis for the WPT is chosen using an entropy-based cost function. The main difference between STFT, WT and WPT is the way each one divides the time-frequency plane (ENGLEHART et al., 1999; ENGLEHART; HUDGIN; PARKER, 2001; WANG et al., 2006).

2.9.2.9 Marginal Discrete Wavelet Transform (mDWT)

Lucas et al. (2008) presented that for EMG classification it is acceptable to preserve only the marginals at each level of the DWT decomposition, removing the time-information from discrete wavelet transform, making it insensitive to wavelet time instants. The mDWT is defined as:

$$m_{x_k}(s) = \sum_{u=0}^{N/2^S-1} |d_{x_k}(s, u)|, s = 1, \dots, S \quad (2.15)$$

Where: x_k is the signal composed of k channels, S is the deepest level of the decomposition, N is the number of coefficients, and d_{x_k} is the set of coefficients ($N = \text{length}(d_{x_k})$).

3 Machine Learning

In the literature, there is an overlapping of the terms Machine Learning (ML), Pattern Recognition (PR), and Data Mining (DM). These terms are often used to refer to the area of artificial intelligence. According to Witten et al. (2016), ML uses computers to simulate human learning and study self-improvement methods, in order to discover new knowledge, identify existing knowledge, and continuously improve performance.

The majority of the recent advancements in AI have been due to the use of supervised algorithms, such as support vector machines and artificial neural networks, applied to several types of datasets. In these algorithms, given a set of inputs and outputs/labels, if given enough examples, they can learn the mapping that relates them. We can then use this mapping to predict new labels, given a set of inputs.

Although, often labels are not available. One solution is to manually label the data in order to produce a set of training data. Another solution is to train the algorithms on unlabeled data, since the vast majority of data in the world has no labels, so if we want to train unsupervised algorithms, i.e. without labels, we can use techniques like clustering and anomaly detection.

Unsupervised algorithms are improving rapidly but there is also room for another class of learning techniques based on trial and error in a dynamic environment. This is called reinforcement learning (RL).

Basically, the idea of reinforcement learning is to learn an optimal strategy through sampling actions, and then looking at which strategy leads to the desired outcome. Unlike the supervised approach, this ideal action is learned not from a label, but from a reward. The goal of RL is to take actions that maximize this reward. While supervised learning tells us how to reach the goal, RL tells you how well we achieved the goal.

3.1 Supervised Learning

Supervised learning is the ML task of inferring a function from labeled training data which is:

Given a training set of i instances (X_i, Y_i) , where $X_i = [x_1, x_2, \dots, x_n]$ is the input feature vector with length n and Y_i is the output class which is an element of a list with size j of classes $y = \{y_1, y_2, \dots, y_j\}$. The main goal is to learn a function which estimates Y given X :

$$\hat{Y} = f(\vec{X}), \text{ where } \hat{Y} \in y$$

The training set exemplified in Table 2 is part of a dataset called Iris (DHEERU; TANISKIDOU, 2017). Its features vectors are the sepal length, sepal width, petal length, petal width and the type of the iris flower (Iris-setosa, Iris-versicolor, Iris-virginica).

Table 2 – Example of a training set

| Sepal Length | Sepal Width | Petal Length | Petal Width | Class |
|--------------|-------------|--------------|-------------|-----------------|
| 5.1 | 3.8 | 1.6 | 0.2 | Iris-setosa |
| 4.6 | 3.2 | 1.4 | 0.2 | Iris-setosa |
| 5.3 | 3.7 | 1.5 | 0.2 | Iris-setosa |
| 5.0 | 3.3 | 1.4 | 0.2 | Iris-setosa |
| 7.0 | 3.2 | 4.7 | 1.4 | Iris-versicolor |
| 6.4 | 3.2 | 4.5 | 1.5 | Iris-versicolor |
| 6.9 | 3.1 | 4.9 | 1.5 | Iris-versicolor |
| 5.5 | 2.3 | 4.0 | 1.3 | Iris-versicolor |

Source – Adapted from Dheeru and Taniskidou (2017)

When the output y is one of a finite set of values such as “Yes” or “No”, the learning problem is called classification. When y is a number such as the grade of a student, the learning problem is called regression.

3.1.1 Support Vector Machines

Proposed by Cortes and Vapnik (1995), Support Vector Machine (SVM) is a supervised machine learning algorithm which is usually used for classification. Given two or more labeled classes of data, the SVM tries to find an optimal hyperplane in order to maximize the margin between the support vectors. Support vectors are the data points that lie closest to the hyperplane. So, when new examples are mapped into the same space, they can be categorized based on which side of the hyperplane they are (CRISTIANINI; SHAWE-TAYLOR et al., 2000).

Given a set of training data points $D = (\vec{X}_i, Y_i)$, where each member is a pair of a point \vec{X}_i and a class label $Y_i = \{-1, +1\}$ corresponding to it. Considering that D is linear separable, we can find the hyperplane that separates the classes “-1” and “+1” (SCHÖLKOPF; SMOLA et al., 2002). The linear classifier (hyperplane) can be described by Equation 3.1:

$$f(\vec{X}) = \vec{w}^T \vec{X} + b \quad (3.1)$$

where \vec{w} is a weight vector perpendicular to the hyperplane, and b is a term to choose among all the hyperplanes that are perpendicular to the normal vector.

Since the data in our example is linear separable, we can select two parallel hyperplanes that separate the two classes of data, so that the distance between them is as

large as possible. The region bounded by these two hyperplanes is called “margin”. The maximum-margin hyperplane is the hyperplane that lies halfway between them. These hyperplanes can be described by Equations 3.2 and 3.3:

$$\vec{w}^T \vec{X} + b = +1 \quad (3.2)$$

$$\vec{w}^T \vec{X} + b = -1 \quad (3.3)$$

3.1.2 Decision Trees

Decision tree is a type of supervised learning algorithm that is most commonly used in classification problems. It works for both categorical and continuous variables. In this technique, we divide the samples into two or more sets based on the most significant divisors on the input variables.

Decision trees models are represented as binary trees. Each root node represents a single input variable (\vec{X}_i) and a split point on that variable. The leaf nodes contain the output variable (Y_i) which is used for prediction.

For instance, considering the example from Table 2, Figure 9, a fictitious decision tree can be represented as a set of rules:

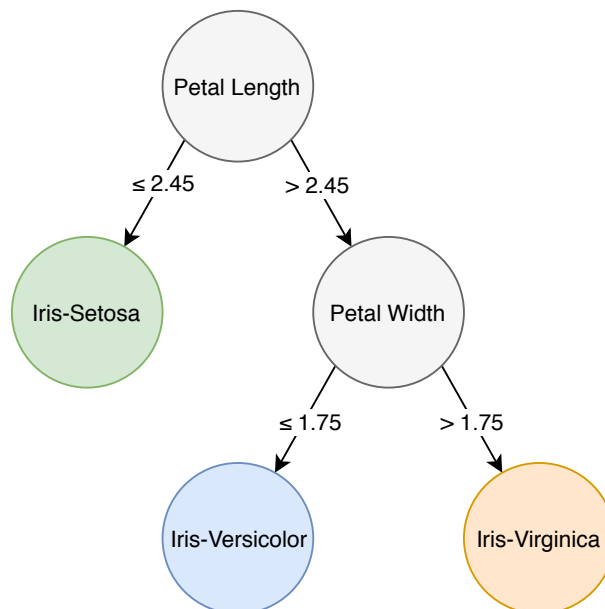


Figure 9 – Fictitious decision tree for Iris dataset

- IF *Petal Length* ≤ 2.45 THEN *Iris – setosa*
- IF *Petal Length* > 2.45 AND *Petal Width* ≤ 1.75 THEN *Iris – versicolor*

- IF *Petal Length* > 2.45 AND *Petal Width* > 1.75 THEN *Iris – virginica*

With the binary tree representation of the decision tree model, it is relatively straightforward to make predictions. For example, given a new input:

$$X_{kPetal\ Length} = 3.00$$

$$X_{kPetal\ Width} = 1.00$$

$$X_{kSepal\ Length} = 6.53$$

$$X_{kSepal\ Width} = 1.24$$

the tree is traversed starting from the root node to the leaves evaluating the input:

- *Petal Length* ≤ 2.45 (FALSE)
- *Petal Length* > 2.45 (TRUE) AND *Petal Width* ≤ 1.75 (TRUE)

THEN: *Iris – versicolor*

Creating a binary decision tree is a numeric procedure where values are aligned, and different split points are tested using a cost function. The division with the best cost is selected. All input variables and all split points are evaluated and selected in a greedy approach.

For classification, a Gini index function, or Gini impurity, is used, which provides an indication of "purity" of the leaf nodes. The Gini index can be computed by Equation 3.4:

$$G = \sum (p_k * (1 - p_k)) \quad (3.4)$$

where, p_k is the probability of an item with label k being chosen. In a multi-label classification with J classes, the Gini index can be calculated as Equation 3.5:

$$I_G(p) = \sum_{i=1}^J p_i \sum_{k \neq i} p_k = \sum_{i=1}^J p_i (1 - p_i) = \sum_{i=1}^J (p_i - p_i^2) = \sum_{i=1}^J p_i - \sum_{i=1}^J p_i^2 = 1 - \sum_{i=1}^J p_i^2 \quad (3.5)$$

In order to stop splitting, a common procedure is to use a minimum count on the number of training instances assigned to each node. If the count is less than the minimum, the division will not be accepted, and the node will be considered as a final leaf node.

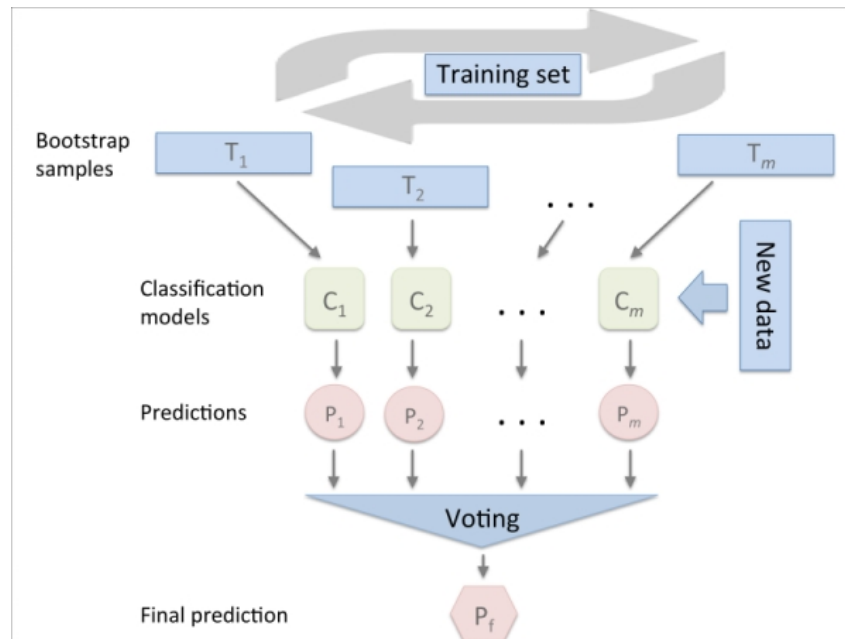


Figure 10 – Steps for Bagging

Source – Raschka, Julian and Hearty (2016)

3.1.2.1 Bagging

Bagging is a technique used to reduce the variance of our predictions by combining the results of several classifiers modeled on different sub-samples of the same dataset. The steps for bagging are (Figure 10):

1. Create multiple datasets: sampling is performed with replacement and new data sets are created; The new data sets may have part of the columns as well as the lines, which are generally hyper parameters in a bagging model;
2. Creation of multiple classifiers: a classifiers is built for each dataset; Generally, the same type of classifier is modeled for each set of data.
3. Aggregate Classifiers: the predictions of all classifiers are aggregated using the average or median from the classifiers or by voting; The combined values are generally more robust than a single model.

There are several implementations that use Bagging. The random forests are one of them and we'll discuss it next.

3.1.2.2 Random Forests

Random Forest is a versatile machine learning method capable of performing regression and classification tasks. It is a kind of ensemble learning method, where a group of weak models combine to form a powerful model.

In the random forest, we created several decision trees. To classify a new object,

each tree predicts a class and then the algorithm counts the “votes” from all the trees for a class. The class with the highest votes is the one chosen as the predicted class. In case of regression, the random forest usually outputs the average output of all trees.

The random forest algorithm works as follows:

Assume that the number of cases in the training set is N . Then, the algorithm takes a sample of these N cases randomly with replacements. This sample will be the training set for a decision tree. A subset of M features is selected randomly and any feature that provides the best division is used to iteratively divide the node. The steps are repeated, and the prediction is based on the number of votes of the N trees.

3.1.3 Convolutional Neural Networks

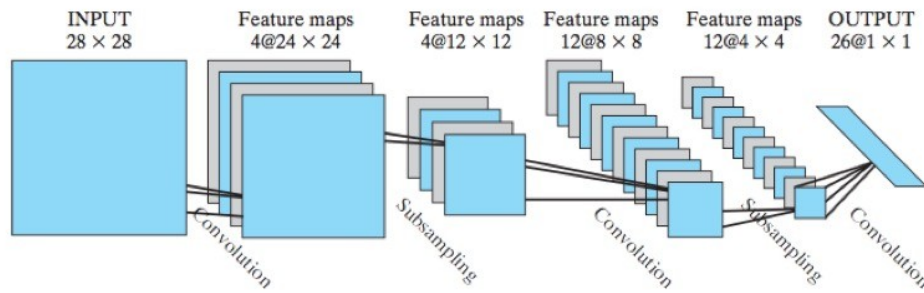
Convolutional Neural Networks (CNN), were proposed by (LECUN et al., 1989). They are a type of artificial neural networks, most commonly applied to computer vision. Haykin et al. (2009) divides the structure of convolutional networks into three main objectives:

Feature extraction: each neuron receives input signals from the previous layer, allowing the extraction of local characteristics. This extraction of local features makes the exact position of each feature irrelevant as long as its position in relation to neighboring features is maintained.

Feature mapping: each layer of the network is composed of several feature maps, which are regions where neurons share the same synaptic weights. These weights are called filters or kernels, and give the model robustness, making it capable of dealing with distortion, rotation and translation in the image. Sharing the weights also enables a drastic reduction in the number of parameters to be optimized.

Subsampling: after each convolution layer a subsampling layer is applied, which is nothing more than a sample collection of each characteristic map. These samplings can be performed by obtaining the sum, taking the mean, selecting the largest (max pooling) or smallest (min pooling) value of the region under analysis. This produces a summary of the features map.

Figure 11 presents an overview of a convolutional neural network applied in an image of 28×28 pixels, using four filters of size 24×24 in the first layer, and then performing a sub-sampling. The process is followed by the application of new filters and sub-samples.

Figure 11 – Overview of a CNN applied in an image of 28×28 pixels

Source – Haykin et al. (2009)

3.1.4 Neural Architecture Search

Neural networks recently gained popularity in broad applications. However, in order to obtain good results, it is necessary to choose a good architecture, which is a difficult manual and empirical task.

Zoph and Le (2016) proposes a Neural Architecture Search (NAS) algorithm, a gradient-based method for finding excellent neural network architectures.

Figure 12 presents an overview of the NAS. At first, the parent network proposes a child model architecture randomly. The child model is then trained and evaluated for a given dataset. Its classification accuracy is used as feedback to inform the parent how to improve its next generation of child architecture, i.e. compute the policy gradient to update the controller. This process is repeated over time, every time generating new architectures, testing them and giving the feedback to the controller to learn from it. Eventually, the controller will give higher probabilities to architectures that achieve best accuracies for a given dataset.

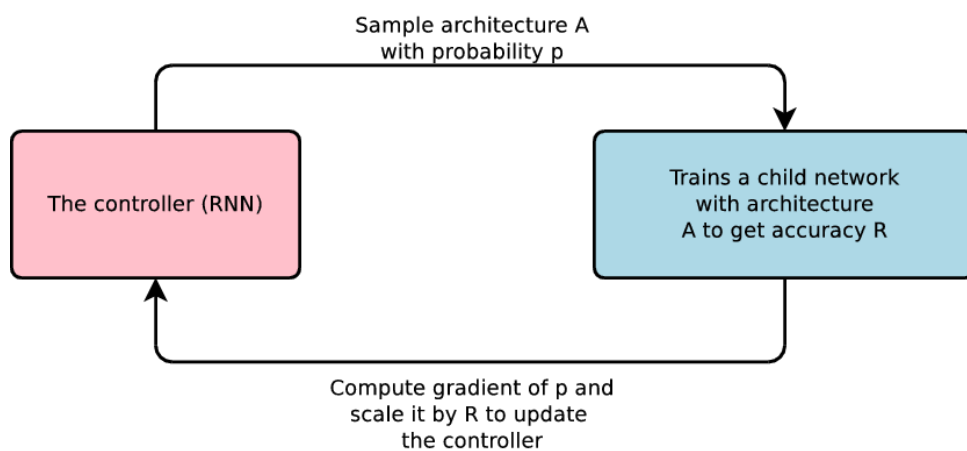


Figure 12 – NAS parent-child network architecture

Source – Zoph and Le (2016)

3.2 Imbalance Classification

Imbalance applies to a large difference in the number of examples between classes. For example, in detection of fraud in telephone calls (FAWCETT; PROVOST, 1997) or in credit card fraudulent transactions (STOLFO et al., 1997), the number of legitimate transactions is much higher than that of fraudulent transactions.

Sampling methods aim to change the distribution of training data in order to increase the accuracy of their models. This is achieved by eliminating cases of the majority class (undersampling) or creating new cases for the minority class (oversampling).

Weiss (2004) divides the sampling methods into: basic sampling methods and advanced sampling methods.

The basic sampling methods are methods that do not use heuristic in the elimination and the replication of cases, that is, they are methods that aim to balance the distribution of classes in a random manner. Basic sampling methods are the random undersampling and the random oversampling.

On the other hand, the advanced sampling methods use heuristics in elimination of cases of the majority class and in the replication of cases of the minority class. Examples of advanced sampling methods are: One-sided Selection, Synthetic Minority Over-Sampling Technique, Cluster-based Oversampling.

3.2.1 Synthetic Minority Oversampling Technique

The simple oversampling techniques are widely criticized by the scientific community, as many of them only replicate existing positive cases. Merely replicating existing cases of the minority class actually increases the classifier's bias for this class, leading the model to overfit, i.e. models are very specific for these replicated cases, therefore, hurting the model's ability to generalize for the class of interest.

Faced with this problem, Chawla et al. (2002) developed a different method to oversample the minority class, which consists in the generation of synthetic cases for the class of interest from the existing cases. These new cases will be generated in the neighborhood of each case of the minority class, in order to grow the decision region and thus increase the model's generalization ability of the classifiers generated for this data. These authors call this new method Synthetic Minority Oversampling Technique (SMOTE)

Figure 13 presents in the R^2 space, the new synthetic cases, that are randomly interpolated along a "line" linking each case of the minority class to one of its nearest randomly selected k neighbors.

Another variation of SMOTE is called SMOTE-SVM, where instead of creating

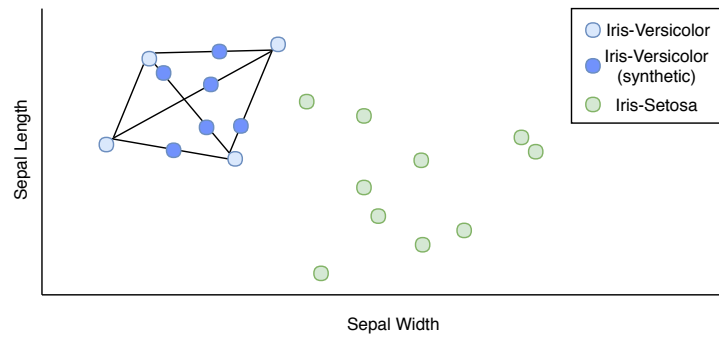


Figure 13 – Example of SMOTE applied to the Iris dataset

the synthetic instances along a “line”, an SVM classifier is used to find the hyperplane that best separates the classes and new minority class instances are created near the hyperplanes. It helps to establish boundary between classes.

4 Pattern Recognition-based Myoelectric Control

In the United States, there are nearly 2 million people living with limb loss. Trauma and vascular diseases are the most common causes of amputations (ZIEGLER-GRAHAM et al., 2008). The use of prostheses represents a technological aid for upper limb amputation and deficiency. There are two dominant prosthetic choices for persons with upper limb amputation: Body Powered (BP) and Myoelectric (MYO) systems. The BP prostheses are fed by the energy of the amputee's body. The movements are actuated through cable and/or harness systems to a terminal device such as hand or hook. Although BP prostheses have been shown to have advantages in durability, training time, maintenance, and feedback, they suffer from the need for energy expenditure with the risk of early fatigue, and less cosmetic aspect than a MYO prosthesis.

Surveys like (CAREY; LURA; HIGHSMITH, 2015; BIDDISS; CHAU, 2007; ATKINS; HEARD; DONOVAN, 1996) shows that 26%–50% of the amputees reject the prosthesis due to its low functionality, poor cosmetic appearance, and low controllability. This situation demands the development of versatile prostheses with intuitive control that will allow amputees to perform tasks for activities of daily living (ADLs). Such control can be developed by extracting information from neuromuscular activities of the amputee in a non-invasive way. Electromyography (EMG) has been used for the prostheses control since 1951 (BERGER; HUPPERT, 1952). It has proven to be an easy and non-invasive method for recording the physiological processes that cause muscle contractions.

At present, pattern recognition in EMG signals plays a key role in the advanced control of motorized prostheses for individuals with upper limbs amputations. It is the most common approach used for controlling active prosthetic hands. Pattern recognition-based myoelectric control usually consists of 5-steps: data collection, data segmentation, feature extraction, classification, and controlling system. Since the beginning until today many researchers use Artificial Neural Network (ANN) to control MYO prostheses (KELLY; PARKER; SCOTT, 1990; HUDGINS; PARKER; SCOTT, 1993; BOCA; PARK, 1994; ENGLEHART et al., 1999; ROSLAN et al., 2016; FAN et al., 2017). However various classifiers such as Linear Discriminant Analysis (LDA) (ENGLEHART; HUDGIN; PARKER, 2001; GUO et al., 2017; ENGLEHART; HUDGINS, 2003; KYRANOU et al., 2016; ENGLEHART et al., 1999), Fuzzy (AJIBOYE; WEIR, 2005; CHAN et al., 2000; PARK; LEE, 1998), Gaussian Mixture Models (GMMs) (HUANG et al., 2005; CHU; LEE, 2009), Hidden Markov Models (HMMs) (CHAN; ENGLEHART, 2005; KHEZRI; JAHED; SADATI, 2007), Support Vector Machines (SVM) (LUCAS et al., 2008; GEETHANJALI;

RAY, 2015; AMSUESS et al., 2016) and many others are used for this task (CHU; LEE, 2009; GEETHANJALI; RAY, 2015; GEETHANJALI, 2015; LEE et al., 1996; PARK; LEE, 1998; AL-TIMEMY et al., 2016).

Saridis and Gootee (1982) were one of the pioneers of applying statistical analysis and pattern recognition in EMG signals. The authors analyzed six different arm movements (Elbow Extension (EE), Elbow Flexion (EF), Humerus Medial Rotation (HMR), Humerus Lateral Rotation (HLR), Wrist Pronation (WP), Wrist Supination (WS)) recorded from EMG electrodes placed on the biceps and triceps of a transhumeral amputee. Their analysis showed good class separability for the six movements. Kelly, Parker and Scott (1990) implemented a multi-function control scheme based on the classification of EMG signals using an ANN. A discrete Hopfield network was used to extract features from four different arm movements (EE, EF, WP, WS) from the biceps and triceps of a transhumeral amputee. The author created a classification model using a two-layer perceptron network which was capable of classifying all the sets of features correctly. Creating new ways of EMG signal analysis. Hudgins, Parker and Scott (1993) recognized four different movements (EE, EF, HMR, HLR) using a 2-channel EMG for data acquisition and a multilayer perceptron (MLP) for classification achieving an accuracy of 88.35%. Boca and Park (1994) proposed a real-time application with an ANN that can recognize three intensities of biceps contraction. EMG features were first extracted through Fourier analysis and clustered using fuzzy c-means algorithm. The features were fed into the ANN having an accuracy of 86.20%. Kwon et al. (1996) built an EMG signal hybrid classifier using a MLP and hidden Markov models (HMM) to classify six arm movements (WP, WS, Wrist Flexion (WF), Wrist Extension (WE), Hand Open (HO), Hand Close (HC)) using four electrodes placed on the biceps and triceps. Achieving an accuracy of 91.16%, the author proved that their method was more accurate than using only a MLP (75%). Lee et al. (1996) proposed a pattern recognition method to identify motion command for the control of a prosthetic arm by using evidence accumulation (EA) with multiple parameters. The author used four electrodes on the biceps and triceps to classify six different movements (EE, EF, HMR, HLR, WP, WS), achieving an accuracy of 46.77%. Kwon et al. (1998) created a several EMG signal hybrid classifiers using MLP, genetic algorithm (GA), counter propagation network (CPN) and HMMs. Six arm movements (WP, WS, WF, WE, HO, HC) were recorded using four electrodes placed on the biceps and triceps. Four hybrid algorithms such as HMM-MLP, HMM-GA-MLP, HMM-CPN, and HMM-GA-CPN were created, having accuracies of 76.9%, 87.7%, 55.6%, 85.6%, respectively. Park and Lee (1998) proposes a method similar to (LEE et al., 1996). Using two electrodes on the biceps and triceps to classify six different movements (EE, EF, HMR, HLR, WP, WS), the proposed method classified 65% of the movements correctly.

Englehart et al. (1999) compared the performance of two classifiers (MLP and LDA) trying to improve the accuracy of transient EMG signal pattern classification.

The approach using MLP and LDA with wavelet packet transform (WPT) and principal components analysis (PCA) outperformed many authors from the literature, achieving an accuracy of 92.75% and 93.75%, respectively. Chan et al. (2000) was one of the first authors that proposed a fuzzy approach for classification of EMG patterns using four electrodes on the biceps and triceps to capture four arm movements (EE, EF, WP, WS). The accuracy of the fuzzy approach was compared with an ANN, being 89.7% and 87.55%, respectively. The authors conclude that the fuzzy has slightly higher recognition rate, it is not sensitive to overtraining, and it has consistent outputs demonstrating higher reliability. Micera, Sabatini and Dario (2000) evaluated comparatively neural and fuzzy networks with a limited amount of data available for learning. The authors used two electrodes on the anterior deltoid (shoulder) to capture three different planar arm pointing movements to reach and grasp (Key Grasp (KG)) an object lying on a table. Four classifiers were used such as self-organizing maps (SOM), fuzzy c-means (FCM), MLP, and The Abe–Lan fuzzy network (Abe-Lan). It is shown that the Abe–Lan classifier had a higher classification accuracy of 93.33%, followed by the MLP (85.75%), FCM (53.30%), and SOM (49.97%). Tsuji et al. (2000) proposed a new ANN approach for the task of EMG classification. The proposed network is combined to form two different neural networks: one is a common back-propagation neural network, and the other a recurrent neural filter. They used four electrodes on the subject’s forearm to classify six movements (WP, WS, WF, WE, HO, Tool Grip (TG)). The network could classify the six movements with an accuracy of about 90%.

Englehart, Hudgin and Parker (2001) used a wavelet-based feature set, PCA to reduce the feature vector dimension and a LDA classifier. The author tested the proposed method in with two sets of data, one performing four movements (WF, WE, HO, HC) and another one six (Wrist Ulnar Deviation (WUD), Wrist Radial Deviation (WRD), WF, WE, HO, HC), recorded from four electrodes placed on the forearm. The proposed system had a high accuracy for both datasets, being 99.5% for the four-class dataset and 98% for the six-class dataset. Zhang et al. (2002) implemented a hybrid classifier using a ANN and Fuzzy called neuro-fuzzy classifier (NFC). The author compared the NFC with an ANN to classify six different movements (EE, EF, WP, WS, HO, HC). The NFC outperformed the ANN, achieving an accuracy of 95% against 90.66% for the ANN. Englehart and Hudgins (2003) presents a continuous classification approach not requiring segmentation of the EMG signal, allowing a continuous stream of class decisions to be delivered to the prosthetic device. The author placed four electrodes on the subject’s forearm to classify four different wrist movements (WUD, WRD, WF, WE), achieving an accuracy of 95%. Ajiboye and Weir (2005) presents a heuristic fuzzy logic approach for EMG signal classification. Using four electrodes placed on the forearm they try to classify four movements (WUD, WF, WE, Finger Flexion (FF)). The authors state that other algorithms in the literature have a long delay, while the presented system has a faster classification

time and good accuracy (97%), making it suitable for real-time applications. Chan and Englehart (2005) used HMM to process four EMG signals from the forearm with task of classifying six movements (WP, WS, WF, WE, HO, HC). A comparison between the proposed HMM method and a MLP was made. The HMM with an accuracy of 94.63% had a statistical significant difference compared to the MLP's accuracy 93.27%. The proposed method is fast because it delivers a continuous stream of classes to the prosthesis and its computational complexity is low, making it suitable for real-time applications. Huang et al. (2005) proposes the use of Gaussian mixture models (GMMs) for EMG signal classification. They used four electrodes on the subject's forearm to classify six movements (WP, WS, WF, WE, HO, HC). The performance of the GMM is compared to three commonly used classifiers: a LDA, a linear perceptron network (LP), and a MLP. The proposed method demonstrates an exceptional classification accuracy of 96.28% against 95.58% of LDA, 95.27% of LP, and 95.38% of MLP. It is a robust method of motion classification with low computational load.

Chu, Moon and Mun (2006) used PCA for dimensionality reduction and self-organizing feature map (SOFM) to make a nonlinear mapping of the features. They fed those new features in a MLP for the classification of eight different movements (WP, WS, WUD, WRD, WF, WE, HO, HC). The proposed method improves class separability and recognition accuracy (97.02%) if compared with the PCA (95.76%). Even though the SOFM had a higher accuracy (97.78%) compared to the PCA+SOFM, its processing time is 36 times higher than the PCA+SOFM approach, making the SOFM not suitable for real time applications. Nagata et al. (2006) proposed the recognition of EMG signals using canonical discriminant analysis (CDA). The author used 96 electrodes placed on the forearm to classify 12 movements of the hand including four finger movements (WP, WS, WUD, WRD, WF, WE, 1234-FF, HO, HC). The proposed system achieved a recognition rate of 85.3%. Tsenov et al. (2006) presents a comparison of three ANNs such as MLP, Radial Basis Function (RBF), and Learning Vector Quantization (LVQ). Tsenov placed two electrodes on the subject's forearm to capture four movements (123-FF, HC). The MLP had an accuracy of 92%, the RBF 84% and the LVQ 89%. Wang et al. (2006) proposed a combination of an auto-regressive (AR) model and ANN to classify EMG signals. The AR model processed the EMG signal and this signal was fed to the ANN. Four pairs of electrodes were attached on the subject's forearm to acquire the signals during six types of finger motions (1st, 2nd and 3rd-Finger Extension (123-FE), 123-FF). They achieved an accuracy of 77%.

Chu et al. (2007) proposed a combination of WPT, LDA and MLP to classify EMG signals. A wavelet packet transform (WPT) is performed to extract a feature vector from four electrodes placed on the forearm. A LDA is used to reduce the feature vector's dimensionality. The reduced feature vector is then fed into an MLP. Eight movements (WP, WS, WUD, WRD, WF, WE) were performed by the subjects. The author

compared the LDA with the PCA approach proposed in the literature. The LDA had an accuracy of 97.4% against the PCA 95.9%. Hargrove, Englehart and Hudgins (2007) compares the three different pre-processing algorithms (AR, Time Domain (TD), TD and sixth-order AR (TDAR)) with two classification algorithms (LDA and MLP). The author used 16 electrodes placed on the forearm to record nine movements (WP, WS, WUD, WRD, WF, WE, HO, KG, Chuck Grip (ChG)). The accuracies achieved for the AR+LDA, AR+MLP, TD+LDA, TD+MLP, TDAR+LDA, and TD+MLP are 97%, 96%, 98%, 97%, 98.5%, 96.5%, respectively. Jung et al. (2007) proposed a method for pattern recognition of EMG signals of hand gesture using spectral estimation and LVQ. Four electrodes were placed on the forearm to record six Korean language hand gestures. Jung achieved 78% accuracy. Khezri, Jahed and Sadati (2007) proposed an adaptive neuro-fuzzy inference system (ANFIS) for EMG signal classification. They used a hybrid method for training a fuzzy system, consisting of back-propagation (BP) and least mean square (LMS). Four electrodes were used to read six movements (WF, WE, FE, FF, HO, HC, Fine Pinch (FP)). The proposed system achieved an accuracy of 96%. Liu, Huang and Weng (2007) proposed a novel EMG classifier called cascaded kernel learning machine (CKLM). It consists of a generalized discriminant analysis (GDA) algorithm, that reduces the dimensionality of the feature vectors, and a SVM algorithm used for the classification. This method achieved an average accuracy of 94.1% on the task of classifying eight movements (WF, HO, ChG, Power Grip (PG), Hook Grip (HG), Lateral Pinch (LaP), Centralized Grasp (CeG), Cylindrical Grasp (CyG)) captured by three electrodes placed on the forearm. Tenore et al. (2007) used time-domain feature extraction methods as inputs to a neural network classifier. The EMG data was collected from 32 electrodes placed on an individual's forearm performing 10 individual finger (12345-FF and 12345-FE) movements and 2 movements of grouped fingers ((345)-FF and (345)-FE). An accuracy of 98% was achieved.

Lucas et al. (2008) proposed a method using Discrete Wavelet Transform (DWT) and SVM to classify EMG signals. Eight electrodes were placed on the forearm to record six movements (WP, WS, WF, WE, HO, HC). The classification method had a classification accuracy of 95.3%. Oskoei and Hu (2008) compares a SVM approach with LDA and MLP for the task of EMG classification. Oskoei placed four electrodes on the forearm to acquire five movements (Finger Abduction (Fab), Finger Adduction (Fad), FE, FF, HO). The SVM accuracy (95.75%) outperformed the LDA (95.5%) and MLP (95%) classifiers. Shenoy et al. (2008) proposed a SVM classification system for EMG signal classification. The author used seven electrodes placed on the forearm to record eight movements (WP, WS, WUD, WRD, WF, WE, HO, PG). The classifier had a 95% accuracy. Sueaseenak et al. (2008) compared an ANN with an independent component analysis (ICA) for the task of EMG classification. Sixteen electrodes were placed on the forearm and captured eight movements (WP, WS, WUD, WRD, WF, WE, HO, HC). The ANN (95.8%) outperformed

the ICA in 2.5% and had a faster training time.

Chu and Lee (2009) presents a new learning method using Conjugate-Prior-Penalized Learning for GMM in order to improve their generalization ability. Chu used four electrodes on the forearm to record nine movements (WP, WS, WUD, WRD, WF, WE, HO, CyG, LG). The author compared the proposed approach, having an accuracy of 95.7%, with Bayesian methods to GMMs, having an accuracy of 93.57%. Tenore et al. (2009) proposed a ANN system that classify individual flexion and extension movements of each finger (12345-FF, 12345-FE) using only EMG signals. The authors compared the system's accuracy with the number of electrodes placed on the individual's forearm. For 19 electrodes, the systems had an accuracy of 91.27%. Using 32 electrodes, the system classified 94.28% of the movements of each finger correctly. Li, Schultz and Kuiken (2010) used a LDA classifier to discriminate 10 movements (WP, WS, WF, WE, HO, KG, ChG, PG, FP, TG) recorded from 12 electrodes placed on the forearm. Li compared the classification accuracy between amputees and healthy subjects. Amputated arms produced significantly lower classification accuracies (79%) than testing on intact arms (94%).

Geethanjali and Ray (2015) developed of a low-cost research platform for EMG prosthetic hand control to evaluate pattern recognition techniques. The author compared seven different algorithms such as simple logistic regression (SLR), C4.5 algorithm (C4.5), logistic model tree (LMT), ANN, LDA, and SVM for the task of EMG classification. Four electrodes were place on the subject's forearm to record six movements (WS, WUD, WRD, WF, WE, HO, HC) which resulted in an accuracy of 87.5% (LDA), 84.5% (ANN), 84.33% (LMT), 84.16% (SLR), 84% (SVM), and 79.5% (C4.5). Geethanjali (2015) Compared five algorithms (SLR, C4.5, LMT, k-Nearest Neighbor classifier (kNN), and ANN) using PCA to classify six hand movements (WUD, WRD, WF, WE, HO, HC) using four EMG electrodes. The author achieved an accuracy of 91% (SLR), 91% (LMT), 90.5% (ANN), 89% (kNN), and 82% (C4.5).

AbdelMaseeh, Chen and Stashuk (2016) proposed an EMG Classification model based on multidimensional dynamic time warping (MD-DTW). The author used the second version of the publicly available database from the Non-Invasive Adaptive Prosthetics (NINAPro) project (ATZORI et al., 2014). The NINAPro database consists of surface EMG signals, kinematic, and force measurement signals acquired from 40 different subjects performing 40 movements. The proposed system was able to classify 89% of the 40 different movements. Adewuyi, Hargrove and Kuiken (2016) demonstrated that using intrinsic and extrinsic hand muscles EMG data it is possible to classify up to 19 different hand grasps and finger motions (1-Fab, 1-Fad, 12345-FE, 12345-FF, HO, KG, ChG, PG, FP, TG). The author placed nine electrodes on the forearm of all subjects, twelve electrodes on health subjects hand, and four electrodes on amputee's hand. An accuracy of 96% for non-amputees and 85% for partial-hand amputees was achieved using a LDA clas-

sifier. Al-Timemy et al. (2016) proposed a novel set of features that reduces the impact of force level variations on prosthesis controlled by amputees. Sixteen electrodes were placed on the subject's forearm to record six movements (12-FF, ChG, PG, FP, HG). In order to evaluate their work, four different classifiers were utilized in the experiments: LDA, Naive Bayes (NB), Random Forest (RF), and kNN with $k=3$. Accuracies of 92.5% for kNN, 92% for LDA, 91.5% for NB and 91% for RF were achieved. Duan et al. (2016) proposed a novel algorithm to recognize six kinds of hand motion commands (WP, WS, WF, WE, HO, HC) using only three EMG electrodes placed on the forearm. The author employed discrete wavelet transform (DWT) and wavelet neural network (WNN) algorithms to improve the recognition rates. The proposed algorithm had an accuracy of 94.67% outperforming the ANN with an accuracy of 93.22%. Kyranou et al. (2016) proposed the use of additional sensors such as accelerometer, gyroscopes and magnetometers to improve the classification accuracy. The author used LDA to classify five different motions (2-FE, HO, ChG, LaP, CyG) using twelve electrodes placed on the forearm having an accuracy of 94.5%. Naik, Al-Timemy and Nguyen (2016) proposed a novel EMG control technique for identification of movements using the minimum number of electrodes based on Independent Component Analysis (ICA) and Icasto clustering. The data was recorded using eleven electrodes on the subject's forearm. The subjects performed eleven finger movements (1-Fab, 12345-FE, 12345-FF). The proposed technique achieved an accuracy of 96.6% using only four out the eleven sensors. Vidovic et al. (2016) proposed a robust EMG classification algorithm that prevents misclassification due to covariate shift, which is the changes on the EMG signal caused by electrode shifts after sweating or varying arm positions. Eight electrodes were placed on the forearm to record seven movements (WP, WS, WF, WE, HO, KG, FP). Vidovic adapted a trained LDA classifier using a calibration set, achieving an accuracy of 92%.

Fan et al. (2017) used pattern recognition algorithms using WNN combined with discrete wavelet transform (DWT) to discriminate six hand motions (WP, WS, WF, WE, HO, HC) using three electrodes on the forearm. The author achieved an average accuracy rate of 91.44%. Guo et al. (2017) used the combination of EMG and mechanomyography (MMG) signals. Four hybrid electrodes were placed on the individual's forearm to record twelve movements (WP, WS, WUD, WRD, WF, WE, 2-FE, HO, HC, ChG, FP, CeG). An accuracy of 95.6% was achieved using a LDA classifier to recognize the 12 classes. Table 3 presents relevant works in MYO classification for prosthesis control. It is sorted historically and contains the works reference, the number of EMG channels, the number of subjects, the algorithm used, the movements performed, the number of classes, the number of repetitions for each movement, and the accuracies.

Table 3 – Pattern Recognition-based Control of Upper Limb Prosthesis

| Author | EMG Ch. | #Subjects | Movements | #Repetitions | Algorithm | Accuracy |
|-------------------------------------|---------|-----------|--------------------------------------|--------------|------------|----------|
| Saridis and Gootee (1982) | 4 | - | EE, EF, HMR, HLR, WP, WS | 20 | - | - |
| Kelly, Parker and Scott (1990) | 2 | 1 Health | EE, EF, WP, WS | 20 | ANN | - |
| Hudgins, Parker and Scott (1993) | 2 | 9H 6A | EE, EF, HMR, HLR | 30 | ANN | 88.35% |
| Boca and Park (1994) | 4 | - | EF (intensities) | - | ANN | 86.20% |
| Kwon et al. (1996) | 4 | 1 Amputee | WP, WS, WF, WE, HO, HC | 30 | HMM-MLP | 91.16% |
| | | | | | MLP | 75.00% |
| Lee et al. (1996) | 4 | 2 Health | EE, EF, HMR, HLR, WP, WS | 50 | EA | 46.77% |
| | | | | | HMM-CPN | 55.60% |
| Kwon et al. (1998) | 4 | 1 Amputee | WP, WS, WF, WE, HO, HC | 30 | HMM-GA-CPN | 85.60% |
| | | | | | HMM-GA-MLP | 87.70% |
| | | | | | HMM-MLP | 76.90% |
| Park and Lee (1998) | 2 | 6 Health | EE, EF, HMR, HLR, WP, WS | 50 | EA | 65.00% |
| Englehart et al. (1999) | 2 | 16 Health | EE, EF, WP, WS | 100 | ANN | 92.75% |
| | | | | | LDA | 93.75% |
| Chan et al. (2000) | 2 | 4 Health | EE, EF, WP, WS | - | Fuzzy | 91.20% |
| | | | | | Abe-Lan | 93.33% |
| Micera, Sabatini and Dario (2000) | 2 | 4 Health | KG (3 planar arm-pointing movements) | 10 | ANN | 85.75% |
| | | | | | FCM | 53.30% |
| | | | | | SOM | 49.97% |
| Tsuji et al. (2000) | 4 | 3H 1A | WP, WS, WF, WE, HO, TG | - | ANN | 90.00% |
| Englehart, Hudgin and Parker (2001) | 4 | 11 Health | WUD, WRD, WF, WE, HO, HC | 80 | LDA | 98.00% |
| | | | WF, WE, HO, HC | | LDA | 99.50% |
| Zhang et al. (2002) | - | - | EE, EF, WP, WS, HO, HC | - | ANN | 90.66% |
| | | | | | NFC | 95.00% |

A: Amputee subjects, **H:** Health subjects

EE: Elbow Extension, **EF:** Elbow Flexion, **HMR:** Humerus Medial Rotation, **HLR:** Humerus Lateral Rotation, **WP:** Wrist Pronation, **WS:** Wrist Supination, **WUD:** Wrist Ulnar Deviation, **WRD:** Wrist Radial Deviation, **WF:** Wrist Flexion, **WE:** Wrist Extension, **xyz-Fab:** xth yth zth-Digit Finger Abduction, **xyz-Fad:** xth yth zth-Digit Finger Adduction, **xyz-FE:** xth yth zth-Digit Finger Extension, **xyz-FF:** xth yth zth-Digit Finger Flexion, **(xyz)-Fab:** Group of xth yth zth-Digit Finger Abduction, **(xyz)-Fad:** Group of xth yth zth-Digit Finger Adduction, **(xyz)-FE:** Group of xth yth zth-Digit Finger Extension, **(xyz)-FF:** Group of xth yth zth-Digit Finger Flexion, **HO:** Hand Open, **HC:** Hand Close, **KG:** Key Grip, **ChG:** Chuck Grip, **PG:** Power Grip, **FP:** Fine Pinch, **TG:** Tool Grip, **HG:** Hook Grip, **LaP:** Lateral Pinch, **CeG:** Centralized Grasp, **CyG:** Cylindrical Grasp

Table 3 – Pattern Recognition-based Control of Upper Limb Prosthesis

| Author | EMG Ch. | #Subjects | Movements | #Repetitions | Algorithm | Accuracy |
|--|---------|-----------|--|--------------|------------|----------|
| Englehart and Hudgins (2003) | 4 | 12 Health | WUD, WRD, WF, WE | 20 | LDA | 95.00% |
| Ajiboye and Weir (2005) | 4 | 3H 1A | WUD, WF, WE, FF | - | Fuzzy | 97.00% |
| Chan and Englehart (2005) | 4 | 11 Health | WP, WS, WF, WE, HO, HC | 8 | ANN | 93.27% |
| | | | | | HMM | 94.63% |
| Huang et al. (2005) | 4 | 12 Health | WP, WS, WF, WE, HO, HC | 4 | GMM | 96.28% |
| | | | | | LDA | 95.58% |
| | | | | | LP | 95.27% |
| | | | | | MLP | 95.38% |
| Chu, Moon and Mun (2006) | 4 | 10 Health | WP, WS, WUD, WRD, WF, WE, HO, HC | 20 | ANN | 97.02% |
| Nagata et al. (2006) | 96 | 3 Health | WP, WS, WUD, WRD, WF, WE, 1234-FF, HO, HC | 10 | CDA | 85.30% |
| | | | | | MLP | 92.00% |
| Tsenov et al. (2006) | 2 | 1 Health | 123-FF, HC | 34 | RBF | 84.00% |
| | | | | | LVQ | 89.00% |
| | | | | | ANN | 77.00% |
| Wang et al. (2006) | 8 | 4 Health | 123-FE, 123-FF | - | ANN | 77.00% |
| Chu et al. (2007) | 4 | 10 Health | WP, WS, WUD, WRD, WF, WE | 20 | LDA+MLP | 97.40% |
| Hargrove, Englehart and Hudgins (2007) | 16 | 6 Health | WP, WS, WUD, WRD, WF, WE, HO, KG, ChG | 36 | ANN | 96.00% |
| | | | | | LDA | 97.50% |
| Jung et al. (2007) | 4 | 1 Health | Korean Characters | 50 | ANN | 78.00% |
| Khezri, Jahed and Sadati (2007) | 4 | 4 Health | WF, WE, FE, FF, HO, HC, FP | 100 | HMM-GA-MLP | 96.00% |
| Liu, Huang and Weng (2007) | 3 | 1H 2A | WF, HO, ChG, PG, HG, LaP, CeG, CyG | 10 | GDA+SVM | 94.10% |
| Tenore et al. (2007) | 32 | 1 Health | 12345(345)FE, 12345(345)FF | 30 | ANN | 98.00% |
| Lucas et al. (2008) | 8 | 6 Health | WP, WS, WF, WE, HO, HC | 40 | SVM | 95.30% |

A: Amputee subjects, **H:** Health subjects

EE: Elbow Extension, **EF:** Elbow Flexion, **HMR:** Humerus Medial Rotation, **HLR:** Humerus Lateral Rotation, **WP:** Wrist Pronation, **WS:** Wrist Supination, **WUD:** Wrist Ulnar Deviation, **WRD:** Wrist Radial Deviation, **WF:** Wrist Flexion, **WE:** Wrist Extension, **xyz-Fab:** xth yth zth-Digit Finger Abduction, **xyz-Fad:** xth yth zth-Digit Finger Adduction, **xyz-FE:** xth yth zth-Digit Finger Extension, **xyz-FF:** xth yth zth-Digit Finger Flexion, **(xyz)-Fab:** Group of xth yth zth-Digit Finger Abduction, **(xyz)-Fad:** Group of xth yth zth-Digit Finger Adduction, **(xyz)-FE:** Group of xth yth zth-Digit Finger Extension, **(xyz)-FF:** Group of xth yth zth-Digit Finger Flexion, **HO:** Hand Open, **HC:** Hand Close, **KG:** Key Grip, **ChG:** Chuck Grip, **PG:** Power Grip, **FP:** Fine Pinch, **TG:** Tool Grip, **HG:** Hook Grip, **LaP:** Lateral Pinch, **CeG:** Centralized Grasp, **CyG:** Cylindrical Grasp

Table 3 – Pattern Recognition-based Control of Upper Limb Prosthesis

| Author | EMG Ch. | #Subjects | Movements | #Repetitions | Algorithm | Accuracy |
|-------------------------------|---------|-----------|--|--------------|-----------|----------|
| Oskoei and Hu (2008) | 4 | 11 Health | Fab, Fad, FE, FF, HO | 2 | ANN | 95.00% |
| | | | | | LDA | 95.50% |
| | | | | | SVM | 95.75% |
| Shenoy et al. (2008) | 7 | 3 Health | WP, WS, WUD, WRD, WF, WE, HO, PG | 5 | SVM | 95.00% |
| Sueaseenak et al. (2008) | 16 | 1 Health | WP, WS, WUD, WRD, WF, WE, HO, HC | 15 | ANN | 95.80% |
| | | | | | ICA | 93.30% |
| Chu and Lee (2009) | 4 | 10 Health | WP, WS, WUD, WRD, WF, WE, HO, CyG | 20 | Bayes | 93.57% |
| | | | | | GMM | 95.70% |
| Tenore et al. (2009) | 19 | 5H 1A | 12345-FF, 12345-FE | 25-30 | ANN | 91.27% |
| | 32 | 5 Health | | | ANN | 94.28% |
| Li, Schultz and Kuiken (2010) | 12 | 5 Amputee | WP, WS, WF, WE, HO, KG, ChG, PG, FP, TG | 2 | LDA | 79.00% |
| | | 1 Health | | | LDA | 94.00% |
| Geethanjali and Ray (2015) | 4 | 10H 2A | WS, WUD, WRD, WF, WE, HO, HC | 8 | ANN | 84.50% |
| | | | | | C4.5 | 79.50% |
| | | | | | LDA | 87.50% |
| | | | | | LMT | 84.33% |
| | | | | | SLR | 84.16% |
| | | | | | SVM | 84.00% |
| Geethanjali (2015) | 4 | 10 Health | WUD, WRD, WF, WE, HO, HC | 8 | ANN | 90.50% |
| | | | | | C4.5 | 82.00% |
| | | | | | kNN | 89.00% |
| | | | | | LMT | 91.00% |
| | | | | | SLR | 91.00% |

A: Amputee subjects, **H:** Health subjects

EE: Elbow Extension, **EF:** Elbow Flexion, **HMR:** Humerus Medial Rotation, **HLR:** Humerus Lateral Rotation, **WP:** Wrist Pronation, **WS:** Wrist Supination, **WUD:** Wrist Ulnar Deviation, **WRD:** Wrist Radial Deviation, **WF:** Wrist Flexion, **WE:** Wrist Extension, **xyz-Fab:** xth yth zth-Digit Finger Abduction, **xyz-Fad:** xth yth zth-Digit Finger Adduction, **xyz-FE:** xth yth zth-Digit Finger Extension, **xyz-FF:** xth yth zth-Digit Finger Flexion, **(xyz)-Fab:** Group of xth yth zth-Digit Finger Abduction, **(xyz)-Fad:** Group of xth yth zth-Digit Finger Adduction, **(xyz)-FE:** Group of xth yth zth-Digit Finger Extension, **(xyz)-FF:** Group of xth yth zth-Digit Finger Flexion, **HO:** Hand Open, **HC:** Hand Close, **KG:** Key Grip, **ChG:** Chuck Grip, **PG:** Power Grip, **FP:** Fine Pinch, **TG:** Tool Grip, **HG:** Hook Grip, **LaP:** Lateral Pinch, **CeG:** Centralized Grasp, **CyG:** Cylindrical Grasp

Table 3 – Pattern Recognition-based Control of Upper Limb Prosthesis

| Author | EMG Ch. | #Subjects | Movements | #Repetitions | Algorithm | Accuracy |
|--------------------------------------|---------|-----------|---|--------------|-----------|----------|
| AbdelMaseeh, Chen and Stashuk (2016) | 12 | 40 Health | NinaPro (ATZORI et al., 2014) | 6 | MD-DTW | 89.00% |
| Adewuyi, Hargrove and Kuiken (2016) | 21 | 9 Health | 1-Fab, 1-Fad, 12345-FE, 12345-FF, | 10 | LDA | 96.00% |
| | 13 | 4 Amputee | HO, KG, ChG, PG, FP, TG | | LDA | 85.00% |
| Al-Timemy et al. (2016) | 16 | 9 Amputee | 12-FF, ChG, PG, FP, HG | 15 - 24 | Bayes | 91.50% |
| | | | | | kNN | 92.50% |
| | | | | | LDA | 92.00% |
| | | | | | RF | 91.00% |
| Duan et al. (2016) | 3 | 6H 2A | WP, WS, WF, WE, HO, HC | 100 | ANN | 93.22% |
| | | | | | WNN | 94.67% |
| Kyranou et al. (2016) | 12 | 8 Health | 2-FE, HO, ChG, LaP, CyG | 5 | LDA | 94.50% |
| Naik, Al-Timemy and Nguyen (2016) | 11 | 5 Amputee | 1-Fab, 12345-FE, 12345-FF | 5-7 | LDA | 96.60% |
| Vidovic et al. (2016) | 8 | 7H 4A | WP, WS, WF, WE, HO, KG, FP | 15 | LDA | 92.00% |
| Fan et al. (2017) | 3 | 3 Health | WP, WS, WF, WE, HO, HC | 10 | ANN | 91.44% |
| Guo et al. (2017) | 4 | 7H 2A | WP, WS, WUD, WRD, WF, WE, 2-FE, HO, HC, ChG, FP, CeG | - | LDA | 95.60% |

A: Amputee subjects, **H:** Health subjects

EE: Elbow Extension, **EF:** Elbow Flexion, **HMR:** Humerus Medial Rotation, **HLR:** Humerus Lateral Rotation, **WP:** Wrist Pronation, **WS:** Wrist Supination, **WUD:** Wrist Ulnar Deviation, **WRD:** Wrist Radial Deviation, **WF:** Wrist Flexion, **WE:** Wrist Extension, **xyz-Fab:** xth yth zth-Digit Finger Abduction, **xyz-Fad:** xth yth zth-Digit Finger Adduction, **xyz-FE:** xth yth zth-Digit Finger Extension, **xyz-FF:** xth yth zth-Digit Finger Flexion, **(xyz)-Fab:** Group of xth yth zth-Digit Finger Abduction, **(xyz)-Fad:** Group of xth yth zth-Digit Finger Adduction, **(xyz)-FE:** Group of xth yth zth-Digit Finger Extension, **(xyz)-FF:** Group of xth yth zth-Digit Finger Flexion, **HO:** Hand Open, **HC:** Hand Close, **KG:** Key Grip, **ChG:** Chuck Grip, **PG:** Power Grip, **FP:** Fine Pinch, **TG:** Tool Grip, **HG:** Hook Grip, **LaP:** Lateral Pinch, **CeG:** Centralized Grasp, **CyG:** Cylindrical Grasp

Analyzing the works in Table 3 we noticed that there are several papers that propose interesting classification approaches, which will be used as ground for our work. However, almost all articles use only the EMG signal for the task of classification.

Kyranou et al. (2016) have observed higher classification accuracy when inertial information measured on the subject's forearm was taken into consideration. Our work aims to verify if the use of multi-modal data can enhance the performance of pattern recognition-based myoelectric control. In the next chapter, we analyze the existing data capture devices that could potentially be used.

5 Human Motion Sensing Techniques

Human motion sensing systems were created to capture spatio-temporal information that represents the movements of a human body or a part of it. The information such as position, acceleration, joint angles, contact pressure, and muscle contraction can be extracted from sensors (LIU et al., 2017).

The sensing techniques for human motions are generally categorized into two types: vision-based sensing and wearable sensing.

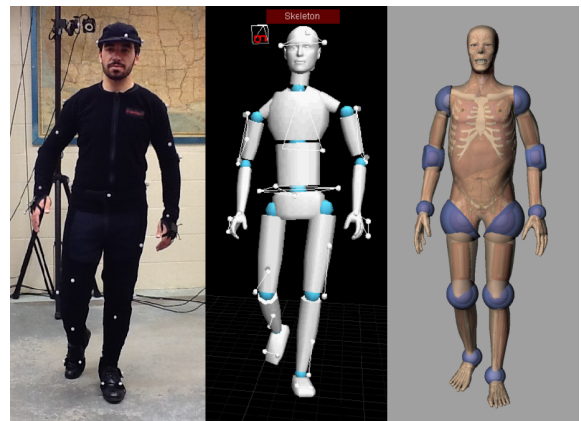
5.1 Vision Based Sensing

Usually cameras are used to track the position of the body. Optical systems use data captured from cameras to triangulate the 3D position of a human between two or more calibrated cameras to provide overlapping projections (HASSAN et al., 2014). Data acquisition is traditionally implemented using special markers attached to an actor. These systems produce data with three degrees of freedom for each marker (Surging, Swaying, Heaving). However, rotational information must be inferred from the relative orientation of markers. The latest hybrid systems combine inertial sensors with optical systems to reduce occlusion and increase the ability to track. Figure 14 shows some examples of vision based systems.



(a) Hand tracking using the Kinect camera

Source Oikonomidis, Kyriazis and Argyros (2011)



(b) Body tracking using passive markers and camera

Source <http://motioncapture3dgaming.blogspot.com.br/>

Figure 14 – Examples of Vision Based Systems

Although there are several interesting works using vision based sensing, it is necessary that the user is in a controlled environment, making this technique impractical for our application.

5.2 Wearable Sensing

Advances in recent technologies have opened up new possibilities for the use of wearable technology to monitor the human body, especially in health care. Integrated with miniature circuits, powerful microcontrollers, wireless data transmission and large capacity battery, wearable sensors are now small enough for people to carry and deploy it in digital health monitoring systems.

These sensors can be integrated into various personal accessories such as clothing, necklaces, hats, gloves, shoes and other devices such as wrist watches, headphones and smartphones. The sensing techniques are mainly based on inertial tracking, ultrasonic and other similar sensing techniques.

According to Liu et al. (2017) data gloves are one of the most important input devices for analyzing the hand movements. Examples of data gloves are shown in Figure 15. Considering the facility of using an off-the-shelf product to perform our research, we conduct an exploratory survey of the existing hand data capture devices, their specifications, price and availability in the market.

Table 4 was created to present the existing hand data capture devices. It is sorted by the application type of the device and contains the device's name, the sensors used, the resolution of the data, the speed that the data is captured, the interface used to communicate with a computer and the market price of the device.



(a) CyberGlove Systems CyberGlove III

Source <http://www.cyberglovesystems.com/>



(b) Synertial IGS Cobra Glove

Source <https://www.synertial.com/>

Figure 15 – Examples of Data Gloves

Table 4 – Glove-Based Systems and Their Applications

| Application | Device | Sensors | Precision | Sample Rate | Interface | Price |
|-------------|--|---------------------|-----------|-------------|-----------|------------|
| Health | YouRehab YouGrabber | AS, OT | - | - | - | - |
| K/M | Peregrine Glove | CS | - | - | USB | \$150.00 |
| K/M | Air Mouse | CS, OT | - | - | - | - |
| K/M | Key Glove | CS | 10 bit | - | Bluetooth | \$200.00 |
| K/M | Mister Gloves | AS, IMU, CS | 8 bit | - | USB | - |
| K/M | Wireless Hand Sensor | IMU, CS | 10 bit | - | Bluetooth | \$50.00 |
| M/A | AC Sensorizer Glove | AS, IMU, CS | 10 bit | - | USB | - |
| M/A | Aura | AS, IMU, CS | - | - | - | - |
| M/A | Crochet Gloves | FS | - | - | - | - |
| M/A | DJ GLove | AS, IMU, US | - | - | Bluetooth | - |
| M/A | Hypersense | AS | 8 bit | 100Hz | USB | - |
| M/A | Imaginary Marching Band | FS, IMU, US, PS, TS | 10 bit | - | USB | - |
| M/A | Musical Glove | AS, OT | 10 bit | - | - | - |
| M/A | mi.mu | AS, IMU | 13 bit | - | WiFi | - |
| M/A | Rachel Yalisove's Conversational Gloves | AS, IMU | 10 bit | - | USB | - |
| M/A | Sensitive Fingertips | FS | 10 bit | - | USB | - |
| M/A | The Lady's Glove | AS, FS, IMU, US, HE | - | - | - | - |
| M/A | Un Doigt, Une Note | FS | 10 bit | - | USB | - |
| M/A | VAMP | AS, FS, IMU | - | - | Zigbee | - |
| M/A | Wireless Midi Glove | FS | - | - | - | - |
| M/A | Wristflickr | Strech | 10 bit | - | Bluetooth | - |
| Robot | Dextrous Hand Master by Exos | HE | 12 bit | 75Hz | - | - |
| Robot | FingerTPS II | FS | 16 bit | 40Hz | Bluetooth | \$2,995.00 |
| SL | Cornell Sign language translation | AS, IMU, CS | 1 bit | - | RF to USB | - |
| SL | EnableTalk sensory gloves | AS, CS | - | - | - | - |

IMU Inertial Measurement Unit, **OT** Optical Tracking, **AS** Angle, **US** Ultrasonic, **CS** Contact, **FS** Force, **PS** Pressure, **TS** Tilt, **HE** Hall, **SS** Strech, **Ab** Abduction, **PA** Palm Arch, **TC** Thumb Crossover

K/M: Keyboard/Mouse, **M/A**: Music and Arts, **SL**: Sign Language, **VR**: Virtual Reality

Table 4 – Glove-Based Systems and Their Applications

| Application | Device | Sensors | Precision | Sample Rate | Interface | Price |
|-------------|--------------------------|-------------------------|-----------|-------------|-------------------|-------------|
| SL | FingerSpell | AS, FS | - | - | - | - |
| SL | Mobile Lorm Glove | CS | - | - | Bluetooth | - |
| SL | UW ASL Glove | AS, IMU | 10 bit | - | Bluetooth | - |
| VR | G-stalt | IMU, OT | - | 100Hz | - | - |
| VR | Matel Power Glove | AS, US | 8 bit | - | - | - |
| VR | 13 Cobra Glove | IMU | - | - | USB/WiFi | \$14,000.00 |
| VR | 16 Cobra Glove | IMU | - | - | USB/WiFi | \$24,500.00 |
| VR | 5DT Glove 14 Ultra | AS, Ab | 10 bit | 75Hz | USB/Bluetooth* | \$5,495.00 |
| VR | 5DT Glove 5 Ultra | AS | 10 bit | 75Hz | USB/Bluetooth* | \$995.00 |
| VR | 7 Cobra Glove | IMU | - | - | USB/WiFi | \$7,500.00 |
| VR | AnthroTronix Acceleglove | IMU | 10 bit | 35Hz | USB | \$499.00 |
| VR | CyberGlove II | AS, Ab, PA | - | 90Hz | WiFi | \$18,000.00 |
| VR | CyberGlove III | AS, Ab, PA | 12 bit | 120Hz | Wi-Fi/SD Card/USB | - |
| VR | CyberWorld P5 | AS, OT | - | 60Hz | USB | \$100.00 |
| VR | DG5 VHand 3.0 | AS, IMU | 12 bit | 100Hz | USB/WiFi | \$750.00 |
| VR | Didjiglove | AS | 10 bit | 70Hz | Serial | \$5,000.00 |
| VR | Fakespace PINCH | CS | 1 bit | - | Serial | \$2,200.00 |
| VR | Homebrew VR Data Glove | AS, IMU | 10 bit | - | USB | - |
| VR | Measurand ShapeHand | AS | - | 80Hz | Serial | \$11,000.00 |
| VR | Pliance® glove sensor | FS | - | - | Analog Interface | - |
| VR | StretchSense | AS | 16 bit | 1kHz | SPI Interface | \$3,050.00 |
| VR | T(ether) | IMU, CS | - | 30Hz | WiFi | - |
| VR | The VPL DataGlove | AS, IMU | - | 60Hz | RS232 | - |
| VR | TouchGloves v2.3 | FS | n/a | n/a | Analog Interface | \$750.00 |
| VR | VMG 10 | AS, FS, IMU | 12 bit | 90Hz | USB/WiFi | - |
| VR | VMG 30 | AS, FS, IMU, Ab, PA, TC | 12 bit | 90Hz | USB/WiFi | - |

IMU Inertial Measurement Unit, **OT** Optical Tracking, **AS** Angle, **US** Ultrasonic, **CS** Contact, **FS** Force, **PS** Pressure, **TS** Tilt, **HE** Hall, **SS** Stretch, **Ab** Abduction, **PA** Palm Arch, **TC** Thumb Crossover

K/M: Keyboard/Mouse, **M/A**: Music and Arts, **SL**: Sign Language, **VR**: Virtual Reality

Table 4 – Glove-Based Systems and Their Applications

| Application | Device | Sensors | Precision | Sample Rate | Interface | Price |
|-------------|--------------|-------------|-----------|-------------|---------------|------------|
| VR | VMG Lite | AS, IMU | 12 bit | 90Hz | USB/Bluetooth | \$750.00 |
| VR | X-IST HR3 3D | AS, FS, IMU | 10 bit | 60Hz | USB/ZigBee | \$5,000.00 |
| VR | X-IST SP1 3D | AS, FS, IMU | 10 bit | 60Hz | USB/ZigBee | \$4,000.00 |

IMU Inertial Measurement Unit, **OT** Optical Tracking, **AS** Angle, **US** Ultrasonic, **CS** Contact, **FS** Force, **PS** Pressure, **TS** Tilt, **HE** Hall, **SS** Stretch, **Ab** Abduction, **PA** Palm Arch, **TC** Thumb Crossover

K/M: Keyboard/Mouse, **M/A**: Music and Arts, **SL**: Sign Language, **VR**: Virtual Reality

As we can see in Table 4 the existing commercial solutions are very expensive and don't provide a variety of sensors. Thus, eliminating the idea of buying an off-the-shelf glove. We used the knowledge acquired from Table 4 to help us build our own hand data acquisition device.

Before starting the design process, we performed experiments applying new machine learning techniques to an open database called Ninapro DB (PIZZOLATO et al., 2017), in order to improve the classification performance. The following chapter presents these experiments.

6 Experiments

The goal of this chapter is to introduce new machine learning (ML) approaches in order to improve the performance of prosthetic hand movements classification. We chose the Ninapro database to perform these experiments, since the NinaPro is a well known database used by several authors in the literature, giving us a baseline to compare our results using new ML approaches.

6.1 Experimental Settings

6.1.1 The Ninapro DB5 database

NinaPro is a project that aims to aid research on hand myoelectric prosthesis making datasets available to everyone. The project has databases using several EMG acquisition setups and the majority of them include data captured from a CyberGlove¹ and an accelerometer.

Pizzolato et al. (2017) created a database using two Myo Armbands, a CyberGlove II and an Accelerometer. Their goal was to compare the EMG classification accuracy of the double-Myo Armband dataset against past NinaPro Datasets, which use state-of-the-art EMG acquisition setups costing more than \$10,000.

The NinaPro DB5 contains data from 10 subjects, where each subject performed 52 movements, grouped in three categories: A) Basic movements of the fingers (12 movements); B) Isometric, isotonic hand configurations and basic wrist movements (17 movements); C) Grasping and functional movements (23 movements), repeating 6 times each movement.

All experiments in this chapter were performed using exercises B, C and Rest from the NinaPro DB5 (exemplified on Figure 16). Repetitions 1, 3, 4 and 6 were used to train the classifiers and repetitions 2 and 5 to validate them.

Experiments #1 through #3 use only EMG data (16 EMG channels) in order to replicate the experimental settings from Pizzolato et al. (2017). Experiment #4 uses all data from the Ninapro DB5, such as 16 EMG channels, 22 Flex sensors and 3-axis accelerometer. All versions of the NinaPro database are available at <<http://ninapro.hevs.ch>>.

Figure 29 presents the class distribution for all the subjects. Because the distribution in the data is not equal, we calculate the Ninapro's DB5 imbalance ratio for exercises

¹ <<http://www.cyberglovesystems.com/>>



Figure 16 – Sets of Movements from NinaPro Database

Source – Adapted from Atzori et al. (2014)

B and C:

$$\begin{aligned}
 IR = \{ & \mathbf{0} : 3.85; \mathbf{1} : 1.39; \mathbf{2} : 1.17; \mathbf{3} : 1.18; \mathbf{4} : 1.20; \mathbf{5} : 1.06; \mathbf{6} : 1.08; \mathbf{7} : 1.23; \mathbf{8} : 1.16; \\
 & \mathbf{9} : 1.27; \mathbf{10} : 1.21; \mathbf{11} : 1.36; \mathbf{12} : 1.22; \mathbf{13} : 1.24; \mathbf{14} : 1.10; \mathbf{15} : 1.00; \mathbf{16} : 1.39; \\
 & \mathbf{17} : 1.28; \mathbf{18} : 1.14; \mathbf{19} : 1.19; \mathbf{20} : 1.17; \mathbf{21} : 1.18; \mathbf{22} : 1.26; \mathbf{23} : 1.43; \mathbf{24} : 1.14; \\
 & \mathbf{25} : 1.23; \mathbf{26} : 1.18; \mathbf{27} : 1.22; \mathbf{28} : 1.30; \mathbf{29} : 1.26; \mathbf{30} : 1.19; \mathbf{31} : 1.30; \mathbf{32} : 1.47; \\
 & \mathbf{33} : 1.30; \mathbf{34} : 1.37; \mathbf{35} : 1.44; \mathbf{36} : 1.33; \mathbf{37} : 1.31; \mathbf{38} : 1.34; \mathbf{39} : 1.53; \mathbf{40} : 1.57 \}
 \end{aligned}$$

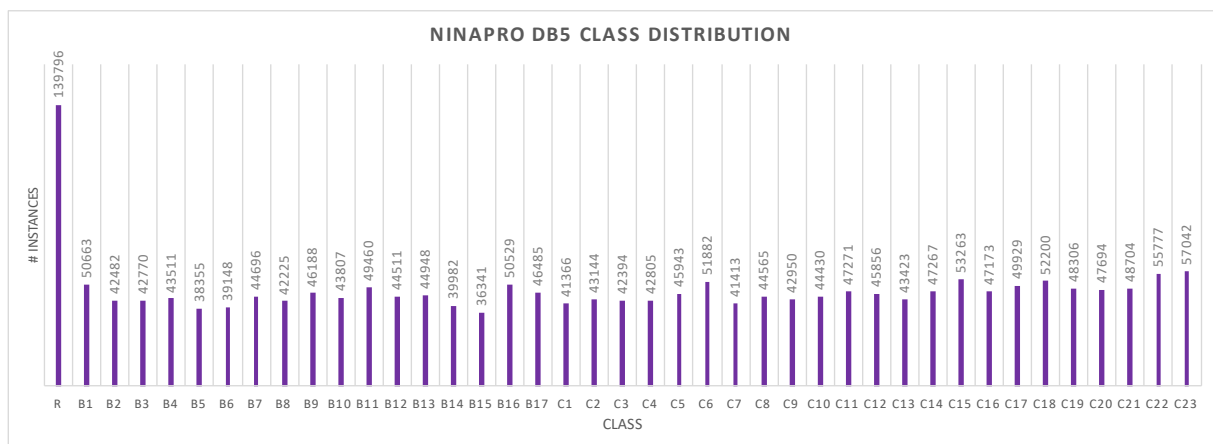


Figure 17 – Class distribution for the Ninapro database. The vertical axis shows the number of examples for all the subjects, the horizontal axis shows the class identification number.

6.1.2 Evaluation Metrics

Based on Chapter 4, to the best of our knowledge, most of the relevant works in the field of Machine Learning for Hand Movements' classification use accuracy to evaluate the performance of the classifier.

According to (FERREIRA et al., 2017), using accuracy as an evaluation metric is inadequate when the objective is to reflect the performance of the classifier for each class, especially on datasets with small classes.

As an example, Figure 18 presents a "mock" dataset with imbalanced classes $C = \{A, B, C\}$ and imbalance ratio $IR = \{A : 100; B : 10; C : 1\}$, with a total of 11,100 instances.



Figure 18 – "Mock" data projected to \mathbb{R}^2

Assume a hypothetical confusion matrix from the "mock" dataset (Figure 19), which describes a model's ability to identify the existing classes in the dataset.

Considering C_i as the class being evaluated, each decision from the confusion matrix can be grouped as:

1. true positive (tp_i): number of times C_i was correctly identified;
2. false negative (fn_i): number of times C_i was incorrectly identified;
3. true negative (tn_i): number of times any class but C_i was correctly identified;
4. false positive (fp_i): number of times any class was incorrectly identified as C_i ;

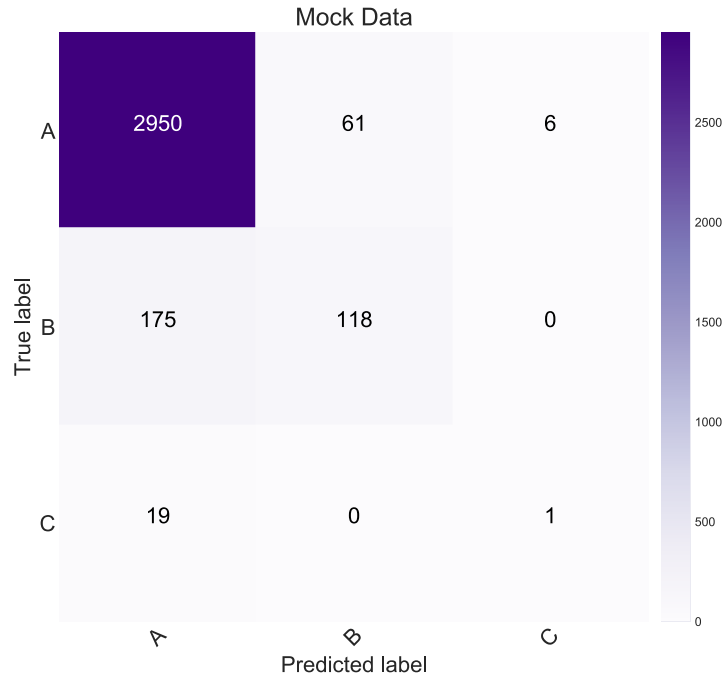


Figure 19 – Confusion matrix shows the predictions from a classifier.

Referring to the confusion matrix (Figure 19) as $CM_{k \times k}$, the classification accuracy is calculated as:

$$Accuracy = \frac{\sum_{i=1}^k CM_{i,i}}{\sum_{j=1}^k CM_{i,j}} \quad (6.1)$$

Evaluating the performance of this algorithm using Equation 6.1, we achieve an accuracy of 92.16% of correctly identified classes. Although, analyzing each class in the confusion matrix, the classifier correctly predicted only 1 out of 20 instances from class C . Therefore, the accuracy is not sufficient to evaluate the performance of the classifier considering each class.

In order to assess the performance of the classifier for each class, it should be considered the model's ability to find all the data points of interest in a dataset; This condition is known as recall (Eq. 6.2).

$$R_i = \frac{tp_i}{tp_i + fn_i} \quad (6.2)$$

However, it is important to point out that as the number of classes increase, the difficulty to evaluate the overall performance of the algorithms, based only on the results per class, also increases. Therefore, it is easier to first evaluate the performance of an algorithm using a single value, and then analyze its performance for each class. Thus, we chose using the Macro Average Geometric (Eq. 6.3), proposed by (SUN; KAMEL; WANG, 2006), as the geometric means of recall values. It is a generalization of the $G - Mean$ for

a multi-class scenario (KUBAT; HOLTE; MATWIN, 1998). Using the *MAvG*, each recall value representing the classification performance of a specific class is equally accounted.

$$MAvG = \left(\prod_{i=1}^J R_i \right)^{\frac{1}{J}} \quad (6.3)$$

In order to observe the difference between the *MAvG* and Accuracy, Table 5 presents the recall, accuracy and *MAvG* metrics to evaluate the performance of a classifier.

Table 5 – Recall per class and overall accuracy and *MAvG* for a classifier.

| Class | Recall |
|-----------------|--------|
| A | 0.9777 |
| B | 0.4027 |
| C | 0.0500 |
| Accuracy | 0.9216 |
| MAvG | 0.2700 |

6.2 Experiment #1: Exploring different algorithms

In this first experiment, we explore the use of different ML algorithms for prosthetic hands movement classification task. The experiments are based on (ENGLEHART; HUDGIN; PARKER, 2001). It consists of applying windows at 200ms with 100ms overlap, feature extraction and classification. Two feature extraction algorithms and five classification methods were employed.

The employed feature extraction algorithms are the Root Mean Square (RMS) and the marginal Discrete Wavelet Transform (mDWT) (LUCAS et al., 2008), using a db7 wavelet and 3 levels (Presented in Chapter 2). These features were chosen because they present the best overall results in the NinaPro database experiments (ATZORI et al., 2014; PIZZOLATO et al., 2017)

We used classifiers from two different categories: Shallow and Deep architectures (PASUPA; SUNHEM, 2016). The shallow architectures are Random Forests (RF), Support Vector Machines (SVM) (AL-TIMEMY et al., 2016; GEETHANJALI; RAY, 2015; LUCAS et al., 2008; SHENOY et al., 2008; LIU; HUANG; WENG, 2007). The deep architectures consist of two Convolutional Neural Networks (CNN). The first network hereafter referred to as *eCNN*, was trained using parameters chosen empirically by the author of this dissertation. The second network, hereafter referred as *NAS-CNN* was trained using a Neural Architecture Search (ZOPH; LE, 2016). It should be noted that in this work we are using the deep architectures after the feature extraction approach, on the grounds that (ATZORI; COGNOLATO; MÜLLER, 2016) shows that applying a CNN direct on the EMG signal presents a bad result.

Table 6 presents the computational results for the four different classifiers with two different feature extraction algorithms.

The experiments presented on table 6 allow us to answer the following questions:

1. Which classification algorithm is the best?
2. Which feature extraction algorithm is better?

It is important to remember that the experiments performed in this section are based on (PIZZOLATO et al., 2017), using 41 classes from the NinaPro DB5 and building a classification model for each individual using repetitions 1,3,4 and 6 for training and repetitions 2 and 5 for testing.

First, the results using the NAS-CNN with RMS outperforms the results from any other classification algorithm regardless of the feature extraction techniques with an *MAvG* of 0.816. Although, analyzing the two different feature extraction algorithms separately, using mDWT, the SVM outperforms the NAS-CNN most likely because creating one model per subject the number of examples provided for the NAS-CNN algorithm was not sufficient for it to find a good function approximation for the problem. On the other hand, it is proven that the SVM performs well with low amount of data (FORMAN; COHEN, 2004).

Although the results obtained are not directly comparable with (PIZZOLATO et al., 2017) because of the evaluation metric. It is important to note that the experiment using SVM with mDWT is equivalent to the best result obtained by (PIZZOLATO et al., 2017). Which means that the NAS-CNN with RMS got better results than the current state of the art.

Second, analyzing the results by feature extraction, it should be noted that regardless of the machine learning algorithm used, the RMS always has the best *MAvG*. Also, it is interesting that even though the RMS has less features (16 features), it gives a better result than using the mDWT (48 features).

The feature extraction is one of the keys for a classifier to achieve a high classification performance. We performed the Wilcoxon signed-rank test to evaluate if there is statistical difference between the chosen features (RMS and mDWT). Surprisingly this type of comparison has not been done before to the best of the authors knowledge. Assuming that the two groups are identical as the null hypothesis and a two-sided level of significance ($\alpha = 0.05$), the test indicated that the *MAvG* for classification of movements for prosthetic hand is significantly greater using RMS ($Mdn = 0.764$) than using mDWT ($Mdn = 0.712$) ($Z = 1367$, $p = 2.066E - 18$).

Table 6 – Results for the subject dependent classifiers.

| Class | Recall | | | | | | | |
|-------------|--------|-------|-------|-------|-------|-------|-------|-------|
| | RMS | | | | mDWT | | | |
| | RF | SVM | eCNN | NAS | RF | SVM | eCNN | NAS |
| R | 0.898 | 0.938 | 0.920 | 0.940 | 0.906 | 0.925 | 0.867 | 0.896 |
| B1 | 0.653 | 0.799 | 0.846 | 0.882 | 0.697 | 0.836 | 0.818 | 0.837 |
| B2 | 0.662 | 0.848 | 0.839 | 0.823 | 0.575 | 0.865 | 0.760 | 0.887 |
| B3 | 0.800 | 0.832 | 0.870 | 0.848 | 0.769 | 0.832 | 0.810 | 0.863 |
| B4 | 0.672 | 0.746 | 0.732 | 0.754 | 0.579 | 0.684 | 0.669 | 0.712 |
| B5 | 0.758 | 0.789 | 0.804 | 0.874 | 0.644 | 0.791 | 0.660 | 0.717 |
| B6 | 0.786 | 0.769 | 0.857 | 0.873 | 0.740 | 0.819 | 0.835 | 0.800 |
| B7 | 0.744 | 0.858 | 0.856 | 0.863 | 0.746 | 0.942 | 0.772 | 0.822 |
| B8 | 0.643 | 0.796 | 0.828 | 0.816 | 0.509 | 0.792 | 0.680 | 0.747 |
| B9 | 0.653 | 0.778 | 0.744 | 0.803 | 0.513 | 0.733 | 0.672 | 0.752 |
| B10 | 0.611 | 0.675 | 0.701 | 0.748 | 0.533 | 0.733 | 0.591 | 0.664 |
| B11 | 0.506 | 0.712 | 0.729 | 0.754 | 0.452 | 0.664 | 0.606 | 0.636 |
| B12 | 0.504 | 0.607 | 0.600 | 0.625 | 0.407 | 0.536 | 0.457 | 0.455 |
| B13 | 0.737 | 0.765 | 0.783 | 0.851 | 0.707 | 0.756 | 0.658 | 0.720 |
| B14 | 0.753 | 0.738 | 0.767 | 0.814 | 0.717 | 0.731 | 0.765 | 0.741 |
| B15 | 0.785 | 0.812 | 0.899 | 0.963 | 0.759 | 0.753 | 0.741 | 0.767 |
| B16 | 0.652 | 0.756 | 0.733 | 0.788 | 0.627 | 0.714 | 0.580 | 0.686 |
| B17 | 0.825 | 0.744 | 0.778 | 0.829 | 0.685 | 0.739 | 0.685 | 0.737 |
| C1 | 0.550 | 0.615 | 0.660 | 0.708 | 0.455 | 0.615 | 0.571 | 0.634 |
| C2 | 0.500 | 0.650 | 0.716 | 0.773 | 0.437 | 0.606 | 0.569 | 0.635 |
| C3 | 0.564 | 0.728 | 0.731 | 0.730 | 0.515 | 0.663 | 0.566 | 0.584 |
| C4 | 0.709 | 0.729 | 0.781 | 0.889 | 0.698 | 0.773 | 0.663 | 0.866 |
| C5 | 0.579 | 0.619 | 0.654 | 0.733 | 0.484 | 0.627 | 0.595 | 0.589 |
| C6 | 0.736 | 0.773 | 0.784 | 0.869 | 0.711 | 0.706 | 0.659 | 0.705 |
| C7 | 0.657 | 0.800 | 0.737 | 0.853 | 0.681 | 0.864 | 0.628 | 0.788 |
| C8 | 0.706 | 0.759 | 0.805 | 0.817 | 0.588 | 0.823 | 0.726 | 0.746 |
| C9 | 0.692 | 0.784 | 0.675 | 0.739 | 0.583 | 0.730 | 0.500 | 0.586 |
| C10 | 0.515 | 0.645 | 0.760 | 0.842 | 0.570 | 0.674 | 0.595 | 0.775 |
| C11 | 0.618 | 0.795 | 0.775 | 0.820 | 0.508 | 0.810 | 0.626 | 0.689 |
| C12 | 0.661 | 0.661 | 0.795 | 0.862 | 0.504 | 0.667 | 0.663 | 0.699 |
| C13 | 0.604 | 0.716 | 0.640 | 0.762 | 0.621 | 0.719 | 0.626 | 0.661 |
| C14 | 0.600 | 0.706 | 0.725 | 0.718 | 0.597 | 0.737 | 0.653 | 0.674 |
| C15 | 0.729 | 0.760 | 0.709 | 0.755 | 0.707 | 0.784 | 0.642 | 0.722 |
| C16 | 0.679 | 0.780 | 0.685 | 0.760 | 0.616 | 0.757 | 0.575 | 0.621 |
| C17 | 0.727 | 0.908 | 0.851 | 0.880 | 0.794 | 0.924 | 0.772 | 0.766 |
| C18 | 0.721 | 0.806 | 0.732 | 0.810 | 0.652 | 0.815 | 0.629 | 0.714 |
| C19 | 0.757 | 0.860 | 0.801 | 0.812 | 0.818 | 0.902 | 0.735 | 0.810 |
| C20 | 0.844 | 0.860 | 0.869 | 0.870 | 0.839 | 0.873 | 0.861 | 0.816 |
| C21 | 0.698 | 0.815 | 0.718 | 0.820 | 0.649 | 0.863 | 0.639 | 0.712 |
| C22 | 0.889 | 0.891 | 0.886 | 0.953 | 0.873 | 0.901 | 0.816 | 0.840 |
| C23 | 0.849 | 0.931 | 0.957 | 0.947 | 0.858 | 0.907 | 0.854 | 0.860 |
| MAvG | 0.681 | 0.765 | 0.770 | 0.816 | 0.629 | 0.764 | 0.671 | 0.724 |

6.3 Experiment #2: Towards a subject independent model

Usually within the movement classification for hand prosthesis community, the models are trained using machine learning algorithms for each subject at a time. i.e. one model is trained and tested for each individual. This is deemed necessary by the community as the different placement of sensors and physiology of the subjects can compromise the classification performance. Therefore, the usual approach is to train and test machine learning classifiers per subject. However, in this work we believe that is possible to use machine learning algorithms to build a subject independent model, i.e. a model which can be used for any subject. For this reason, the motivation behind this second experiment is to evaluate what happens when we use the traditional approach for movement classification using the data from the Ninapro DB5 with different machine learning classifiers. To the best of our knowledge, this type of experiment has never been done before, which puzzles us, as it would make a lot of sense to build off the shelves devices, rather than buying a device and then having to train it in order to use it.

Table 7 presents the results experiment using the same classifiers and feature extraction algorithms from Experiment #1 (Section 6.2). The main difference is that the results presented on Table 7 are from using the movement classification regardless of the individual, i.e. a subject independent model. It is expected to be more challenging than subject dependent classification. It can be one of the reasons that, to the best of our knowledge, it has not been done before.

The experiments presented on table 7 allow us to answer the following questions:

1. Which classification algorithm is the best?
2. Which feature extraction algorithm is better?
3. What is the difference between the subject dependent and subject independent results?

The results using the NAS-CNN with RMS outperforms the results from the other classifiers regardless of the feature extraction techniques with an *MAvG* of 0.705. Different from the results in Table 6, analyzing the algorithm's performances using mDWT for a subject independent model, the NAS-CNN achieves better *MAvG* than the SVM. This happens because deep learning algorithms perform better when they have more data.

Analyzing the results by feature extraction, regardless of the machine learning algorithm used, the RMS still always has the best *MAvG* compared to the mDWT. We performed the Wilcoxon signed-rank test to evaluate if there is statistical difference between the chosen features (RMS and mDWT). Assuming that the two groups are identical as the null hypothesis and a two-sided level of significance ($\alpha = 0.05$), the test indicated

Table 7 – Results for the subject independent classifiers.

| Class | Recall | | | | | | | |
|-------------|--------|-------|-------|-------|-------|-------|-------|-------|
| | RMS | | | | mDWT | | | |
| | RF | SVM | eCNN | NAS | RF | SVM | eCNN | NAS |
| R | 0.855 | 0.834 | 0.897 | 0.856 | 0.818 | 0.715 | 0.898 | 0.916 |
| B1 | 0.628 | 0.479 | 0.817 | 0.889 | 0.630 | 0.314 | 0.862 | 0.798 |
| B2 | 0.575 | 0.397 | 0.796 | 0.785 | 0.460 | 0.293 | 0.703 | 0.726 |
| B3 | 0.739 | 0.712 | 0.857 | 0.774 | 0.609 | 0.483 | 0.768 | 0.811 |
| B4 | 0.570 | 0.444 | 0.670 | 0.789 | 0.467 | 0.204 | 0.582 | 0.707 |
| B5 | 0.481 | 0.429 | 0.719 | 0.837 | 0.414 | 0.348 | 0.533 | 0.693 |
| B6 | 0.655 | 0.538 | 0.743 | 0.903 | 0.617 | 0.378 | 0.673 | 0.786 |
| B7 | 0.725 | 0.484 | 0.702 | 0.743 | 0.695 | 0.305 | 0.731 | 0.829 |
| B8 | 0.457 | 0.263 | 0.703 | 0.730 | 0.425 | 0.227 | 0.543 | 0.632 |
| B9 | 0.504 | 0.432 | 0.593 | 0.605 | 0.394 | 0.189 | 0.660 | 0.510 |
| B10 | 0.543 | 0.466 | 0.626 | 0.630 | 0.472 | 0.291 | 0.566 | 0.483 |
| B11 | 0.439 | 0.281 | 0.564 | 0.667 | 0.355 | 0.355 | 0.520 | 0.549 |
| B12 | 0.448 | 0.333 | 0.500 | 0.569 | 0.359 | 0.214 | 0.338 | 0.440 |
| B13 | 0.647 | 0.701 | 0.697 | 0.845 | 0.573 | 0.358 | 0.645 | 0.760 |
| B14 | 0.742 | 0.519 | 0.631 | 0.762 | 0.621 | 0.228 | 0.621 | 0.703 |
| B15 | 0.687 | 0.389 | 0.600 | 0.825 | 0.590 | 0.209 | 0.582 | 0.766 |
| B16 | 0.594 | 0.477 | 0.667 | 0.691 | 0.561 | 0.301 | 0.610 | 0.574 |
| B17 | 0.774 | 0.659 | 0.630 | 0.794 | 0.693 | 0.229 | 0.475 | 0.561 |
| C1 | 0.431 | 0.410 | 0.538 | 0.619 | 0.371 | 0.266 | 0.421 | 0.485 |
| C2 | 0.457 | 0.297 | 0.550 | 0.629 | 0.306 | 0.167 | 0.408 | 0.358 |
| C3 | 0.346 | 0.289 | 0.448 | 0.626 | 0.409 | 0.269 | 0.412 | 0.532 |
| C4 | 0.527 | 0.425 | 0.568 | 0.604 | 0.422 | 0.177 | 0.537 | 0.559 |
| C5 | 0.490 | 0.377 | 0.489 | 0.608 | 0.362 | 0.284 | 0.372 | 0.469 |
| C6 | 0.572 | 0.417 | 0.701 | 0.758 | 0.528 | 0.227 | 0.542 | 0.675 |
| C7 | 0.459 | 0.405 | 0.556 | 0.762 | 0.400 | 0.272 | 0.529 | 0.634 |
| C8 | 0.596 | 0.430 | 0.632 | 0.732 | 0.505 | 0.330 | 0.733 | 0.617 |
| C9 | 0.540 | 0.272 | 0.538 | 0.557 | 0.455 | 0.233 | 0.494 | 0.559 |
| C10 | 0.537 | 0.413 | 0.602 | 0.694 | 0.440 | 0.246 | 0.579 | 0.508 |
| C11 | 0.491 | 0.459 | 0.511 | 0.512 | 0.360 | 0.110 | 0.389 | 0.493 |
| C12 | 0.419 | 0.359 | 0.676 | 0.729 | 0.400 | 0.296 | 0.414 | 0.505 |
| C13 | 0.400 | 0.299 | 0.546 | 0.575 | 0.418 | 0.098 | 0.442 | 0.544 |
| C14 | 0.524 | 0.379 | 0.460 | 0.602 | 0.477 | 0.280 | 0.576 | 0.545 |
| C15 | 0.660 | 0.432 | 0.629 | 0.770 | 0.582 | 0.241 | 0.584 | 0.653 |
| C16 | 0.570 | 0.410 | 0.604 | 0.518 | 0.525 | 0.234 | 0.400 | 0.438 |
| C17 | 0.675 | 0.438 | 0.647 | 0.775 | 0.624 | 0.346 | 0.577 | 0.555 |
| C18 | 0.609 | 0.500 | 0.542 | 0.684 | 0.496 | 0.289 | 0.509 | 0.473 |
| C19 | 0.677 | 0.390 | 0.723 | 0.744 | 0.636 | 0.381 | 0.705 | 0.699 |
| C20 | 0.692 | 0.513 | 0.692 | 0.818 | 0.638 | 0.342 | 0.694 | 0.685 |
| C21 | 0.604 | 0.340 | 0.492 | 0.649 | 0.533 | 0.208 | 0.349 | 0.589 |
| C22 | 0.752 | 0.605 | 0.748 | 0.765 | 0.667 | 0.404 | 0.720 | 0.684 |
| C23 | 0.806 | 0.531 | 0.720 | 0.804 | 0.701 | 0.320 | 0.750 | 0.704 |
| MAvG | 0.570 | 0.429 | 0.626 | 0.705 | 0.499 | 0.268 | 0.555 | 0.602 |

that the *MAvG* for classification of movements for prosthetic hand is significantly greater using RMS ($Mdn = 0.602$) than using mDWT ($Mdn = 0.505$) ($Z = 599$, $p = 4.329E-24$).

Creating an independent model using the classic algorithms from the literature to classify movements has lower *MAvG* compared to the results from Table 6. Although adopting new approaches such as *e*CNN and NAS-CNN, we could achieve an *MAvG* for a subject independent model close or even better than subject dependent models using classic algorithms.

6.4 Experiment #3: Improving the results with Synthetic Samples

Considering the variability given by the sensors depending on the subject information as well as the precise location where they are placed. In this third experiment we are interested in investigating whether or not it is possible to improve the classification results (for both subject-dependent classification as well as subject-independent classification) using methods that automatically generates synthetic samples in order to balance the database.

In this experiment, we used Synthetic Minority Over-Sampling Technique (SMOTE) and its variation known as SMOTE-SVM (Presented in Chapter 2), to resample our data in order to decrease the imbalance ratio of the original data set. It follows the same protocol as Section 6.2, with the difference that we have more data, since we generated synthetic examples for each class using the SMOTE algorithm with the standard hyper-parameters from (LEMAÎTRE; NOGUEIRA; ARIDAS, 2017) implementation.

Section 6.4.1, presents the results using SMOTE and SMOTE-SVM for the subject dependent approach, i.e. train and test one classification model for each subject. Section 6.4.2, presents the results using SMOTE and SMOTE-SVM for the subject independent approach, i.e. train and test one classification model for all subjects.

6.4.1 SMOTE and SMOTE-SVM in a Subject Dependent Approach

Tables 8 and 9 present the computational results for the four different classifiers with two different feature extraction algorithms. The results allow us to answer the following questions:

1. Which classification algorithm is the best?
2. Which feature extraction algorithm is better?
3. Does using SMOTE improve the results?

In regard to Table 8, the results using the NAS-CNN with RMS still outperforms the results from other classification algorithm regardless of the feature extraction techniques with an *MAvG* of 0.818. Comparing the results in Table 8 using SMOTE with the results on Table 6, we noticed that the synthetic oversampling using SMOTE substantially increased the *MAvG* for the Random Forests and NAS-CNN algorithms, improving it in an average of 6.05% and 3.20%, respectively, despite of the feature extraction used.

Analyzing Table 9, the outcome using the NAS-CNN with RMS has better results than any other classification algorithm presented in this dissertation, regardless of the feature extraction techniques with an *MAvG* of 0.831. Observing the results on Table 9, we also noticed that the synthetic oversampling using SMOTE-SVM considerably increased the *MAvG* for all classification algorithms.

A Wilcoxon signed-rank test shows that there is statistical difference between the chosen features (RMS and mDWT) for using SMOTE and SMOTE-SVM. Assuming that the two groups are identical as the null hypothesis and a two-sided level of significance ($\alpha = 0.05$), the test indicated that the *MAvG* for classification of movements for prosthetic hand is significantly greater using RMS ($Mdn_{SMOTE} = 0.774$ and $Mdn_{SMOTE-SVM} = 0.791$) than using mDWT ($Mdn_{SMOTE} = 0.752$ and $Mdn_{SMOTE-SVM} = 0.773$) ($Z_{SMOTE} = 5209$, $p_{SMOTE} = 1.063E-02$ and $Z_{SMOTE-SVM} = 4154$, $p_{SMOTE-SVM} = 2.784E-05$).

To evaluate if the improvements on the results with and without SMOTE and SMOTE-SVM are statistically significant, we performed a Friedman test. The test shows that there is a statistically significant difference between using or not using the SMOTE and SMOTE-SVM, $\chi^2(2) = 170.140$, $p = 1.1336E-37$. Post hoc analysis with Wilcoxon signed-rank tests was conducted with a Bonferroni correction applied, resulting in a significance level set at $p < 0.017$. There are significant differences between the noSMOTE and SMOTE results ($Z = -7.594$, $p = 3.0906E-14$), the noSMOTE and SMOTE-SVM ($Z = -11.813$, $p = 3.3306E-32$), and the SMOTE and SMOTE-SVM ($Z = -7.217$, $p = 5.2991E-13$).

Although the difference between the results seems small, using SMOTE-SVM is significantly better than using SMOTE or not using any synthetic algorithms for a subject dependent approach.

6.4.2 SMOTE and SMOTE-SVM in a Subject Independent Approach

In this section, Tables 8 and 9 present the computational results for three classifiers, such as Random Forest, *e*CNN and NAS-CNN, with two different feature extraction algorithms, RMS and mDWT. The results allow us to answer the following questions:

1. Which classification algorithm has the best classification performance?

Table 8 – Results for subject dependent classifiers using SMOTE

| Class | Recall | | | | | | | |
|-------------|--------|-------|-------|-------|-------|-------|-------|-------|
| | RMS | | | | mDWT | | | |
| | RF | SVM | eCNN | NAS | RF | SVM | eCNN | NAS |
| R | 0.805 | 0.760 | 0.763 | 0.780 | 0.797 | 0.750 | 0.704 | 0.732 |
| B1 | 0.788 | 0.841 | 0.850 | 0.938 | 0.782 | 0.847 | 0.942 | 0.875 |
| B2 | 0.768 | 0.848 | 0.825 | 0.864 | 0.730 | 0.881 | 0.896 | 0.865 |
| B3 | 0.813 | 0.832 | 0.847 | 0.850 | 0.806 | 0.831 | 0.912 | 0.864 |
| B4 | 0.710 | 0.736 | 0.756 | 0.793 | 0.620 | 0.689 | 0.748 | 0.797 |
| B5 | 0.679 | 0.768 | 0.804 | 0.854 | 0.649 | 0.789 | 0.701 | 0.863 |
| B6 | 0.710 | 0.756 | 0.830 | 0.933 | 0.772 | 0.819 | 0.852 | 0.874 |
| B7 | 0.802 | 0.872 | 0.860 | 0.878 | 0.842 | 0.931 | 0.817 | 0.867 |
| B8 | 0.709 | 0.804 | 0.777 | 0.825 | 0.632 | 0.806 | 0.764 | 0.776 |
| B9 | 0.679 | 0.769 | 0.780 | 0.819 | 0.669 | 0.729 | 0.832 | 0.797 |
| B10 | 0.661 | 0.694 | 0.658 | 0.718 | 0.631 | 0.740 | 0.686 | 0.817 |
| B11 | 0.718 | 0.711 | 0.733 | 0.819 | 0.610 | 0.669 | 0.629 | 0.707 |
| B12 | 0.575 | 0.619 | 0.598 | 0.642 | 0.538 | 0.526 | 0.464 | 0.524 |
| B13 | 0.748 | 0.772 | 0.786 | 0.817 | 0.745 | 0.758 | 0.685 | 0.778 |
| B14 | 0.723 | 0.745 | 0.676 | 0.853 | 0.750 | 0.731 | 0.725 | 0.820 |
| B15 | 0.776 | 0.852 | 0.873 | 0.925 | 0.707 | 0.773 | 0.753 | 0.914 |
| B16 | 0.683 | 0.739 | 0.701 | 0.784 | 0.651 | 0.723 | 0.654 | 0.679 |
| B17 | 0.750 | 0.748 | 0.705 | 0.837 | 0.742 | 0.752 | 0.737 | 0.739 |
| C1 | 0.624 | 0.611 | 0.622 | 0.729 | 0.555 | 0.604 | 0.697 | 0.734 |
| C2 | 0.620 | 0.673 | 0.728 | 0.782 | 0.566 | 0.603 | 0.606 | 0.669 |
| C3 | 0.626 | 0.698 | 0.748 | 0.816 | 0.551 | 0.673 | 0.649 | 0.755 |
| C4 | 0.647 | 0.729 | 0.721 | 0.869 | 0.728 | 0.780 | 0.726 | 0.728 |
| C5 | 0.598 | 0.673 | 0.643 | 0.669 | 0.570 | 0.648 | 0.643 | 0.694 |
| C6 | 0.733 | 0.770 | 0.769 | 0.860 | 0.723 | 0.706 | 0.745 | 0.815 |
| C7 | 0.798 | 0.781 | 0.789 | 0.867 | 0.716 | 0.857 | 0.839 | 0.862 |
| C8 | 0.737 | 0.791 | 0.807 | 0.787 | 0.722 | 0.833 | 0.869 | 0.823 |
| C9 | 0.809 | 0.745 | 0.830 | 0.779 | 0.810 | 0.794 | 0.708 | 0.786 |
| C10 | 0.658 | 0.633 | 0.669 | 0.739 | 0.638 | 0.679 | 0.677 | 0.739 |
| C11 | 0.638 | 0.793 | 0.721 | 0.772 | 0.679 | 0.817 | 0.730 | 0.748 |
| C12 | 0.628 | 0.669 | 0.706 | 0.812 | 0.689 | 0.667 | 0.682 | 0.773 |
| C13 | 0.620 | 0.729 | 0.650 | 0.757 | 0.670 | 0.726 | 0.658 | 0.684 |
| C14 | 0.638 | 0.712 | 0.722 | 0.824 | 0.682 | 0.739 | 0.762 | 0.795 |
| C15 | 0.762 | 0.752 | 0.754 | 0.804 | 0.810 | 0.823 | 0.795 | 0.827 |
| C16 | 0.758 | 0.771 | 0.678 | 0.767 | 0.735 | 0.789 | 0.670 | 0.694 |
| C17 | 0.824 | 0.903 | 0.809 | 0.890 | 0.788 | 0.922 | 0.845 | 0.874 |
| C18 | 0.788 | 0.812 | 0.788 | 0.815 | 0.753 | 0.824 | 0.787 | 0.803 |
| C19 | 0.827 | 0.859 | 0.800 | 0.807 | 0.804 | 0.916 | 0.871 | 0.852 |
| C20 | 0.908 | 0.860 | 0.852 | 0.881 | 0.884 | 0.873 | 0.850 | 0.913 |
| C21 | 0.765 | 0.796 | 0.782 | 0.826 | 0.722 | 0.863 | 0.675 | 0.771 |
| C22 | 0.856 | 0.890 | 0.825 | 0.927 | 0.875 | 0.913 | 0.859 | 0.868 |
| C23 | 0.897 | 0.924 | 0.878 | 0.924 | 0.884 | 0.907 | 0.829 | 0.893 |
| MAvG | 0.724 | 0.763 | 0.755 | 0.818 | 0.707 | 0.767 | 0.742 | 0.786 |

Table 9 – Results for subject dependent classifiers using SMOTE-SVM

| Class | Recall | | | | | | | |
|-------------|--------|-------|-------|-------|-------|-------|-------|-------|
| | RMS | | | | mDWT | | | |
| | RF | SVM | eCNN | NAS | RF | SVM | eCNN | NAS |
| R | 0.809 | 0.774 | 0.798 | 0.809 | 0.804 | 0.762 | 0.756 | 0.795 |
| B1 | 0.827 | 0.841 | 0.872 | 0.857 | 0.848 | 0.881 | 0.856 | 0.894 |
| B2 | 0.785 | 0.862 | 0.857 | 0.898 | 0.775 | 0.858 | 0.896 | 0.860 |
| B3 | 0.862 | 0.854 | 0.861 | 0.923 | 0.845 | 0.840 | 0.929 | 0.922 |
| B4 | 0.730 | 0.790 | 0.765 | 0.779 | 0.696 | 0.732 | 0.686 | 0.776 |
| B5 | 0.778 | 0.814 | 0.816 | 0.900 | 0.762 | 0.809 | 0.670 | 0.789 |
| B6 | 0.854 | 0.819 | 0.819 | 0.952 | 0.754 | 0.838 | 0.864 | 0.887 |
| B7 | 0.891 | 0.889 | 0.858 | 0.846 | 0.789 | 0.933 | 0.855 | 0.883 |
| B8 | 0.676 | 0.787 | 0.779 | 0.845 | 0.561 | 0.772 | 0.750 | 0.782 |
| B9 | 0.635 | 0.797 | 0.846 | 0.846 | 0.634 | 0.766 | 0.781 | 0.784 |
| B10 | 0.697 | 0.707 | 0.705 | 0.784 | 0.688 | 0.775 | 0.757 | 0.820 |
| B11 | 0.669 | 0.697 | 0.752 | 0.798 | 0.631 | 0.724 | 0.735 | 0.748 |
| B12 | 0.570 | 0.634 | 0.609 | 0.644 | 0.516 | 0.546 | 0.477 | 0.582 |
| B13 | 0.766 | 0.795 | 0.860 | 0.839 | 0.736 | 0.763 | 0.788 | 0.805 |
| B14 | 0.778 | 0.783 | 0.786 | 0.873 | 0.733 | 0.776 | 0.789 | 0.785 |
| B15 | 0.745 | 0.865 | 0.919 | 0.918 | 0.855 | 0.781 | 0.839 | 0.897 |
| B16 | 0.738 | 0.773 | 0.762 | 0.800 | 0.708 | 0.741 | 0.627 | 0.721 |
| B17 | 0.817 | 0.772 | 0.824 | 0.806 | 0.798 | 0.750 | 0.752 | 0.807 |
| C1 | 0.593 | 0.639 | 0.663 | 0.800 | 0.600 | 0.604 | 0.620 | 0.739 |
| C2 | 0.593 | 0.652 | 0.750 | 0.768 | 0.507 | 0.650 | 0.628 | 0.701 |
| C3 | 0.576 | 0.733 | 0.796 | 0.812 | 0.617 | 0.740 | 0.664 | 0.740 |
| C4 | 0.707 | 0.729 | 0.789 | 0.782 | 0.724 | 0.761 | 0.735 | 0.882 |
| C5 | 0.600 | 0.692 | 0.720 | 0.676 | 0.550 | 0.664 | 0.588 | 0.728 |
| C6 | 0.713 | 0.792 | 0.794 | 0.901 | 0.697 | 0.742 | 0.771 | 0.820 |
| C7 | 0.712 | 0.827 | 0.869 | 0.857 | 0.758 | 0.848 | 0.848 | 0.857 |
| C8 | 0.773 | 0.750 | 0.829 | 0.825 | 0.706 | 0.843 | 0.798 | 0.835 |
| C9 | 0.773 | 0.712 | 0.743 | 0.882 | 0.698 | 0.796 | 0.775 | 0.758 |
| C10 | 0.705 | 0.699 | 0.764 | 0.824 | 0.682 | 0.669 | 0.764 | 0.746 |
| C11 | 0.731 | 0.800 | 0.750 | 0.843 | 0.723 | 0.803 | 0.769 | 0.896 |
| C12 | 0.681 | 0.702 | 0.802 | 0.852 | 0.676 | 0.686 | 0.736 | 0.758 |
| C13 | 0.660 | 0.760 | 0.766 | 0.831 | 0.624 | 0.757 | 0.642 | 0.791 |
| C14 | 0.675 | 0.732 | 0.754 | 0.758 | 0.726 | 0.756 | 0.772 | 0.779 |
| C15 | 0.755 | 0.783 | 0.763 | 0.767 | 0.739 | 0.815 | 0.773 | 0.855 |
| C16 | 0.738 | 0.767 | 0.727 | 0.786 | 0.673 | 0.794 | 0.727 | 0.761 |
| C17 | 0.844 | 0.883 | 0.856 | 0.866 | 0.837 | 0.893 | 0.897 | 0.909 |
| C18 | 0.769 | 0.796 | 0.768 | 0.848 | 0.771 | 0.818 | 0.779 | 0.796 |
| C19 | 0.843 | 0.859 | 0.833 | 0.841 | 0.853 | 0.918 | 0.881 | 0.890 |
| C20 | 0.938 | 0.885 | 0.837 | 0.900 | 0.858 | 0.874 | 0.770 | 0.868 |
| C21 | 0.776 | 0.785 | 0.748 | 0.819 | 0.689 | 0.875 | 0.743 | 0.868 |
| C22 | 0.938 | 0.937 | 0.863 | 0.904 | 0.910 | 0.919 | 0.872 | 0.917 |
| C23 | 0.916 | 0.918 | 0.958 | 0.910 | 0.921 | 0.924 | 0.901 | 0.880 |
| MAvG | 0.741 | 0.779 | 0.793 | 0.831 | 0.717 | 0.780 | 0.756 | 0.809 |

2. Which feature extraction algorithm is better?
3. Does using SMOTE improve the results?

The increase in the number of examples for training, due to the synthetic instances, requires more processing and may require a longer run-time for some classification algorithms, as was the case with SVM. The main limitation of this algorithm for large amount of data is the need to compare each pair of examples for each characteristic of the problem. This comparison demands an exponential increase in the number of processes as the number of training examples increases. The training time complexity of SVM is $O(n^3)$ and its space complexity is at least quadratic (ABDIANSAH; WARDOYO, 2015).

Table 10 shows that the results using the NAS-CNN with RMS performs better than any other subject-independent-classification algorithm, regardless of the feature extraction techniques, with an *MAvG* of 0.731.

Comparing the results in Table 10 with the results on Table 7, we observed that using the SMOTE increased the *MAvG* for the Random Forests and NAS-CNN algorithms, improving it in an average of 12.25% and 3.80%, respectively, despite of the feature extraction used. Analyzing Table 11, the outcome using the NAS-CNN with RMS and SMOTE-SVM shows even better results for a subject independent model, achieving an *MAvG* of 0.735.

A Wilcoxon signed-rank test shows that there is statistical difference between the chosen features (RMS and mDWT) for using SMOTE and SMOTE-SVM. Assuming that the two groups are identical as the null hypothesis and a two-sided level of significance ($\alpha = 0.05$), the test indicated that the *MAvG* for classification of movements for prosthetic hand is significantly greater using RMS ($Mdn_{SMOTE} = 0.676$ and $Mdn_{SMOTE-SVM} = 0.695$) than using mDWT ($Mdn_{SMOTE} = 0.621$ and $Mdn_{SMOTE-SVM} = 0.646$) ($Z_{SMOTE} = 595$, $p_{SMOTE} = 4.574E-16$ and $Z_{SMOTE-SVM} = 1310$, $p_{SMOTE-SVM} = 4.431E-10$).

We performed a Friedman test in order to evaluate if the improvements on the results with and without SMOTE and SMOTE-SVM are statistically significant. The test shows that there is a statistically significant difference between using or not using the SMOTE and SMOTE-SVM, $\chi^2(2) = 86.780$, $p = 1.432E-19$. Post hoc analysis with Wilcoxon signed-rank tests was conducted with a Bonferroni correction applied, resulting in a significance level set at $p < 0.017$. There are significant differences between the noSMOTE and SMOTE results ($Z = -7.203$, $p = 5.8804E-13$), the noSMOTE and SMOTE-SVM ($Z = -8.813$, $p = 3.3306E-32$), and the SMOTE and SMOTE-SVM ($Z = -3.152$, $p = 1.62E-03$).

Observing the results in Tables 9 to 11, we noticed that the synthetic oversampling

using SMOTE-SVM considerably increased the *MAvG* for all classification algorithms. Even though the results obtained are not directly comparable with (PIZZOLATO et al., 2017) because they use a different evaluation metric and a subject dependent approach. It is important to observe that the experiments using SMOTE in a subject independent model, achieve results very close to the current state-of-the-art using a subject dependent model. This means that we have been able to create a user-independent prosthetic control model with almost the same precision as a user-dependent system that the user would need to spend hours training before starting using the prosthesis.

Table 10 – Results for subject independent classifiers using SMOTE

| Class | Recall | | | | | |
|-------------|--------|-------|-------|-------|-------|-------|
| | RMS | | | mDWT | | |
| | RF | eCNN | NAS | RF | eCNN | NAS |
| R | 0.758 | 0.820 | 0.728 | 0.715 | 0.684 | 0.700 |
| B1 | 0.762 | 0.734 | 0.912 | 0.745 | 0.780 | 0.863 |
| B2 | 0.732 | 0.713 | 0.807 | 0.653 | 0.670 | 0.798 |
| B3 | 0.824 | 0.764 | 0.912 | 0.746 | 0.776 | 0.841 |
| B4 | 0.697 | 0.653 | 0.773 | 0.572 | 0.547 | 0.776 |
| B5 | 0.688 | 0.568 | 0.796 | 0.602 | 0.709 | 0.779 |
| B6 | 0.669 | 0.699 | 0.783 | 0.645 | 0.667 | 0.735 |
| B7 | 0.761 | 0.695 | 0.850 | 0.759 | 0.689 | 0.816 |
| B8 | 0.623 | 0.643 | 0.753 | 0.574 | 0.576 | 0.634 |
| B9 | 0.633 | 0.594 | 0.743 | 0.547 | 0.581 | 0.692 |
| B10 | 0.576 | 0.611 | 0.720 | 0.558 | 0.516 | 0.580 |
| B11 | 0.576 | 0.570 | 0.686 | 0.570 | 0.442 | 0.605 |
| B12 | 0.554 | 0.434 | 0.578 | 0.467 | 0.412 | 0.454 |
| B13 | 0.684 | 0.614 | 0.760 | 0.705 | 0.646 | 0.752 |
| B14 | 0.760 | 0.772 | 0.793 | 0.667 | 0.673 | 0.728 |
| B15 | 0.677 | 0.692 | 0.820 | 0.640 | 0.571 | 0.687 |
| B16 | 0.678 | 0.571 | 0.637 | 0.639 | 0.524 | 0.619 |
| B17 | 0.783 | 0.731 | 0.748 | 0.732 | 0.595 | 0.601 |
| C1 | 0.579 | 0.495 | 0.703 | 0.583 | 0.439 | 0.557 |
| C2 | 0.496 | 0.469 | 0.670 | 0.400 | 0.412 | 0.434 |
| C3 | 0.543 | 0.467 | 0.657 | 0.490 | 0.467 | 0.522 |
| C4 | 0.663 | 0.513 | 0.664 | 0.591 | 0.466 | 0.612 |
| C5 | 0.557 | 0.504 | 0.632 | 0.521 | 0.483 | 0.540 |
| C6 | 0.708 | 0.662 | 0.790 | 0.654 | 0.576 | 0.712 |
| C7 | 0.734 | 0.548 | 0.729 | 0.703 | 0.535 | 0.649 |
| C8 | 0.733 | 0.596 | 0.683 | 0.716 | 0.652 | 0.626 |
| C9 | 0.640 | 0.491 | 0.586 | 0.600 | 0.513 | 0.530 |
| C10 | 0.571 | 0.574 | 0.698 | 0.587 | 0.385 | 0.625 |
| C11 | 0.618 | 0.529 | 0.667 | 0.576 | 0.443 | 0.533 |
| C12 | 0.617 | 0.565 | 0.692 | 0.565 | 0.440 | 0.673 |
| C13 | 0.616 | 0.542 | 0.625 | 0.556 | 0.385 | 0.542 |
| C14 | 0.650 | 0.611 | 0.723 | 0.577 | 0.533 | 0.618 |
| C15 | 0.795 | 0.636 | 0.740 | 0.761 | 0.629 | 0.759 |
| C16 | 0.713 | 0.554 | 0.661 | 0.620 | 0.457 | 0.516 |
| C17 | 0.772 | 0.667 | 0.829 | 0.775 | 0.603 | 0.781 |
| C18 | 0.671 | 0.623 | 0.655 | 0.696 | 0.611 | 0.621 |
| C19 | 0.780 | 0.669 | 0.800 | 0.763 | 0.718 | 0.783 |
| C20 | 0.841 | 0.626 | 0.815 | 0.787 | 0.703 | 0.746 |
| C21 | 0.641 | 0.528 | 0.676 | 0.670 | 0.393 | 0.608 |
| C22 | 0.796 | 0.642 | 0.840 | 0.753 | 0.632 | 0.706 |
| C23 | 0.894 | 0.720 | 0.818 | 0.880 | 0.682 | 0.755 |
| MAvG | 0.679 | 0.606 | 0.731 | 0.635 | 0.555 | 0.652 |

Table 11 – Results for subject independent classifiers using SMOTE-SVM

| Class | Recall | | | | | |
|-------------|--------|-------|-------|-------|-------|-------|
| | RMS | | | mDWT | | |
| | RF | eCNN | NAS | RF | eCNN | NAS |
| R | 0.740 | 0.807 | 0.836 | 0.731 | 0.734 | 0.721 |
| B1 | 0.773 | 0.820 | 0.859 | 0.709 | 0.797 | 0.776 |
| B2 | 0.701 | 0.761 | 0.817 | 0.619 | 0.781 | 0.727 |
| B3 | 0.836 | 0.748 | 0.941 | 0.762 | 0.833 | 0.847 |
| B4 | 0.707 | 0.705 | 0.775 | 0.607 | 0.595 | 0.705 |
| B5 | 0.703 | 0.704 | 0.812 | 0.660 | 0.630 | 0.744 |
| B6 | 0.722 | 0.747 | 0.827 | 0.633 | 0.667 | 0.810 |
| B7 | 0.739 | 0.750 | 0.832 | 0.775 | 0.784 | 0.811 |
| B8 | 0.598 | 0.620 | 0.828 | 0.565 | 0.559 | 0.702 |
| B9 | 0.632 | 0.747 | 0.833 | 0.564 | 0.650 | 0.664 |
| B10 | 0.631 | 0.562 | 0.752 | 0.538 | 0.464 | 0.676 |
| B11 | 0.598 | 0.558 | 0.703 | 0.563 | 0.504 | 0.758 |
| B12 | 0.521 | 0.509 | 0.670 | 0.488 | 0.387 | 0.437 |
| B13 | 0.768 | 0.766 | 0.579 | 0.697 | 0.594 | 0.687 |
| B14 | 0.760 | 0.627 | 0.778 | 0.732 | 0.811 | 0.790 |
| B15 | 0.711 | 0.611 | 0.822 | 0.713 | 0.590 | 0.722 |
| B16 | 0.667 | 0.604 | 0.688 | 0.629 | 0.619 | 0.576 |
| B17 | 0.717 | 0.640 | 0.870 | 0.712 | 0.595 | 0.638 |
| C1 | 0.591 | 0.533 | 0.679 | 0.570 | 0.472 | 0.534 |
| C2 | 0.565 | 0.475 | 0.636 | 0.500 | 0.420 | 0.636 |
| C3 | 0.510 | 0.529 | 0.580 | 0.426 | 0.511 | 0.544 |
| C4 | 0.623 | 0.571 | 0.816 | 0.604 | 0.553 | 0.706 |
| C5 | 0.559 | 0.476 | 0.608 | 0.564 | 0.479 | 0.515 |
| C6 | 0.698 | 0.789 | 0.773 | 0.658 | 0.545 | 0.605 |
| C7 | 0.658 | 0.625 | 0.698 | 0.690 | 0.509 | 0.653 |
| C8 | 0.664 | 0.669 | 0.810 | 0.628 | 0.726 | 0.726 |
| C9 | 0.706 | 0.598 | 0.822 | 0.667 | 0.549 | 0.608 |
| C10 | 0.550 | 0.578 | 0.693 | 0.556 | 0.482 | 0.688 |
| C11 | 0.600 | 0.522 | 0.603 | 0.651 | 0.504 | 0.673 |
| C12 | 0.630 | 0.564 | 0.557 | 0.646 | 0.450 | 0.639 |
| C13 | 0.674 | 0.619 | 0.788 | 0.640 | 0.562 | 0.580 |
| C14 | 0.577 | 0.535 | 0.689 | 0.603 | 0.525 | 0.602 |
| C15 | 0.795 | 0.605 | 0.629 | 0.775 | 0.626 | 0.639 |
| C16 | 0.695 | 0.612 | 0.758 | 0.570 | 0.477 | 0.507 |
| C17 | 0.805 | 0.662 | 0.849 | 0.754 | 0.687 | 0.677 |
| C18 | 0.676 | 0.580 | 0.564 | 0.659 | 0.683 | 0.656 |
| C19 | 0.772 | 0.707 | 0.599 | 0.715 | 0.677 | 0.786 |
| C20 | 0.811 | 0.775 | 0.870 | 0.802 | 0.627 | 0.746 |
| C21 | 0.648 | 0.512 | 0.583 | 0.647 | 0.470 | 0.587 |
| C22 | 0.761 | 0.711 | 0.775 | 0.761 | 0.720 | 0.761 |
| C23 | 0.838 | 0.787 | 0.845 | 0.883 | 0.750 | 0.768 |
| MAvG | 0.676 | 0.635 | 0.735 | 0.644 | 0.589 | 0.667 |

6.5 Experiment #4: Improving the results with additional sensors

The results of the previous experiments show that the use of NAS-CNN is the best option for a subject independent classification approach using EMG signals. The use of SMOTE-SVM improves the classifier’s performance but there is still room for improvements. In this section we perform experiments using the NAS-CNN with RMS using the all data from the Ninapro dataset. As stated in Section 6.1.1, additional sensors from a CyberGlove II were captured along with the EMG during the Ninapro DB5’s acquisition protocol. We conduct experiments comparing the classification performance between the Ninapro DB5 using only EMG data and the Ninapro DB5 using EMG and CyberGlove II.

In this experiment we included 25 additional data signals to the EMG signal from the Ninapro DB5, having a total of 41 channels. This additional data was collected by Pizzolato et al. (2017) using a CyberGlove II, with 22 flex sensors and a 3-axis accelerometer. We performed the RMS feature extraction in all sensors. Subsequently, we trained the NAS-CNN algorithm with this data, achieving an *MAvG* of 0.884, an improvement of 20% compared to the results from Experiment #3. We then applied SMOTE-SVM in the new data and one more time, trained the NAS-CNN to classify the 41 different movements. The obtained results were better than the results from the previous experiments. Table 12 presents the recall per class for each dataset using NAS-CNN with RMS as the classifier.

Table 12 – Results for subject independent classifier NAS-CNN using RMS as feature extraction. The first column presents the results using NAS-CNN with RMS from Table 11; The second column present the experiments using EMG and the CyberGlove II; The third column shows the experiments using EMG and CyberGlove II with synthetic examples from SMOTE-SVM.

| Class | Recall | | |
|-------------|------------------|-----------|------------------------|
| | EMG SMOTE-SVM | EMG+GLOVE | EMG+GLOVE SMOTE-SVM |
| R | 0.836 | 0.945 | 0.752 |
| B1 | 0.859 | 0.938 | 0.992 |
| B2 | 0.817 | 0.872 | 1.000 |
| B3 | 0.941 | 0.932 | 0.957 |
| B4 | 0.775 | 0.956 | 0.942 |
| B5 | 0.812 | 0.814 | 0.893 |
| B6 | 0.827 | 0.917 | 0.980 |
| B7 | 0.832 | 0.982 | 0.991 |
| B8 | 0.828 | 0.737 | 0.956 |
| B9 | 0.833 | 0.822 | 0.850 |
| B10 | 0.752 | 0.884 | 0.885 |
| B11 | 0.703 | 0.737 | 0.930 |
| B12 | 0.670 | 0.734 | 0.762 |
| B13 | 0.579 | 0.978 | 0.825 |
| B14 | 0.778 | 0.928 | 0.932 |
| B15 | 0.822 | 0.988 | 0.978 |
| B16 | 0.688 | 0.724 | 0.804 |
| B17 | 0.870 | 0.857 | 0.912 |
| C1 | 0.679 | 0.927 | 0.939 |
| C2 | 0.636 | 0.764 | 0.930 |
| C3 | 0.580 | 0.895 | 0.956 |
| C4 | 0.816 | 0.835 | 0.928 |
| C5 | 0.608 | 0.835 | 0.921 |
| C6 | 0.773 | 0.927 | 0.972 |
| C7 | 0.698 | 0.960 | 0.970 |
| C8 | 0.810 | 0.963 | 0.965 |
| C9 | 0.822 | 0.878 | 0.966 |
| C10 | 0.693 | 0.875 | 0.973 |
| C11 | 0.603 | 0.800 | 0.875 |
| C12 | 0.557 | 0.875 | 0.944 |
| C13 | 0.788 | 0.849 | 0.878 |
| C14 | 0.689 | 0.827 | 0.950 |
| C15 | 0.629 | 0.977 | 0.930 |
| C16 | 0.758 | 0.927 | 0.917 |
| C17 | 0.849 | 0.969 | 0.963 |
| C18 | 0.564 | 0.956 | 0.932 |
| C19 | 0.599 | 0.932 | 0.969 |
| C20 | 0.870 | 0.952 | 0.967 |
| C21 | 0.583 | 0.855 | 0.930 |
| C22 | 0.775 | 0.906 | 0.967 |
| C23 | 0.845 | 0.959 | 0.968 |
| MAvG | 0.735 | 0.884 | 0.926 |

7 Prototype Development

Due to the elevated cost of the data capture devices and the few options of sensors, such as CyberGlove II, one of the goals of this project is to develop a low-cost hand movement data acquisition device. Resulting in capturing acceleration, orientation, finger joint angles, proximity of each finger to an object, and physical pressure on each finger while grasping an object for example.

7.1 System Overview

Figure 20 presents an overview of the system. The system is composed of two parts: A sensor unit, which is a glove with sensors to capture movements which is worn by the user, and a base unit which is positioned on the individual's forearm for signal processing and store data locally.

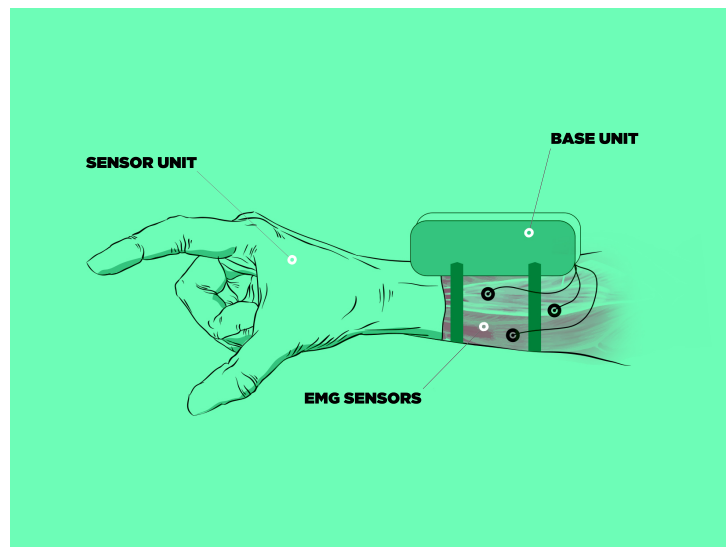


Figure 20 – Overview of the system

The base unit contains a computing platform, a battery, a battery charger circuit, and the circuits required for proper acquisition of sensor data. The data is organized and saved in a Comma Separated Value (CSV) file.

In order to optimize the weight distribution, the base unit is fixed in the individual's forearm as shown in Figure 20. The EMG sensor is placed over the muscles: *Flexor Digitorum Superficialis*, *Flexor Carpi Radialis*, *Extensor Carpi Radialis Longus* as recommended by Keating (2013) and Thalmic Labs (2016b), the device's manufacturer.

Figure 21 illustrates the components in the sensor unit. The main role of the sensor unit is to keep the sensors in place and wire them to the base unit.

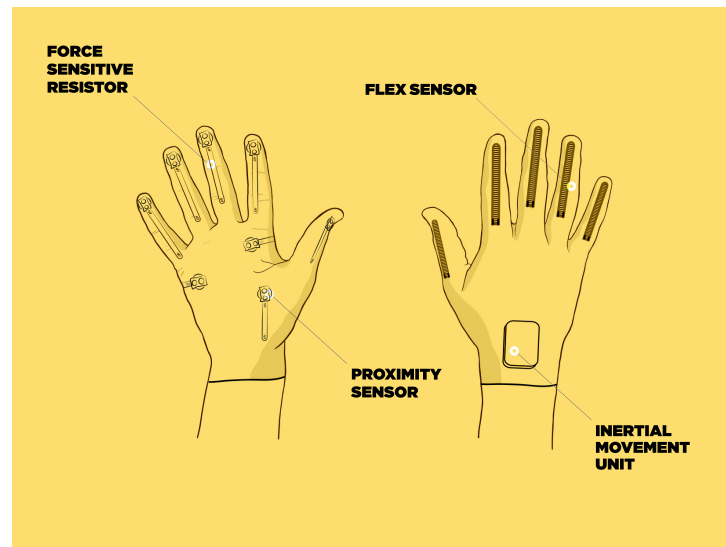


Figure 21 – Sensor Unit Overview

7.1.1 Project Specifications

The device must be robust to be used in research experiments. In order to assure quality in the experiments, requirements must be completed such as: sensors must be integrated into the system; in order to collect more natural movements inside and outside the laboratory, the system must be lightweight and operable for a long period of time. These are some examples of the project's specific requirements we set for our device. The full list of requirements and requirement achievements are available in Appendix ??, Table 13.

7.2 Hardware Implementation

7.2.1 Electronic Design

This section presents the choices made for the electronic design including sensor selection and PCB layout.

7.2.1.1 Computing Platform

The Intel Edison was chosen to be our processor. It has a 22nm Intel SoC that includes a dual-core Intel Atom CPU at 500 MHz and a 32-bit Intel Quark microcontroller (MCU) at 100 MHz. The main advantage of having a MCU is that the data can be pre-processed in it and then delivered to the CPU for heavier processing.

The Intel Edison includes a 1 GB LPDDR3 POP memory, 4 GB eMMC storage, Wi-Fi dual-band and Bluetooth 4.0 integrated (INTEL CORPORATION, 2014). One of the main advantage of the Intel Edison is that it includes all this features with a very low

power consumption.

We chose an Arduino Breakout Board to be used with the Edison. This breakout board is designed to be hardware and software pin-compatible with Arduino shields designed for the Arduino Uno R3. The board also has a microSD card slot, micro USB connector, USB 2.0 Host connector and many others features as seen on Figure 22.

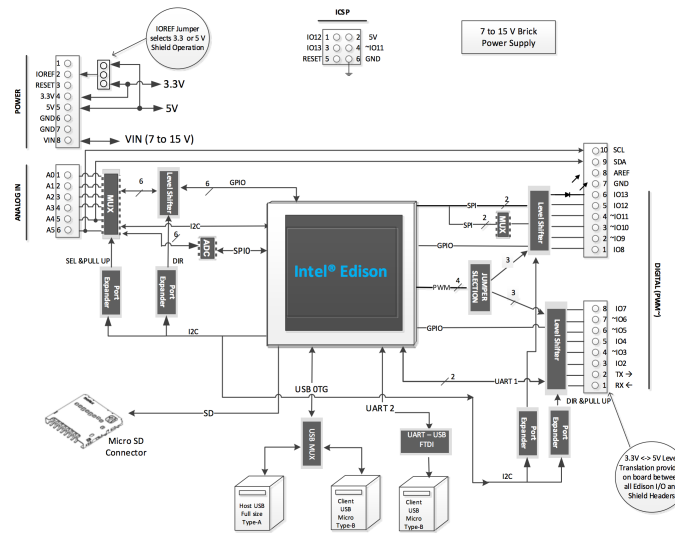


Figure 22 – Intel Edison kit for Arduino block diagram

Source – Intel Corporation (2015b)

7.2.1.2 Electromyography Sensor

Since our goal is to create a low-cost device, we chose the Myo Armband as our EMG sensor. The Myo Armband is an intelligent armband for gesture control. It detects motion in two ways: muscle activity and motion sensing (NUWER, 2013).

As seen on Thalmic Labs (2016a), the Myo Armband uses Bluetooth 4.0 Low Energy to communicate with other devices. It has on-board rechargeable Lithium-Ion batteries and an ARM Cortex M4 Processor. Its sensors are eight Medical Grade Stainless Steel EMG surface electrodes, and highly sensitive nine-axis IMU with three-axis gyroscope, three-axis accelerometer, and three-axis magnetometer, making it the perfect candidate as our EMG/IMU sensor, costing only \$200.

7.2.1.3 FSR, Flex and Proximity Sensors

As seen in section 7.1, our device is completely customized for our application. Therefore, for the sensors that are attached to the glove, we chose to create our own circuits. Being able to fully customize the sensors for our device.

As the FSR, we chose the Interlink Electronics FSR402, a force sensitive resistor that can measure from 0.1 to 10^{02} Newtons of force (ELECTRONICS, 2015). The flex

sensor was the Spectra Symbol FS-L-0055-253-ST, measuring angular displacements from 0 to 180 degrees (SPECTRA SYMBOL, 2014). We chose the Vishay VCNL4040 as our proximity sensor. It is a tiny sensor (4.0mm x 2.0mm x 1.1mm) which detects objects within a range of 200mm (VISHAY SEMICONDUCTORS, 2015).

7.2.2 Printed Circuit Board Design

We first designed a wiring diagram, presented on Figure 23, of how the hardware is connected, including the communication protocols used.

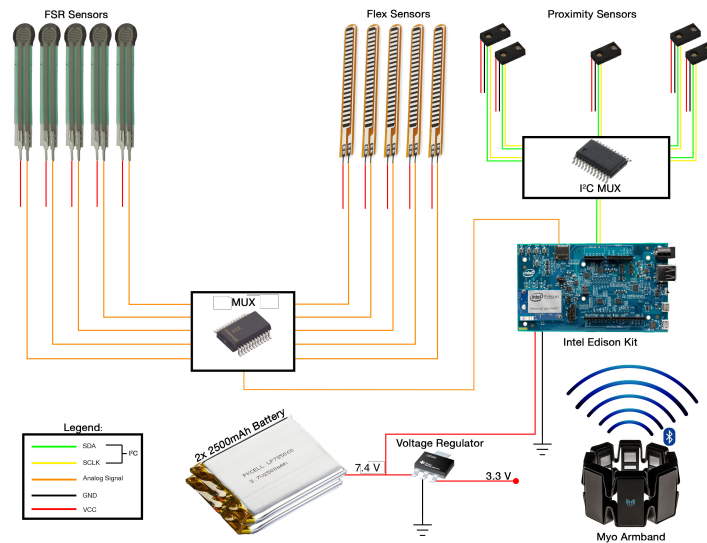


Figure 23 – Overview of the hardware connection

In order to translate the connections presented on Figure 23 with fidelity to our system, we designed a printed circuit board (PCB), hereafter referred to as base board. Due to the dimensions of the proximity sensors, we had to design a specific breakout board for it. This breakout board gives access to the I^2C , V_{cc} and GND pins.

The base board is the most important part of the system. This board contains signal conditioning, analog to digital converters, multiplexers and power supply circuits to have a high-fidelity data acquisition from all sensors. It has the shape of an Arduino Uno Shield to better fit the Intel Edison Arduino Expansion Board pins.

Figure 24 presents the PCBs for the proximity breakout board and the base board.

For a better understanding of the circuits, the electric schematics are shown on Appendix B.

7.2.3 Mechanical Design

In the design process for the sensor unit, we opt to use a glove made out of cotton. The sensors slide into pockets sew on the glove. This pocket approach is useful because

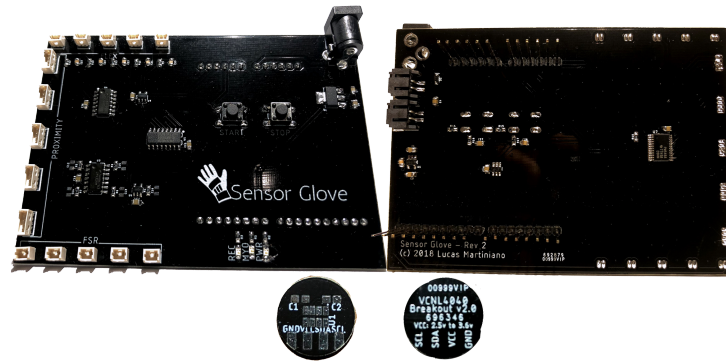


Figure 24 – Overview of base board and proximity sensor breakout board

it facilitates the removal of the sensors for eventual repairs.

An enclosure box was designed to fit all the components used in this project. It was designed using the software Solidworks (Figure 25) and printed in a 3D printer.

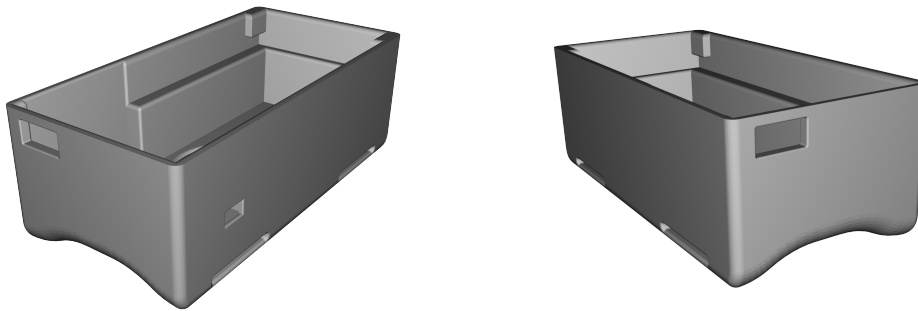


Figure 25 – 3D Printed Box

7.3 Software Implementation

7.3.1 Operating System

The Edison Module combines a dual-core Atom processor running Yocto Linux at 500MHz with an Intel's MCU Quark processor clocked at 100MHz. The Quark co-processor runs Viper RTOS, a real-time operating system (INTEL CORPORATION, 2015a).

The Yocto Project is a collaborative open-source project that provides templates, tools and methods to assist in the creation of Linux-based systems for embedded systems, regardless of the hardware architecture used (PROJECTS, 2016). Viper provides basic OS function support, including thread scheduling, memory management, interrupt dispatch, and more. The MCU is a separate CPU that handles the interface with the outside world. The advantage of the Intel Edison OS is that we can ignore this separation because the

main CPU (Intel Atom) communicates with the MCU by itself as can be seen in Figure 26.

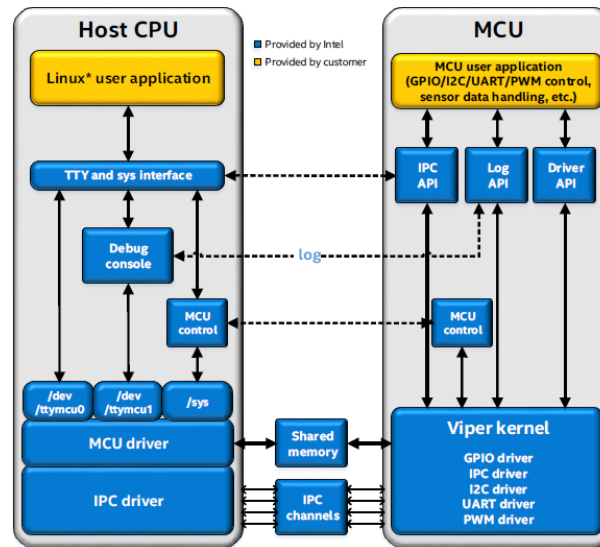


Figure 26 – CPU + MCU Integration

Source – Intel Corporation (2015a)

7.3.2 Application

This section focuses on the design of the application that controls our device. It handles all calculations, peripheral communication, sensor integration and data storing.

The software was coded in Node.js because of its support with the package Noble¹. It is a package for writing programs that interact with Bluetooth Low Energy devices, making it possible to communicate the Intel Edison with the Myo Armband.

The algorithm first initializes the variables and defines the GPIOs that are be used, then it configures the I^2C , analog ports and connects via Bluetooth with the Myo Armband. The system waits for the user to press the record button to start recording the sensor's data in a CSV file. To stop recording, the user needs to press the stop button. After the system finishes recording each movement, it waits for the user to press the record button again, making process of the data collection more efficient. Figure 27 illustrates the flow of the system.

7.4 Results

In this section we discuss the outcomes of our prototype. A multi-modal data capture device was especially designed to record hand movement data following the specifications established by the author (Figure 28).

¹ <<https://github.com/sandeepmistry/noble>>

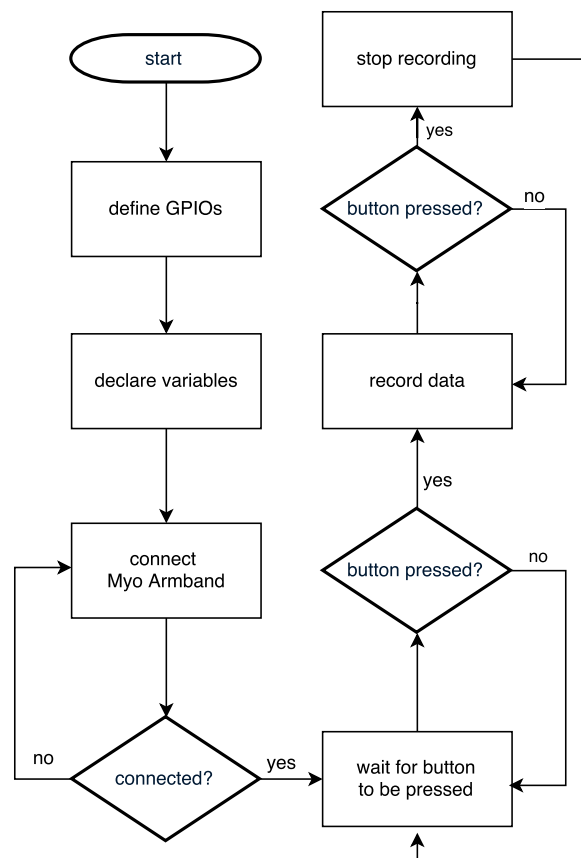


Figure 27 – Activity diagram

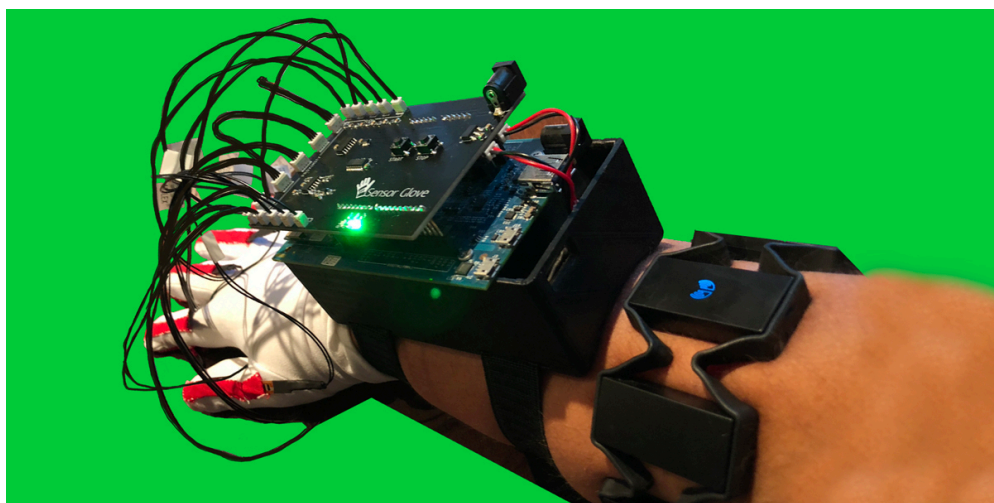


Figure 28 – Final prototype. This picture shows the final configuration of the device. All principal electric components were placed in the 3d printed box to protect the equipment from sweat contact.

Table 13 – Comparison of project’s requirements and prototype’s achievements

| Number | Name | Description | Threshold | Objective | Completed |
|-------------------|---------------------|---|--|---|--------------------------|
| MECHANICAL | | | | | |
| M001 | Overall size | Overall dimensional constraints of the device | Fit into ski glove | Fit into golf/driving glove | ✓Driving Glove |
| | Sensor size | Dimensional limits on any single finger or palm sensor | 25 x 13mm | 20 x 8mm | ✓ < 20 x 8mm |
| | Base unit size | External controller unit size | 145mmx70mmx80mm | 70mmx60mmx20mm | ✓ |
| POWER | | | | | |
| P001 | Op Voltage | Operating voltage | DC <14.4V | | ✓7.4V |
| P002 | Battery life | Battery life for 100% operation | 10 hours (continuous) | 24 hours (continuous) | ✓≈ 25 hours (continuous) |
| P003A1 | Charging | Charge time | <5 Hours | <3 Hours | ✓2.5 hours |
| P003A2 | Charge cable | | USB | Wireless standard compliant | ✓MiniUSB |
| P003B | Replacement | Replaceable battery option | Commercially available | | ✓Li-Ion Batteries |
| ELECTRICAL | | | | | |
| E001 | μP | μP Capabilities and Speed | Sufficient to meet sensor requirements and processing at 100ms intervals | Sufficient to meet sensor requirements and processing at 50ms intervals | ✓Intel Edison @ 5ms |
| E002 | Connectors | Connectorization of sensors and wiring | All sensors shall be connectorized for easy repair/replacement | | ✓Molex connectors |
| DATA | | | | | |
| D001 | Finger sensor range | Distance to detect object | 3” | 6” | ✓7.8” |
| D002 | Accelerometer | Accelerometer resolution | +/-3g at 12 bit | +/-3g at 14 bit | ✓+/-3g at 12 bit |
| D003 | Magnetometer | | 12 bit | 14 bit | ✓12 bit |
| D004 | Gyro | | 12 bit | 14 bit | ✓12 bit |
| D005 | Myo Data | | 2 Myo channels at 12 bit | 2 Myo channels at 14 bit | ✓8 channels at 12 bit |
| UI | | | | | |
| UI001 | Display | Representation of recording state and result of decision making | LED indication of power, recording, and decision output, at least 4 unique items | Character display | ✓LED |
| UI002 | Input | Ability to tag data and interface | Controls for power, begin/end recording, and 3 data event tags | Controls for power, begin/end recording, and six data event tags | ✓Begin/end recording |
| SOFTWARE | | | | | |
| SW001 | Language | | Common programming language | | ✓JavaScript |

The device was designed to be used in research experiments. For this reason, we defined requirements for it. Table 13 shows the requirements recommended for the device and how our design fulfills these requirements.

7.4.1 Costs

Since the purpose of our device is to be low-cost compared to the similar ones available on the market, Table 14 shows a detailed price breakdown of our device.

Table 14 – Price breakdown of our device

| Qty | Description | Price | Total |
|--------------|-------------------------|----------|-----------------|
| 2 | Push Button | \$0.35 | \$0.70 |
| 1 | Schottky Diode | \$0.33 | \$0.33 |
| 3 | LED | \$0.17 | \$0.51 |
| 25 | Capacitor | \$0.03 | \$0.75 |
| 18 | Resistor | \$0.02 | \$0.36 |
| 15 | Sensor Connector | \$0.25 | \$3.75 |
| 1 | Multiplexer | \$0.62 | \$0.62 |
| 3 | Power Connector | \$0.75 | \$2.25 |
| 2 | Voltage Regulator | \$0.79 | \$1.58 |
| 4 | Operational Amplifier | \$1.15 | \$4.60 |
| 1 | Schmitt trigger | \$0.54 | \$0.54 |
| 1 | I2C Multiplexer | \$1.51 | \$1.51 |
| 6 | PCB Manufacturer | \$0.49 | \$2.94 |
| 1 | Cotton Glove | \$5.00 | \$5.00 |
| 1 | Myo Armband | \$200.00 | \$200.00 |
| 5 | Flex Sensor | \$7.00 | \$35.00 |
| 5 | FSR Sensor | \$7.00 | \$35.00 |
| 5 | Proximity Sensor | \$1.63 | \$8.15 |
| 15 | Wire | \$2.20 | \$33.00 |
| 2 | Battery | \$14.95 | \$29.90 |
| 1 | Battery Charger | \$12.50 | \$12.50 |
| 1 | Intel Edison + Breakout | \$79.00 | \$79.00 |
| Total | | | \$457.99 |

Comparing our device cost with products presented in Chapter 5, our glove has a lower cost with virtually the same or better functionality. For instance, a CyberGlove II, which to the best of our knowledge is the most used data glove in the literature consisting of 22 flex sensors and an accelerometer, costs around \$18,000. Price-wise our device is more than 39 times cheaper than the CyberGlove II and it has a broader number and variety of sensors such as EMG, IMU, force and proximity sensors.

7.5 Data Collection

Before starting the data collection task, we submitted the project to the Seattle Pacific University Institutional Review Board (IRB), also known as ethical committee. The data acquisition protocol was approved by the Seattle Pacific University IRB (IRB number: 171801010).

In the data collection process, we recruited 5 subjects via email solicitations and texts. Each subject was requested to give informed consent and to answer questions including age, sex, height, weight and laterality. Afterwards, they were asked to wear the data collection device, sit in at desk on an office chair and comfortable rest the arms on the desk. A screen was placed in front of them randomly showing the movements they should perform. Each subject performed 6 repetitions of 21 grasping and functional movements, including rest position. The set of movements were selected from Feix et al. (2016) with the goal of replicating most of the activities of daily living (ADL), and are available at Appendix C.

The database, hereafter referred to as Sensor Glove database (SGDB), contains one csv file with synchronized variables for each subject. The variables included in the files are:

- subject (1 column): subject id
- emg (16 columns): two samples of sEMG signal of 8 electrodes
- imu (10 columns): signal from the Myo armband's IMU
- flex (5 columns): signal from the 5 flex sensors of our glove
- fsr (5 columns): signal from the 5 FSR sensors of our glove
- prox (5 columns): signal from the 5 proximity sensors of our glove
- repetition (1 column): repetition of the movement
- movement (1 column): movement id

Figure 29 presents the class distribution for all the subjects. Because the distribution in the data is not equal, we calculate the SGBD's imbalance ratio:

$$IR = \{\mathbf{0} : 1.07; \mathbf{1} : 1.10; \mathbf{2} : 1.22; \mathbf{3} : 1.30; \mathbf{4} : 1.11; \\ \mathbf{5} : 1.11; \mathbf{6} : 1.22; \mathbf{7} : 1.31; \mathbf{8} : 1.24; \mathbf{9} : 1.37; \\ \mathbf{10} : 1.23; \mathbf{11} : 1.15; \mathbf{12} : 1.16; \mathbf{13} : 1.31; \mathbf{14} : 1.16; \\ \mathbf{15} : 1.00; \mathbf{16} : 1.24; \mathbf{17} : 1.11; \mathbf{18} : 1.21; \mathbf{19} : 1.17; \mathbf{20} : 1.32\}$$

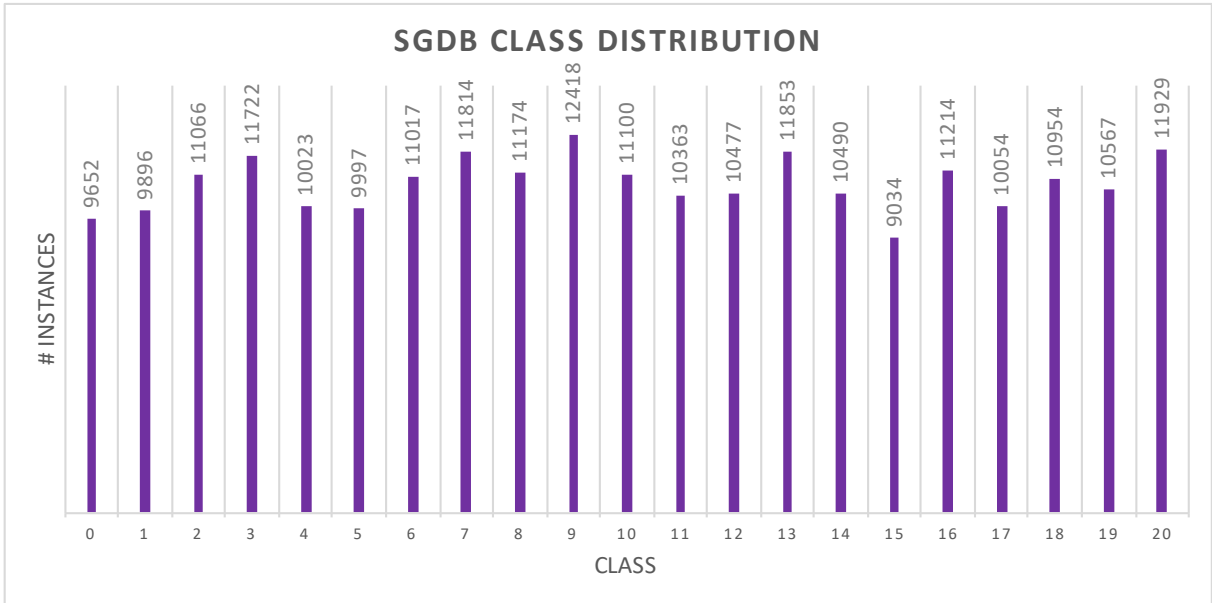


Figure 29 – Class distribution for the Sensor Glove database. The vertical axis shows the number of examples for all the subjects, the horizontal axis shows the class identification number.

7.6 Low-cost sensor glove validation

This section aims to verify the functionalities of the proposed device. We performed experiments using 20 movements + rest (i.e. 21 classes) from the SGDB. We applied the algorithm NAS-CNN using RMS as a subject independent approach (Chapter 6, Section 6.3) in the SGDB using only EMG signals and in the SGDB using all 41 signals. It should be noted that the results obtained using the SGDB cannot be direct compared with the results from Chapter 6, because the SGDB’s data acquisition protocol differs from the Ninapro DB5. The data from the Ninapro DB5 is submitted throughout several signal processing steps such as: synchronization of the data using linear or nearest neighbor interpolation; relabeling the data to perfect match only the performed movement, using a generalize likelihood ratio algorithm; and filtering the data to remove noise.

Table 15 presents the recall for each movement and $MAvG$ for each configuration of the database. Analyzing the results using our device, it is noticeable that the classification performance improved from $MAvG = 0.370$ using only EMG signals to $MAvG = 0.581$ using additional sensors. Proving that the use of additional sensors from our device along with the EMG signal improves the classification performance.

Table 15 – Results for the SGDB with EMG only and with all sensors. Using NAS-CNN classifier with RMS as feature extraction in a subject independent approach.

| Class | Recall | |
|-------------|------------------|-------|
| | SGDB EMG only | SGDB |
| R | 0.900 | 0.750 |
| C1 | 1.000 | 0.938 |
| C2 | 0.500 | 0.657 |
| C3 | 0.387 | 0.778 |
| C4 | 0.349 | 0.678 |
| C5 | 0.762 | 0.761 |
| C6 | 0.172 | 0.659 |
| C7 | 0.111 | 0.240 |
| C8 | 0.500 | 0.406 |
| C9 | 0.312 | 0.318 |
| C10 | 0.165 | 0.469 |
| C11 | 0.429 | 0.732 |
| C12 | 0.167 | 0.625 |
| C13 | 0.750 | 0.410 |
| C14 | 0.794 | 0.788 |
| C15 | 0.200 | 0.560 |
| C16 | 0.300 | 0.468 |
| C17 | 0.243 | 0.581 |
| C18 | 0.800 | 0.726 |
| C19 | 0.102 | 0.486 |
| C20 | 0.750 | 0.796 |
| MAvG | 0.370 | 0.581 |

8 Concluding Remarks

This work presents new machine learning approaches in order to improve the current results for classification of hand movements for prosthetic devices presented in the literature. In addition, due to the high cost of data capture devices, we built a new multi-sensor device for capturing hand movements. With this device we created a database with 21 hand movements. Finally, we verified the functionalities of the device we proposed, by comparing our database with the data from the Ninapro database, a database that uses a setup similar to ours.

To the best of our knowledge, nearly all of the authors use accuracy to evaluate the classification of hand movements, which is usually an imbalanced problem. We propose the use of a metric called *MAvG*, which accounts each value representing the classification performance for a specific class equally. It is also important to point out that most of the authors do not specify whether they train one algorithm specifically for each subject or if they train one algorithm for all subjects, we named that Subject Dependent and Subject Independent approaches, respectively.

We performed experiments to evaluate how different machine learning techniques affect the results of the Ninapro DB5. The results using a subject dependent approach shows significant improvements when deep learning techniques, more specifically convolutional neural networks generated by a neural architecture search algorithm, are applied on the Ninapro data. When these techniques are applied in a subject independent approach, the results are worse, but considering that the classification model will be deployed in a prosthetic hand, it will save the user the hassle of having to spend their time and money training the prosthesis specifically for their use.

Considering the variability given by the sensors depending on the subject information as well as the precise location where they are placed. We performed experiments to investigate whether or not it is possible to improve the classification results (for both subject-dependent and subject-independent approaches) using methods that automatically generates synthetic samples in order to balance the database. The results show that the use of synthetic samples to balance the database improve the classification performance significantly. It is important to point out that using synthetic sampling and deep learning techniques for a subject-independent approach, improves even more the classification, achieving results very close to the current state-of-the-art using a subject dependent model. This means that we have been able to create a user-independent prosthetic control model with almost the same precision as a user-dependent system that the user would need to spend hours training before starting using the prosthesis.

Besides using only EMG signals, we suggest that the use of additional sensors along with the EMG, improve the classification results. Applying the ML techniques proposed on the previous experiments, using the Ninapro DB5 with the sensors from 2 Myo armbands (16 EMG channels) and a CyberGlove II (22 flex sensors and a 3-axis accelerometer), we were able to classify 92.6% of the movements correctly, proving that the use of additional sensors help to improve the classification performance for hand movements. However, the CyberGlove II has an extremely high price.

Thus, in order to find an alternative to the CyberGlove II, we created a low-cost hand motion capture device. We performed tests using the SGDB, a database of hand movements using the motion capture device created by the author of this dissertation. The results for a subject-independent approach using NAS-CNN, shows that using our device along with the EMG sensors from the Myo Armband, improves the classification performance for classification of hand movements, showing that our glove is a viable alternative to the CyberGlove II.

Bibliography

- ABBR. Associação Brasileira Beneficente de Reabilitação. *Estatísticas*. 2016. Available from Internet: <www.abbr.org.br>. Cited July, 2017. 14
- ABDELMASEEH, M.; CHEN, T. W.; STASHUK, D. W. Extraction and classification of multichannel electromyographic activation trajectories for hand movement recognition. *IEEE Transactions on Neural Systems and Rehabilitation Engineering*, v. 24, n. 6, p. 662–673, June 2016. ISSN 1534-4320. 43, 48
- ABDIANSAH, Abdiansah; WARDOYO, Retantyo. Time complexity analysis of support vector machines (svm) in libsvm. *International Journal Computer and Application*, 2015. 69
- ADAFRUIT LEARN. *Force Sensitive Resistor (FSR)*. 2012. Available from Internet: <<https://learn.adafruit.com/force-sensitive-resistor-fsr/>>. Cited August 2017. 22
- ADEWUYI, A. A.; HARGROVE, L. J.; KUIKEN, T. A. An analysis of intrinsic and extrinsic hand muscle emg for improved pattern recognition control. *IEEE Transactions on Neural Systems and Rehabilitation Engineering*, v. 24, n. 4, p. 485–494, April 2016. ISSN 1534-4320. 43, 48
- AJIBOYE, A. B.; WEIR, R. F. A heuristic fuzzy logic approach to emg pattern recognition for multifunctional prosthesis control. *IEEE Transactions on Neural Systems and Rehabilitation Engineering*, v. 13, n. 3, p. 280–291, Sept 2005. ISSN 1534-4320. 38, 40, 46
- AL-TIMEMY, A. H.; KHUSHABA, R. N.; BUGMANN, G.; ESCUDERO, J. Improving the performance against force variation of emg controlled multifunctional upper-limb prostheses for transradial amputees. *IEEE Transactions on Neural Systems and Rehabilitation Engineering*, v. 24, n. 6, p. 650–661, June 2016. ISSN 1534-4320. 39, 44, 48, 60
- AMPUTEE COALITION. Prosthetic devices for upper-extremity amputees. *Military in-Step*, 2014. 14
- AMPUTEE COALITION; O&P EDGE. Amputee patient comfort and compliance. *inMotion*, v. 21, September/October 2011. 14
- AMSUESS, S.; VUJAKLIJA, I.; GOEBEL, P.; ROCHE, A. D.; GRAIMANN, B.; ASZMANN, O. C.; FARINA, D. Context-dependent upper limb prosthesis control for natural and robust use. *IEEE Transactions on Neural Systems and Rehabilitation Engineering*, v. 24, n. 7, p. 744–753, July 2016. ISSN 1534-4320. 38, 39
- ANG, Wei-Tech; Khosla , Pradeep; RIVIERE, Cameron. Design of all-accelerometer inertial measurement unit for tremor sensing in hand-held microsurgical instrument. In: *IEEE International Conference on Robotics and Automation*. : IEEE, 2003. p. 1781–1786. 21

ATKINS, Diane J; HEARD, Denise CY; DONOVAN, William H. Epidemiologic overview of individuals with upper-limb loss and their reported research priorities. *JPO: Journal of Prosthetics and Orthotics*, LWW, v. 8, n. 1, p. 2–11, 1996. 38

ATZORI, Manfredo; COGNOLATO, Matteo; MÜLLER, Henning. Deep learning with convolutional neural networks applied to electromyography data: a resource for the classification of movements for prosthetic hands. *Frontiers in neurorobotics*, Frontiers, v. 10, p. 9, 2016. 15, 60

ATZORI, Manfredo; GIJSBERTS, Arjan; CASTELLINI, Claudio; CAPUTO, Barbara; HAGER, Anne-Gabrielle Mittaz; ELSIG, Simone; GIATSIDIS, Giorgio; BASSETTO, Franco; MÜLLER, Henning. Electromyography data for non-invasive naturally-controlled robotic hand prostheses. *Scientific data*, Nature Publishing Group, v. 1, p. 140053, 2014. 43, 48, 57, 60

BASMAJIAN, J.V.; LUCA, C.J. De. *Muscles Alive: Their Functions Revealed by Electromyography*. Williams & Wilkins, 1985. ISBN 9780683004144. Available from Internet: <<https://books.google.com.br/books?id=H9pqAAAAMAAJ>>. 20

BENET, Gines; BLANES, Francisco; SIMÓ, José E; PÉREZ, Pascual. Using infrared sensors for distance measurement in mobile robots. *Robotics and autonomous systems*, Elsevier, v. 40, n. 4, p. 255–266, 2002. 23

BERGER, Norman; HUPPERT, Curtis R. The use of electrical and mechanical muscular forces for the control of an electrical prosthesis. *The American journal of occupational therapy: official publication of the American Occupational Therapy Association*, v. 6, n. 3, p. 110, 1952. 38

BIDDISS, Elaine A; CHAU, Tom T. Upper limb prosthesis use and abandonment: a survey of the last 25 years. *Prosthetics and orthotics international*, SAGE Publications Sage UK: London, England, v. 31, n. 3, p. 236–257, 2007. 38

BOCA, Adrian Del; PARK, Dong C. Myoelectric signal recognition using fuzzy clustering and artificial neural networks in real time. In: IEEE. *1994 IEEE International Conference on Neural Networks*. 1994. v. 5, p. 3098–3103. 38, 39, 45

BONIVENTO, Claudio; DAVALLI, Angelo; FANTUZZI, Cesare; SACCHETTI, Rinaldo; TERENCEZI, Sabina. Automatic tuning of myoelectric prostheses. *Journal of rehabilitation research and development*, REHABILITATION RESEARCH & DEVELOPMENT SERVICE, v. 35, p. 294–304, 1998. 19

CAMPBELL, JD. An infrared distance sensor, analysis and test results. 1984. 23

CAREY, Stephanie L; LURA, Derek J; HIGHSMITH, M Jason. Differences in myoelectric and body-powered upper-limb prostheses: Systematic literature review. *Journal of Rehabilitation Research & Development*, v. 52, n. 3, 2015. 38

CHAN, Adrian DC; ENGLEHART, Kevin B. Continuous myoelectric control for powered prostheses using hidden markov models. *IEEE Transactions on Biomedical Engineering*, IEEE, v. 52, n. 1, p. 121–124, 2005. 38, 41, 46

CHAN, Francis HY; YANG, Yong-Sheng; LAM, FK; ZHANG, Yuan-Ting; PARKER, Philip A. Fuzzy emg classification for prosthesis control. *IEEE transactions on rehabilitation engineering*, IEEE, v. 8, n. 3, p. 305–311, 2000. 24, 38, 40, 45

CHAWLA, Nitesh V; BOWYER, Kevin W; HALL, Lawrence O; KEGELMEYER, W Philip. Smote: synthetic minority over-sampling technique. *Journal of artificial intelligence research*, v. 16, p. 321–357, 2002. 36

CHOROST, Michael. *A True Bionic Limb Remains Far Out of Reach*. 2012. Available from Internet: <http://www.wired.com/2012/03/ff_prosthetics/>. Cited August 2017. 19

CHOWDHURY, Suman Kanti; NIMBARTE, Ashish D; JARIDI, Majid; CREESE, Robert C. Discrete wavelet transform analysis of surface electromyography for the fatigue assessment of neck and shoulder muscles. *Journal of Electromyography and Kinesiology*, Elsevier, v. 23, n. 5, p. 995–1003, 2013. 28

CHU, Jun-Uk; LEE, Yun-Jung. Conjugate-prior-penalized learning of gaussian mixture models for multifunction myoelectric hand control. *IEEE Transactions on Neural Systems and Rehabilitation Engineering*, IEEE, v. 17, n. 3, p. 287–297, 2009. 38, 39, 43, 47

CHU, Jun-Uk; MOON, Inhyuk; LEE, Yun-Jung; KIM, Shin-Ki; MUN, Mu-Seong. A supervised feature-projection-based real-time emg pattern recognition for multifunction myoelectric hand control. *IEEE/ASME Transactions on Mechatronics*, IEEE, v. 12, n. 3, p. 282–290, 2007. 41, 46

CHU, J. U.; MOON, I.; MUN, M. S. A real-time emg pattern recognition system based on linear-nonlinear feature projection for a multifunction myoelectric hand. *IEEE Transactions on Biomedical Engineering*, v. 53, n. 11, p. 2232–2239, Nov 2006. ISSN 0018-9294. 41, 46

CORTES, Corinna; VAPNIK, Vladimir. Support-vector networks. *Machine learning*, Springer, v. 20, n. 3, p. 273–297, 1995. 30

COSTA, Francisco M. V. *Grande Dicionário de Enfermagem Atual*. Rio de Janeiro: Revisão Editorial Ltda e R.B.E editorial, 2006. 17

CRISTIANINI, Nello; SHAWE-TAYLOR, John et al. *An introduction to support vector machines and other kernel-based learning methods*. : Cambridge university press, 2000. 30

DHEERU, Dua; TANISKIDOU, Efi Karra. *UCI Machine Learning Repository*. 2017. Available from Internet: <<http://archive.ics.uci.edu/ml>>. 30

DICTIONARY.COM. "prosthesis," in *Dictionary.com Unabridged*. 2015. Available from Internet: <<http://dictionary.reference.com/browse/prostheses>>. Cited August 2017. 18

DUAN, Feng; DAI, Lili; CHANG, Wennan; CHEN, Zengqiang; ZHU, Chi; LI, Wei. semg-based identification of hand motion commands using wavelet neural network combined with discrete wavelet transform. *IEEE Transactions on Industrial Electronics*, IEEE, v. 63, n. 3, p. 1923–1934, 2016. 44, 48

ELECTRONICS, Interlink. *FSR® Integration Guide*. 2015. Available from Internet: <<http://www.interlinkelectronics.com>>. Cited August 2017. 22, 77

ENGINEERSHANDBOOK.COM. *Sensors: Proximity*. 2006. Available from Internet: <<http://www.engineershandbook.com/>>. Cited August 2017. 23

- ENGLEHART, K.; HUDGIN, B.; PARKER, P. A. A wavelet-based continuous classification scheme for multifunction myoelectric control. *IEEE Transactions on Biomedical Engineering*, v. 48, n. 3, p. 302–311, March 2001. ISSN 0018-9294. [27](#), [28](#), [38](#), [40](#), [45](#), [60](#)
- ENGLEHART, K.; HUDGINS, B. A robust, real-time control scheme for multifunction myoelectric control. *IEEE Transactions on Biomedical Engineering*, v. 50, n. 7, p. 848–854, July 2003. ISSN 0018-9294. [38](#), [40](#), [46](#)
- ENGLEHART, Kevin; HUDGINS, Bernard; PARKER, Philip A; STEVENSON, Maryhelen. Classification of the myoelectric signal using time-frequency based representations. *Medical engineering & physics*, Elsevier, v. 21, n. 6, p. 431–438, 1999. [27](#), [28](#), [38](#), [39](#), [45](#)
- FAN, X.; DAI, L.; CHANG, W.; REN, X.; SHENG, S.; DUAN, F. Verifying the gesture identification effect of wnn and dwt for an interference driven prosthetic hand. In: *2017 29th Chinese Control And Decision Conference (CCDC)*. 2017. p. 5862–5867. [38](#), [44](#), [48](#)
- FARLEY, Pete. *Study Puts More Natural Movement for Artificial Limbs within Reach*. 2014. UCSF News Center. Available from Internet: <www.ucsf.edu/news/>. [15](#)
- FARRY, Kristin A; WALKER, Ian D; BARANIUK, Richard G. Myoelectric teleoperation of a complex robotic hand. *IEEE Transactions on Robotics and Automation*, IEEE, v. 12, n. 5, p. 775–788, 1996. [26](#)
- FAWCETT, Tom; PROVOST, Foster. Adaptive fraud detection. *Data mining and knowledge discovery*, Springer, v. 1, n. 3, p. 291–316, 1997. [36](#)
- FEIX, Thomas; ROMERO, Javier; SCHMIEDMAYER, Heinz-Bodo; DOLLAR, Aaron M; KRAGIC, Danica. The grasp taxonomy of human grasp types. *IEEE Transactions on Human-Machine Systems*, IEEE, v. 46, n. 1, p. 66–77, 2016. [84](#), [109](#)
- FERREIRA, Luis Eduardo Boiko; BARDDAL, Jean Paul; GOMES, Heitor Murilo; ENEMBRECK, Fabrício. Improving credit risk prediction in online peer-to-peer (p2p) lending using imbalanced learning techniques. In: IEEE. *Tools with Artificial Intelligence (ICTAI), 2017 IEEE 29th International Conference on*. 2017. p. 175–181. [58](#)
- FINLEY, F Ray; WIRTA, Roy W. Myocoder studies of multiple myopotential response. *Archives of physical medicine and rehabilitation*, v. 48, n. 11, p. 598, 1967. [15](#)
- FORMAN, George; COHEN, Ira. Learning from little: Comparison of classifiers given little training. In: SPRINGER. *European Conference on Principles of Data Mining and Knowledge Discovery*. 2004. p. 161–172. [61](#)
- GEETHANJALI, P. Comparative study of pca in classification of multichannel emg signals. *Australasian physical & engineering sciences in medicine*, Springer, v. 38, n. 2, p. 331–343, 2015. [39](#), [43](#), [47](#)
- GEETHANJALI, P; RAY, KK. A low-cost real-time research platform for emg pattern recognition-based prosthetic hand. *IEEE/ASME Transactions on mechatronics*, IEEE, v. 20, n. 4, p. 1948–1955, 2015. [38](#), [39](#), [43](#), [47](#), [60](#)
- GERRISH, William E. Dugger Jr. Howard H.; ROBERTS, Richard M. *Electricity & Electronics*. 9th. ed. : Goodheart-Willcox, 2004. [21](#)

- GRIGORIE, Teodor Lucian; BOTEZ, Ruxandra Mihaela. precision improvement of aircrafts attitude estimation through gyro sensors data fusion in a redundant inertial measurement unit. In: IEEE PRESS. *Proceedings of the 13th international symposium on Information processing in sensor networks*. 2014. p. 301–302. 21
- GRUSIN, Mike. *Flex Sensor 2.2" - Small Retail*. 2011. Available from Internet: <<https://www.sparkfun.com/tutorials/270>>. Cited August 2017. 23
- GUO, W.; SHENG, X.; LIU, H.; ZHU, X. Mechanomyography assisted myoelectric sensing for upper-extremity prostheses: A hybrid approach. *IEEE Sensors Journal*, v. 17, n. 10, p. 3100–3108, May 2017. ISSN 1530-437X. 38, 44, 48
- HALL, J.E. *Guyton and Hall Textbook of Medical Physiology*. Elsevier Health Sciences, 2010. (Guyton Physiology). ISBN 9781437726749. Available from Internet: <<https://books.google.com.br/books?id=Po0zyO0BFzwC>>. 20
- HAN, Jeong-Su; SONG, Won-Kyung; KIM, Jong-Sung; BANG, Won-Chul; LEE, Heyoung; BIEN, Zeungnam. New emg pattern recognition based on soft computing techniques and its application to control of a rehabilitation robotic arm. In: *Proceedings of 6th International Conference on Soft Computing*. 2000. p. 890–897. 27
- HARGROVE, L. J.; ENGLEHART, K.; HUDGINS, B. A comparison of surface and intramuscular myoelectric signal classification. *IEEE Transactions on Biomedical Engineering*, v. 54, n. 5, p. 847–853, May 2007. ISSN 0018-9294. 42, 46
- HASSAN, Muhammad; AHMAD, Tasweer; LIAQAT, Nudrat; FAROOQ, Ali; ALI, Syed Asghar; HASSAN, Syed Rizwan. A review on human actions recognition using vision based techniques. *Journal of Image and Graphics*, v. 2, n. 1, p. 28–32, 2014. 50
- HAYKIN, Simon S; HAYKIN, Simon S; HAYKIN, Simon S; HAYKIN, Simon S. *Neural networks and learning machines*. : Pearson Upper Saddle River, NJ, USA:, 2009. 34, 35
- HSIAO, K.; NANGERONI, Paul; HUBER, M.; SAXENA, A.; NG, A.Y. Reactive grasping using optical proximity sensors. In: *IEEE International Conference on Robotics and Automation*. 2009. p. 2098–2105. ISSN 1050-4729. 23
- HUANG, Yonghong; ENGLEHART, K. B.; HUDGINS, B.; CHAN, A. D. C. A gaussian mixture model based classification scheme for myoelectric control of powered upper limb prostheses. *IEEE Transactions on Biomedical Engineering*, v. 52, n. 11, p. 1801–1811, Nov 2005. ISSN 0018-9294. 25, 26, 38, 41, 46
- HUDGINS, Bernard; PARKER, Philip; SCOTT, Robert N. A new strategy for multifunction myoelectric control. *IEEE Transactions on Biomedical Engineering*, IEEE, v. 40, n. 1, p. 82–94, 1993. 24, 25, 26, 38, 39, 45
- IBGE. Instituto Brasileiro de Geografia e Estatística. *Censo Demográfico*. 2010. Available from Internet: <<http://www.ibge.gov.br>>. Cited August 2017. 14
- INTEL CORPORATION. *Intel Edison Development Platform*. 2014. 76
- INTEL CORPORATION. *Creating applications with the MCU SDK for the Intel® Edison board*. 2015. Available from Internet: <<https://software.intel.com/node/545142>>. 79, 80

- INTEL CORPORATION. *Intel® Edison Kit for Arduino Hardware Guide*. 2015. 77
- JUNG, Kyung Kwon; KIM, Joo Woong; LEE, Hyun Kwan; CHUNG, Sung Boo; EOM, Ki Hwan. Emg pattern classification using spectral estimation and neural network. In: IEEE. 2007. p. 1108–1111. 42, 46
- KAMEN, Gary; GABRIEL, David. *Essentials of electromyography*. : Human Kinetics, 2010. 20
- KEATING, Jennifer. *Anatomical surface EMG placement on the forearm*. 2013. 75
- KELLY, Michael F; PARKER, Philip A; SCOTT, Robert N. The application of neural networks to myoelectric signal analysis: A preliminary study. *IEEE Transactions on Biomedical Engineering*, IEEE, v. 37, n. 3, p. 221–230, 1990. 38, 39, 45
- KHEZRI, M; JAHED, M; SADATI, N. Neuro-fuzzy surface emg pattern recognition for multifunctional hand prosthesis control. In: IEEE. *IEEE International Symposium on Industrial Electronics*. 2007. p. 269–274. 38, 42, 46
- KUBAT, Miroslav; HOLTE, Robert C; MATWIN, Stan. Machine learning for the detection of oil spills in satellite radar images. *Machine learning*, Springer, v. 30, n. 2-3, p. 195–215, 1998. 60
- KWON, Jangwoo; LEE, Donghoon; LEE, Sangmin; KIM, Naghwan; HONG, Seunghong. Emg signals recognition for continuous prosthetic arm control purpose. In: IEEE. *IEEE Asia Pacific Conference on Circuits and Systems*. 1996. p. 365–368. 39, 45
- KWON, Jangwoo; LEE, Sangjean; SHIN, Chulkyu; JANG, Younggun; HONG, Seunghong. Signal hybrid hmm-ga-mlp classifier for continuous emg classification purpose. In: IEEE. *Proceedings of the 20th Annual International Conference of the IEEE Engineering in Medicine and Biology Society*. 1998. v. 3, p. 1404–1407. 39, 45
- KYRANOU, I.; KRASOULIS, A.; ERDEN, M. S.; NAZARPOUR, K.; VIJAYAKUMAR, S. Real-time classification of multi-modal sensory data for prosthetic hand control. In: *2016 6th IEEE International Conference on Biomedical Robotics and Biomechatronics (BioRob)*. 2016. p. 536–541. 15, 38, 44, 48, 49
- LAWRENCE, P; HERBERTS, P; KADEFORS, R. Experiences with a multifunctional hand prosthesis controlled by myoelectric patterns. *Advances in External Control of Human Extremities*, p. 47–65, 1973. 15
- LEBLANC, Maurice. Give hope-give a hand. *The Ellen Meadow Prosthetic Hand Foundation, San Francisco, CA*, v. 5, p. 2017, 2011. 14
- LECUN, Yann et al. Generalization and network design strategies. *Connectionism in perspective*, Citeseer, p. 143–155, 1989. 34
- LEE, Seok-Pil; PARK, Sang-Hui; KIM, Jeong-Seop; KIM, Ig-Jae. Emg pattern recognition based on evidence accumulation for prosthesis control. In: IEEE. *Proceedings of 18th Annual International Conference of the IEEE Engineering in Medicine and Biology Society*. 1996. v. 4, p. 1481–1483. 39, 45

- LEMAÎTRE, Guillaume; NOGUEIRA, Fernando; ARIDAS, Christos K. Imbalanced-learn: A python toolbox to tackle the curse of imbalanced datasets in machine learning. *The Journal of Machine Learning Research*, JMLR. org, v. 18, n. 1, p. 559–563, 2017. 65
- LI, G.; SCHULTZ, A. E.; KUIKEN, T. A. Quantifying pattern recognition-based myoelectric control of multifunctional transradial prostheses. *IEEE Transactions on Neural Systems and Rehabilitation Engineering*, v. 18, n. 2, p. 185–192, April 2010. ISSN 1534-4320. 43, 47
- LICHTER, P. A.; LANGE, E. H.; RIEHLE, T. H.; ANDERSON, S. M.; HEDIN, D. S. Rechargeable wireless EMG sensor for prosthetic control. *Conf Proc IEEE Eng Med Biol Soc*, v. 2010, p. 5074–5076, 2010. 15
- LIMBLESS ASSOCIATION. *Types of Amputation*. 2012. Available from Internet: <<http://www.limbless-association.org>>. Cited August 2017. 18
- LIU, Honghai; JU, Zhaojie; JI, Xiaofei; CHAN, Chee Seng; KHOURY, Mehdi. *Human Motion Sensing and Recognition: A Fuzzy Qualitative Approach*. : Springer, 2017. 50, 51
- LIU, Yi-Hung; HUANG, Han-Pang; WENG, Chang-Hsin. Recognition of electromyographic signals using cascaded kernel learning machine. *IEEE/ASME Transactions on Mechatronics*, IEEE, v. 12, n. 3, p. 253–264, 2007. 26, 42, 46, 60
- LUCAS, Marie-Françoise; GAUFRIAU, Adrien; PASCUAL, Sylvain; DONCARLI, Christian; FARINA, Dario. Multi-channel surface emg classification using support vector machines and signal-based wavelet optimization. *Biomedical Signal Processing and Control*, Elsevier, v. 3, n. 2, p. 169–174, 2008. 28, 38, 39, 42, 46, 60
- LYMAN, JH; FREEDY, A; PRIOR, R. Fundamental and applied research related to the design and development of upper-limb externally powered prostheses. *Bull. Prosthetics Res*, p. 184–195, 1976. 15
- MARKS, G.E. *Manual of Artificial Limbs: Artificial Toes, Feet, Legs, Fingers, Hands, Arms, for Amputations and Deformities, Appliances for Excisions, Fractures, and Other Disabilities of Lower and Upper Extremities, Suggestions on Amputations, Treatment of Stumps, History, Etc., Etc., Etc. : an Exhaustive Exposition of Prosthesis*. A.A. Marks, 1905. Available from Internet: <<https://books.google.com.br/books?id=S-ktAAAAIAAJ>>. 18
- MEHTA, Arpit. High-speed op amp enables infrared (ir) proximity sensing. 2009. 23
- MICERA, Silvestro; SABATINI, Angelo M; DARIO, Paolo. On automatic identification of upper-limb movements using small-sized training sets of emg signals. *Medical engineering & physics*, Elsevier, v. 22, n. 8, p. 527–533, 2000. 40, 45
- NAGATA, Kentaro; ADNO, Keiichi; MAGATANI, K; YAMADA, M. A classification method of hand movements using multi channel electrode. In: IEEE. *27th Annual International Conference of the Engineering in Medicine and Biology Society*. 2006. p. 2375–2378. 41, 46
- NAIK, G. R.; AL-TIMEMY, A. H.; NGUYEN, H. T. Transradial amputee gesture classification using an optimal number of semg sensors: An approach using ica clustering. *IEEE Transactions on Neural Systems and Rehabilitation Engineering*, v. 24, n. 8, p. 837–846, Aug 2016. ISSN 1534-4320. 44, 48

- NAZMI, Nurhazimah; RAHMAN, Mohd Azizi Abdul; YAMAMOTO, Shin-Ichiroh; AHMAD, Siti Anom; ZAMZURI, Hairi; MAZLAN, Saiful Amri. A review of classification techniques of emg signals during isotonic and isometric contractions. *Sensors*, Multidisciplinary Digital Publishing Institute, v. 16, n. 8, p. 1304, 2016. [24](#)
- NHS CHOICES. *Amputation*. 2014. Available from Internet: <<http://www.nhs.uk/conditions/amputation>>. Cited August 2017. [17](#)
- NUWER, Rachel. Armband adds a twitch to gesture control. *New Scientist*, v. 217, n. 2906, p. 21 –, 2013. ISSN 0262-4079. Available from Internet: <<http://www.sciencedirect.com/science/article/pii/S0262407913605424>>. [77](#)
- OIKONOMIDIS, Iason; KYRIAZIS, Nikolaos; ARGYROS, Antonis A. Efficient model-based 3d tracking of hand articulations using kinect. In: . 2011. v. 1, n. 2, p. 3. [50](#)
- OSKOEI, Mohammadreza Asghari; HU, Huosheng. Ga-based feature subset selection for myoelectric classification. In: IEEE. *IEEE International Conference on Robotics and Biomimetics*. 2006. p. 1465–1470. [26](#), [27](#)
- OSKOEI, Mohammadreza Asghari; HU, Huosheng. Support vector machine-based classification scheme for myoelectric control applied to upper limb. *IEEE transactions on biomedical engineering*, IEEE, v. 55, n. 8, p. 1956–1965, 2008. [26](#), [42](#), [47](#)
- PANAHANDEH, Ghazaleh; SKOG, Isaac; JANSSON, Magnus. Calibration of the accelerometer triad of an inertial measurement unit, maximum likelihood estimation and cramer-rao bound. In: IEEE. *International Conference on Indoor Positioning and Indoor Navigation*. 2010. p. 1–6. [21](#)
- PARK, Sang-Hui; LEE, Seok-Pil. Emg pattern recognition based on artificial intelligence techniques. *IEEE transactions on Rehabilitation Engineering*, IEEE, v. 6, n. 4, p. 400–405, 1998. [24](#), [26](#), [38](#), [39](#), [45](#)
- PASUPA, Kitsuchart; SUNHEM, Wisuwat. A comparison between shallow and deep architecture classifiers on small dataset. In: IEEE. *Information Technology and Electrical Engineering (ICITEE), 2016 8th International Conference on*. 2016. p. 1–6. [60](#)
- PHINYOMARK, Angkoon; KHUSHABA, Rami N; SCHEME, Erik. Feature extraction and selection for myoelectric control based on wearable emg sensors. *Sensors*, Multidisciplinary Digital Publishing Institute, v. 18, n. 5, p. 1615, 2018. [15](#)
- PIZZOLATO, Stefano; TAGLIAPIETRA, Luca; COGNOLATO, Matteo; REGGIANI, Monica; MÜLLER, Henning; ATZORI, Manfredo. Comparison of six electromyography acquisition setups on hand movement classification tasks. *PloS one*, Public Library of Science, v. 12, n. 10, p. e0186132, 2017. [55](#), [56](#), [60](#), [61](#), [70](#), [73](#)
- PRAHM, Cosima; VUJAKLIJA, Ivan; KAYALI, Fares; PURGATHOFER, Peter; ASZMANN, Oskar C. Game-based rehabilitation for myoelectric prosthesis control. *JMIR serious games*, JMIR Publications Inc., v. 5, n. 1, 2017. [25](#)
- PROJECTS, Linux Foundation Collaborative. *About Yocto Project*. 2016. Available from Internet: <<https://www.yoctoproject.org/about>>. [79](#)
- RASCHKA, Sebastian; JULIAN, David; HEARTY, John. *Python: deeper insights into machine learning*. : Packt Publishing Ltd, 2016. [33](#)

- ROSLAN, M. R.; SIDEK, S. N.; SIDEK, S.; KHALID, M. S. bin Mohd. Emg based classification of thumb posture using portable thumb training system. In: *2016 IEEE EMBS Conference on Biomedical Engineering and Sciences (IECBES)*. 2016. p. 758–762. [38](#)
- SARIDIS, G. N.; GOOTEE, T. P. Emg pattern analysis and classification for a prosthetic arm. *IEEE Transactions on Biomedical Engineering*, BME-29, n. 6, p. 403–412, June 1982. ISSN 0018-9294. [39](#), [45](#)
- SCHÖLKOPF, Bernhard; SMOLA, Alexander J et al. *Learning with kernels: support vector machines, regularization, optimization, and beyond*. : MIT press, 2002. [30](#)
- SHENOY, P.; MILLER, K. J.; CRAWFORD, B.; RAO, R. P. N. Online electromyographic control of a robotic prosthesis. *IEEE Transactions on Biomedical Engineering*, v. 55, n. 3, p. 1128–1135, March 2008. ISSN 0018-9294. [25](#), [42](#), [47](#), [60](#)
- SPECTRA SYMBOL. *Flex Sensor FS*. 2014. Rev. A. [78](#)
- SPICHLER, E. R.; SPICHLER, D.; LESSA, I.; FORTI, A. Costa e; FRANCO, L. J.; LAPORTE, R. E. Capture-recapture method to estimate lower extremity amputation rates in Rio de Janeiro, Brazil. *Rev. Panam. Salud Publica*, v. 10, n. 5, p. 334–340, Nov 2001. [14](#)
- STEWART, R.E.; FERSHT, S.N. *Three axis inertial measurement unit with counterbalanced mechanical oscillator*. Google Patents, 1991. US Patent 4,996,877. Available from Internet: <<https://www.google.com.ar/patents/US4996877>>. [21](#)
- STOLFO, Salvatore; FAN, David W; LEE, Wenke; PRODROMIDIS, Andreas; CHAN, P. Credit card fraud detection using meta-learning: Issues and initial results. In: *AAAI-97 Workshop on Fraud Detection and Risk Management*. 1997. [36](#)
- STRAIT, Erin. Prosthetics in developing countries. *Prosthetic Resident*, 2006. [18](#), [19](#)
- SUEASEENAK, Direk; WIBIRAMA, Sunu; CHANWIMALUEANG, Theerasak; PINTAVIROOJ, Chuchart; SANGWORASIL, Manus. Comparison study of muscular-contraction classification between independent component analysis and artificial neural network. In: *IEEE. International Symposium on Communications and Information Technologies*. 2008. p. 468–472. [42](#), [47](#)
- SUN, Yanmin; KAMEL, Mohamed S; WANG, Yang. Boosting for learning multiple classes with imbalanced class distribution. In: *IEEE. Data Mining, 2006. ICDM'06. Sixth International Conference on*. 2006. p. 592–602. [59](#)
- TENORE, Francesco; RAMOS, Ander; FAHMY, Amir; ACHARYA, Soumyadipta; ETIENNE-CUMMINGS, Ralph; THAKOR, Nitish V. Towards the control of individual fingers of a prosthetic hand using surface emg signals. In: *IEEE. 29th Annual International Conference of the IEEE Engineering in Medicine and Biology Society*. 2007. p. 6145–6148. [42](#), [46](#)
- TENORE, Francesco VG; RAMOS, Ander; FAHMY, Amir; ACHARYA, Soumyadipta; ETIENNE-CUMMINGS, Ralph; THAKOR, Nitish V. Decoding of individuated finger movements using surface electromyography. *IEEE transactions on biomedical engineering*, IEEE, v. 56, n. 5, p. 1427–1434, 2009. [24](#), [25](#), [43](#), [47](#)

Thalmic Labs. *Myo Armband Tech Specs*. 2016. Available from Internet: <<https://www.myo.com/techspecs>>. 77

Thalmic Labs. *Myo Gesture Control Armband: Important Information Guide*. 2016. Available from Internet: <<https://s3.amazonaws.com/thalmonicdownloads/information+guide/important-information-guide-v01.pdf>>. 75

TSENOV, G; ZEGHBIB, AH; PALIS, F; SHOYLEV, N; MLADENOV, V. Neural networks for online classification of hand and finger movements using surface emg signals. In: IEEE. *8th Seminar on Neural Network Applications in Electrical Engineering*. 2006. p. 167–171. 41, 46

TSUJI, Toshio; FUKUDA, R Osamu; KANEKO, Makoto; ITO, Koji. Pattern classification of time-series emg signals using neural networks. *INTERNATIONAL JOURNAL OF ADAPTIVE CONTROL AND SIGNAL PROCESSING*, v. 14, p. 829–848, 2000. 40, 45

VANDERWERKER, JR. EARL E. A brief review of the history of amputations and prostheses. *ICIB*, v. 15, n. 5, p. 15–16, 1976. 14

VERLE, Milan. *PIC Microcontrollers - Programming in Assembly*. 2016. Available from Internet: <<https://www.mikroe.com/ebooks/pic-microcontrollers-programming-in-assembly/introduction>>. 21

VERPLAETSE, Christopher. Can a pen remember what it has written using inertial navigation?: An evaluation of current accelerometer technology. 1995. 22

VIDOVIC, M. M. C.; HWANG, H. J.; AMSÜSS, S.; HAHNE, J. M.; FARINA, D.; MÜLLER, K. R. Improving the robustness of myoelectric pattern recognition for upper limb prostheses by covariate shift adaptation. *IEEE Transactions on Neural Systems and Rehabilitation Engineering*, v. 24, n. 9, p. 961–970, Sept 2016. ISSN 1534-4320. 44, 48

VISHAY SEMICONDUCTORS. *Fully Integrated Proximity and Ambient Light Sensor with Infrared Emitter and I2C Interface*. 2015. Rev. 1.4. 78

WANG, JZ; WANG, RC; LI, F; JIANG, MW; JIN, DW. Emg signal classification for myoelectric teleoperating a dexterous robot hand. In: IEEE. *27th Annual International Conference of the Engineering in Medicine and Biology Society*. 2006. p. 5931–5933. 28, 41, 46

WEISS, Gary M. Mining with rarity: a unifying framework. *ACM Sigkdd Explorations Newsletter*, ACM, v. 6, n. 1, p. 7–19, 2004. 36

WHO. World Health Organization and MossRehab. *The Rehabilitation of People with Amputations*. United States, 2004. 14

WININGS, T.R.; SAMSON, R. *Automated dispenser for disinfectant with proximity sensor*. Google Patents, 1997. US Patent 5,695,091. Available from Internet: <<https://www.google.com/patents/US5695091>>. 23

WITTEN, I.H.; FRANK, E.; HALL, M.A.; PAL, C.J. *Data Mining: Practical Machine Learning Tools and Techniques*. Elsevier Science, 2016. (The Morgan Kaufmann Series in Data Management Systems). ISBN 9780128043578. Available from Internet: <<https://books.google.com.br/books?id=1SylCgAAQBAJ>>. 29

- WOODMAN, Oliver J. An introduction to inertial navigation. *University of Cambridge, Computer Laboratory, Tech. Rep. UCAMCL-TR-696*, v. 14, p. 15, 2007. [21](#)
- ZARDOSHTI-KERMANI, Mahyar; WHEELER, Bruce C; BADIE, Kambiz; HASHEMI, Reza M. Emg feature evaluation for movement control of upper extremity prostheses. *IEEE Transactions on Rehabilitation Engineering*, IEEE, v. 3, n. 4, p. 324–333, 1995. [26](#)
- ZECCA, Micera; MICERA, Silvestro; CARROZZA, Maria C; DARIO, Paolo. Control of multifunctional prosthetic hands by processing the electromyographic signal. *Critical ReviewsTM in Biomedical Engineering*, Begel House Inc., v. 30, n. 4-6, 2002. [27](#)
- ZHANG, Xiaowen; YANG, Yupu; XU, Xiaoming; ZHANG, Ming. Wavelet based neuro-fuzzy classification for emg control. In: IEEE. *International Conference on Communications, Circuits and Systems and West Sino Expositions*. 2002. v. 2, p. 1087–1089. [40](#), [45](#)
- ZIEGLER-GRAHAM, K.; MACKENZIE, E. J.; EPHRAIM, P. L.; TRAVISON, T. G.; BROOKMEYER, R. Estimating the prevalence of limb loss in the United States: 2005 to 2050. *Arch Phys Med Rehabil*, v. 89, n. 3, p. 422–429, Mar 2008. [14](#), [38](#)
- ZOPH, Barret; LE, Quoc V. Neural architecture search with reinforcement learning. *arXiv preprint arXiv:1611.01578*, 2016. [35](#), [60](#)

Appendix

APPENDIX A – Neural Networks Architectures

We train the weights of our networks to minimize the cross-entropy between the estimated class probabilities and the “true” distribution. Figure 30 shows the network architecture, which consists of four layers, including a normalization layer, one convolutional layer, one max-pooling layer and one fully connected layer.

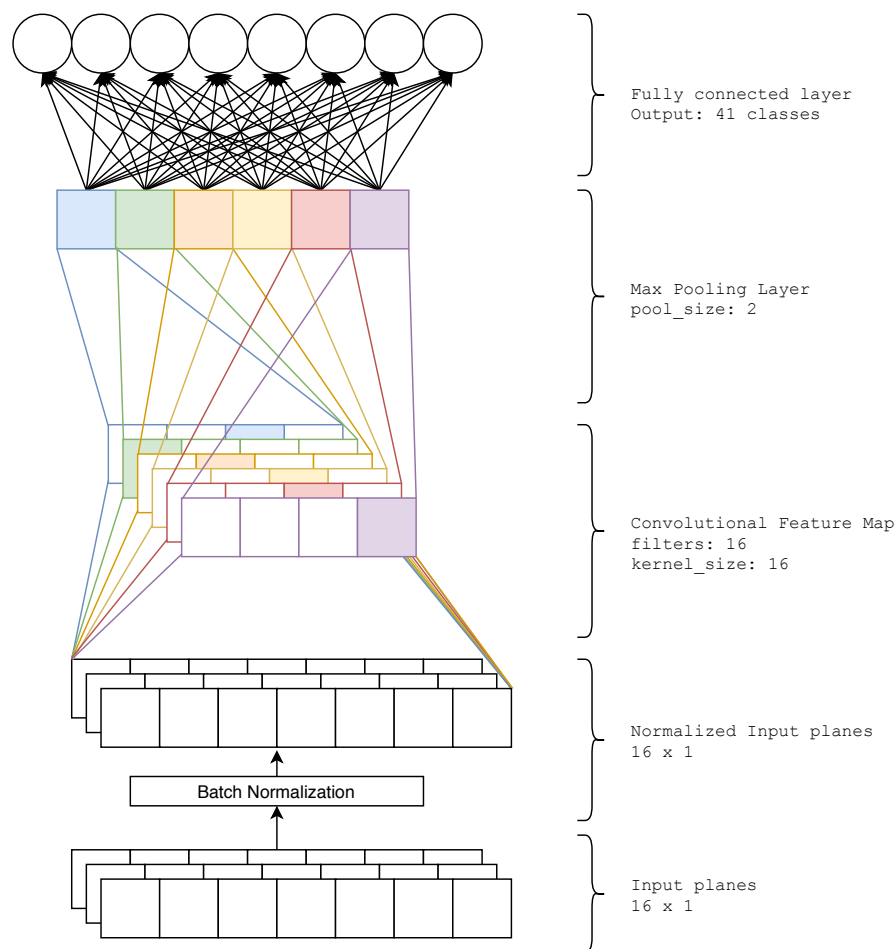


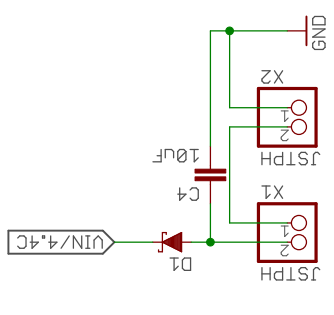
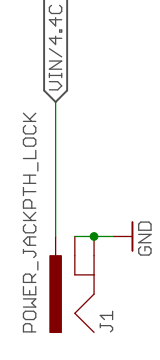
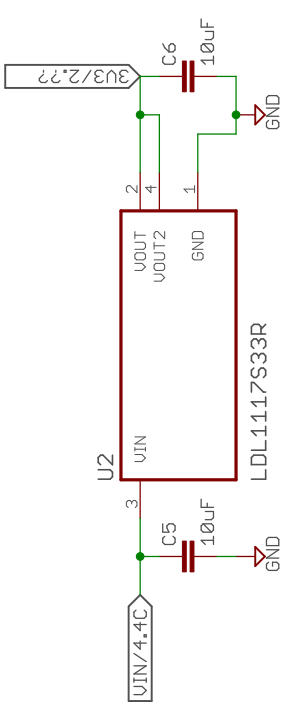
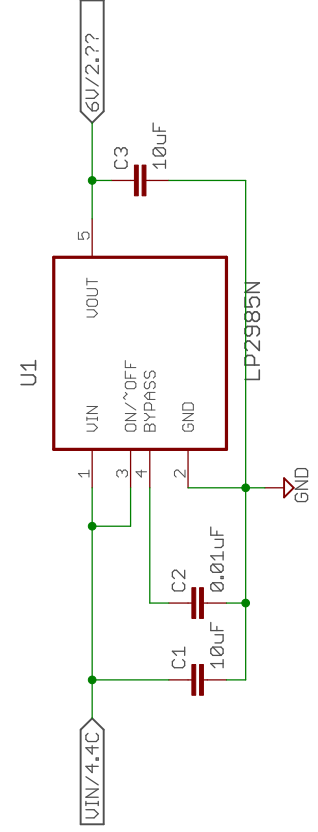
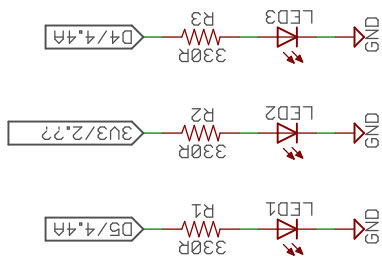
Figure 30 – Neural Network Architecture for the eCNN trained with 500 epochs and dropout rate of 0.2

The architectures generated by the NAS-CNN are presented on Table 16. It follows the same architecture in Figure 30, changing the hyper-parameters: kernel_size, #filters, pool_size and dropout rate.

Table 16 – Neural Network Architectures generated by the NAS algorithm

| | | RMS | | | | | | mDWT | | | |
|----------------------------|---------|-------------|---------|-------------|---------|----------------------------|---------|-------------|---------|-------------|---------|
| Experiment | Subject | Kernel Size | Filters | Max Pooling | Dropout | Experiment | Subject | Kernel Size | Filters | Max Pooling | Dropout |
| 1 | 1 | 62 | 46 | 5 | 0.02 | 1 | 1 | 5 | 56 | 5 | 0.20 |
| | 2 | 70 | 74 | 5 | 0.02 | | 2 | 8 | 76 | 5 | 0.20 |
| | 3 | 64 | 51 | 5 | 0.11 | | 3 | 70 | 74 | 5 | 0.02 |
| | 4 | 70 | 74 | 5 | 0.02 | | 4 | 5 | 76 | 5 | 0.20 |
| | 5 | 70 | 74 | 5 | 0.02 | | 5 | 70 | 74 | 5 | 0.02 |
| | 6 | 70 | 74 | 5 | 0.02 | | 6 | 25 | 30 | 5 | 0.20 |
| | 7 | 49 | 68 | 5 | 0.02 | | 7 | 70 | 74 | 5 | 0.02 |
| | 8 | 76 | 62 | 5 | 0.02 | | 8 | 34 | 62 | 5 | 0.03 |
| | 9 | 70 | 74 | 5 | 0.02 | | 9 | 5 | 51 | 5 | 0.02 |
| | 10 | 70 | 74 | 5 | 0.02 | | 10 | 70 | 74 | 5 | 0.02 |
| 2 | All | 70 | 74 | 5 | 0.02 | 2 | All | 70 | 74 | 5 | 0.02 |
| 3 SMOTE | 1 | 40 | 14 | 5 | 0.02 | 3 SMOTE | 1 | 67 | 72 | 5 | 0.20 |
| | 2 | 70 | 74 | 5 | 0.02 | | 2 | 46 | 5 | 5 | 0.20 |
| | 3 | 70 | 74 | 5 | 0.02 | | 3 | 62 | 76 | 5 | 0.02 |
| | 4 | 75 | 75 | 5 | 0.02 | | 4 | 70 | 74 | 5 | 0.02 |
| | 5 | 15 | 36 | 5 | 0.06 | | 5 | 70 | 74 | 5 | 0.02 |
| | 6 | 70 | 74 | 5 | 0.02 | | 6 | 62 | 67 | 5 | 0.10 |
| | 7 | 70 | 74 | 5 | 0.02 | | 7 | 76 | 76 | 5 | 0.02 |
| | 8 | 76 | 75 | 4 | 0.02 | | 8 | 62 | 5 | 5 | 0.01 |
| | 9 | 63 | 76 | 7 | 0.01 | | 9 | 33 | 40 | 54 | 0.20 |
| | 10 | 7 | 45 | 5 | 0.20 | | 10 | 29 | 16 | 5 | 0.01 |
| 3 SMOTE SVM | 1 | 59 | 58 | 5 | 0.01 | 3 SMOTE SVM | 1 | 58 | 62 | 5 | 0.02 |
| | 2 | 70 | 74 | 5 | 0.02 | | 2 | 46 | 5 | 5 | 0.02 |
| | 3 | 76 | 76 | 76 | 0.01 | | 3 | 68 | 9 | 5 | 0.04 |
| | 4 | 5 | 75 | 5 | 0.02 | | 4 | 28 | 28 | 4 | 0.20 |
| | 5 | 72 | 13 | 5 | 0.06 | | 5 | 29 | 5 | 5 | 0.20 |
| | 6 | 76 | 5 | 5 | 0.03 | | 6 | 15 | 5 | 1 | 0.02 |
| | 7 | 46 | 75 | 5 | 0.02 | | 7 | 76 | 16 | 8 | 0.01 |
| | 8 | 58 | 39 | 5 | 0.01 | | 8 | 52 | 64 | 5 | 0.20 |
| | 9 | 63 | 75 | 75 | 0.20 | | 9 | 51 | 64 | 5 | 0.02 |
| | 10 | 25 | 75 | 5 | 0.02 | | 10 | 70 | 74 | 5 | 0.02 |
| 3 SMOTE | All | 75 | 63 | 5 | 0.20 | 3 SMOTE | All | 62 | 50 | 5 | 0.20 |
| 3 SMOTE SVM | All | 76 | 64 | 3 | 0.20 | 3 SMOTE SVM | All | 72 | 62 | 5 | 0.20 |

APPENDIX B – Schematics



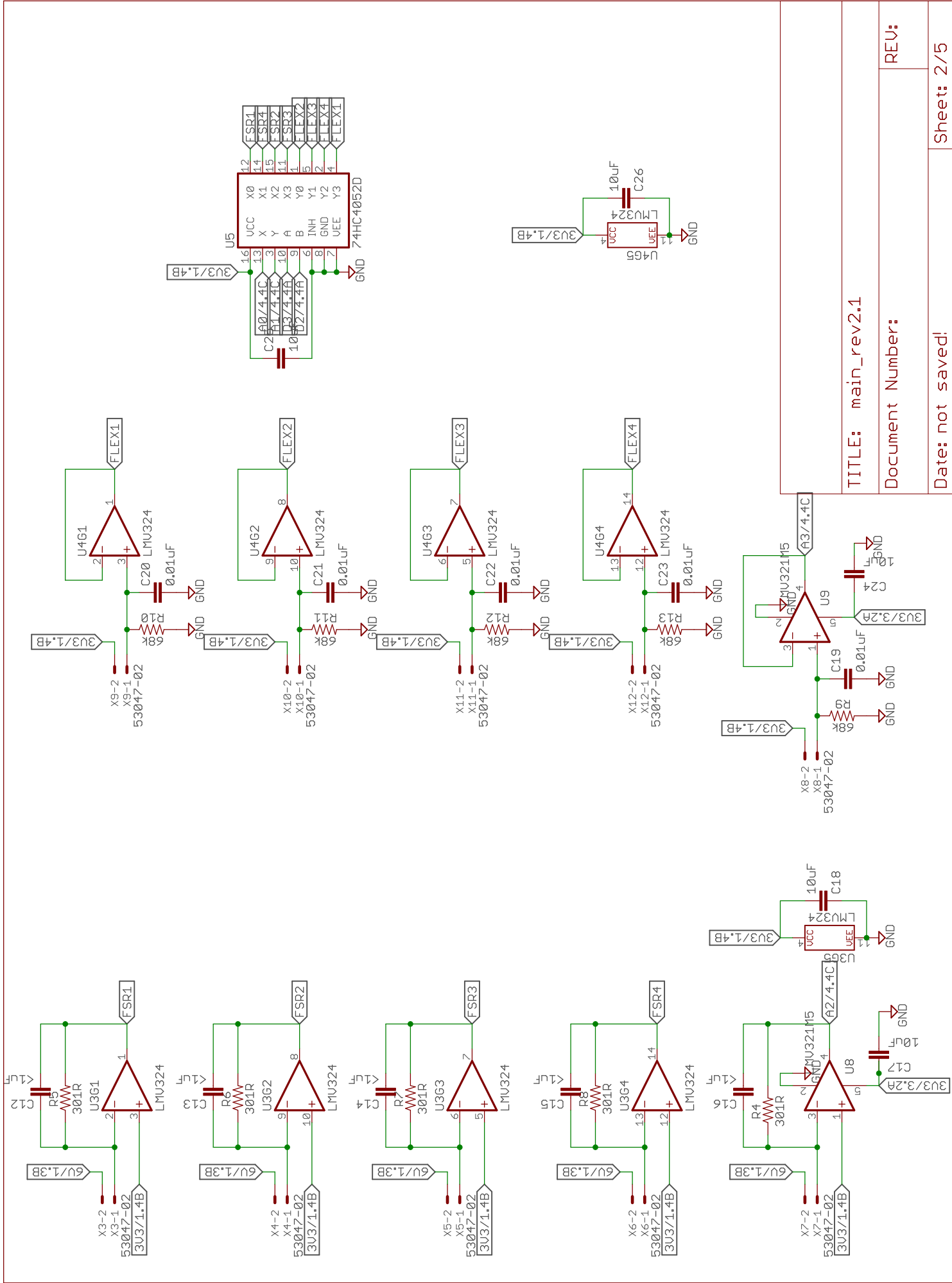
TITLE: main_rev2.1

Document Number:

REV:

Date: not saved!

Sheet: 1/5



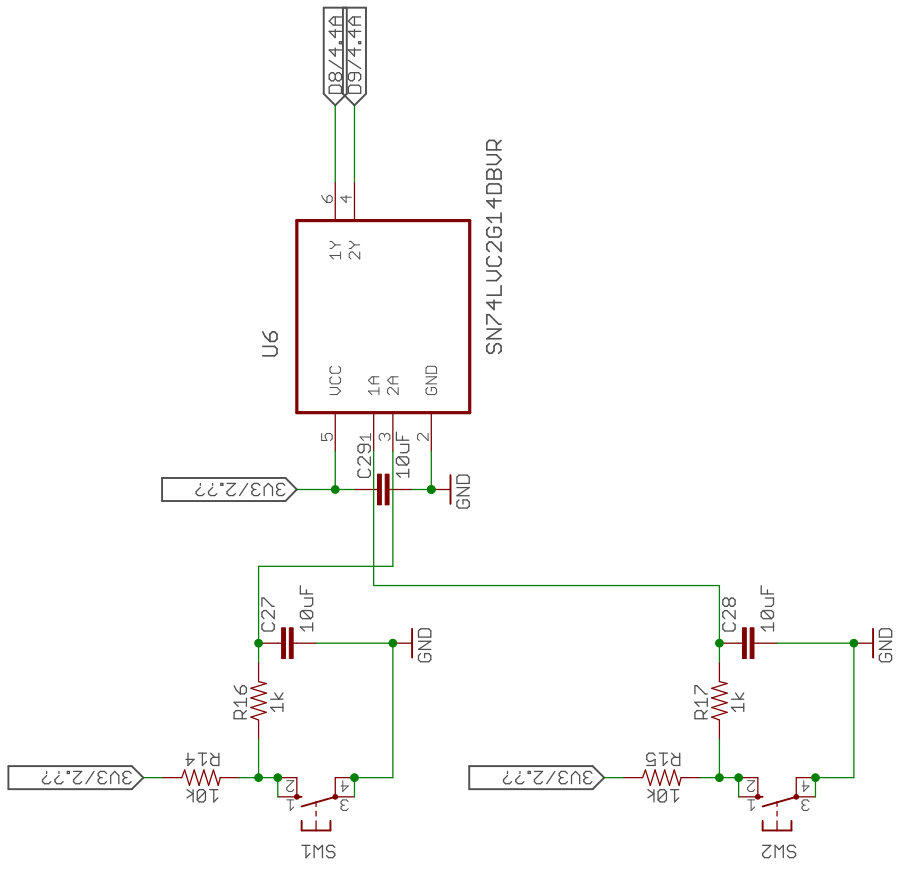
TITLE: main_rev2.1

Document Number:

REV:

Date: not saved!

Sheet: 2/5



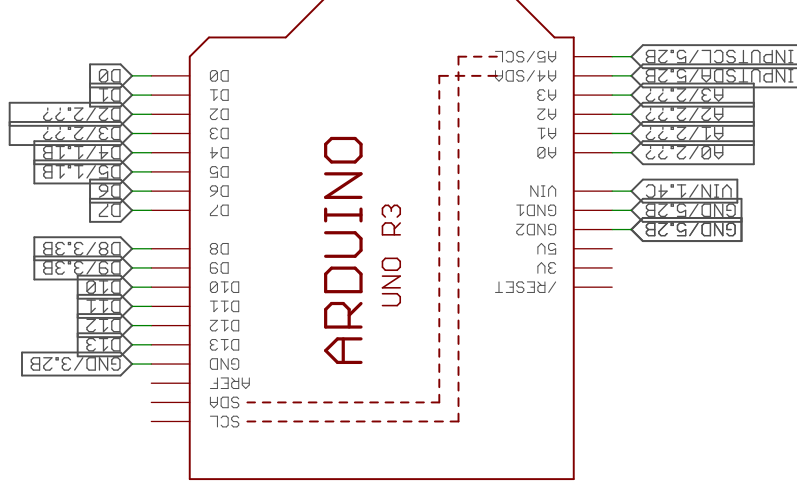
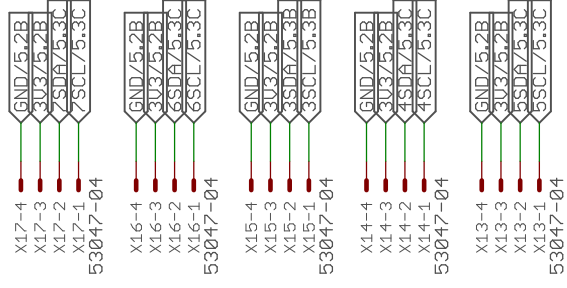
TITLE: main_rev2.1

Document Number:

REV:

Date: not saved!

Sheet: 3/5



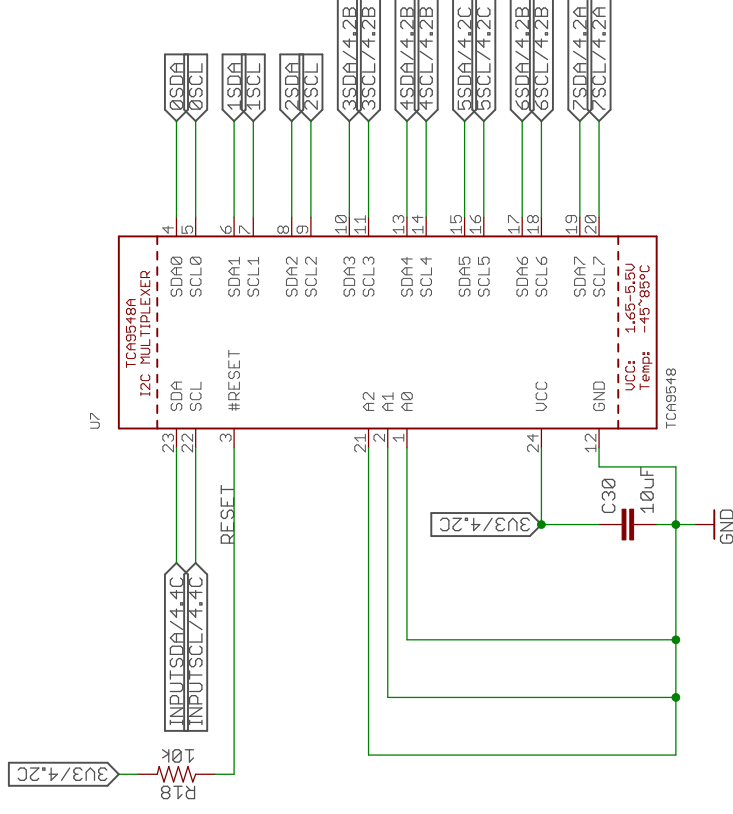
TITLE: main_rev2.1

Document Number:

REV:

Date: not saved!

Sheet: 4/5



TITLE: main_rev2.1

Document Number:





REV:





Date: not saved!





Sheet: 5/5





APPENDIX C – Movements SGDB




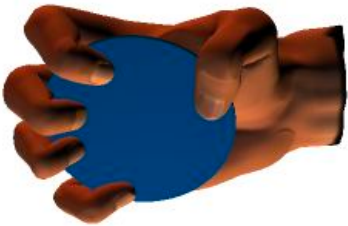
The movements chosen for the SGDB were selected from Feix et al. (2016).

| Mov. Id | Name | Picture | Type | Opp.Type | Thumb Pos. |
|---------|------------------------|---|-------|----------|------------|
| 1 | Large Diameter |  | Power | Palm | Abd |
| 2 | Small Diameter |  | Power | Palm | Abd |
| 3 | Fixed Hook |  | Power | Palm | Add |
| 4 | Index Finger Extension |  | Power | Palm | Add |

| Mov. Id | Name | Picture | Type | Opp.Type | Thumb Pos. |
|---------|--------------------|---|--------------|----------|------------|
| 5 | Medium Wrap |  | Power | Palm | Abd |
| 6 | Ring |  | Power | Pad | Abd |
| 7 | Prismatic 4 Finger |  | Precision | Pad | Abd |
| 8 | Stick |  | Intermediate | Side | Add |

| Mov. Id | Name | Picture | Type | Opp.Type | Thumb Pos. |
|---------|------------------|---|-----------|----------|------------|
| 9 | Writing Tripod |  | Precision | Side | Abd |
| 10 | Power Sphere |  | Power | Palm | Abd |
| 11 | Sphere 3 Finger |  | Power | Pad | Abd |
| 12 | Precision Sphere |  | Precision | Pad | Abd |

| Mov. Id | Name | Picture | Type | Opp.Type | Thumb Pos. |
|---------|--------------|---|-----------|----------|------------|
| 13 | Tripod |  | Precision | Pad | Abd |
| 14 | Palmar Pinch |  | Precision | Pad | Abd |
| 15 | Tip Pinch |  | Precision | Pad | Abd |
| 16 | Quadpod |  | Precision | Pad | Abd |

| Mov. Id | Name | Picture | Type | Opp.Type | Thumb Pos. |
|---------|--------------------|---|--------------|----------|------------|
| 17 | Lateral |  | Intermediate | Side | Add |
| 18 | Parallel Extension |  | Precision | Pad | Add |
| 19 | Extension Type |  | Power | Pad | Abd |
| 20 | Power Disk |  | Power | Palm | Abd |